



HEALTH & SAFETY
LABORATORY

ETI High Hydrogen Phase 2 Test Programme Report

Author(s):

B.C.R. Ewan, PhD.

K. Moodie, MSc.

W. Rattigan, BSc.

Report Number:

EA/19/12

ETI High Hydrogen Phase 2 Test Programme Report

Report approved by:	Phil Hooker
Report authorised for issue to Energy Technology Institute by:	Stuart Hawksworth PhD
Date of Issue:	01/08/2019
Lead Authors:	K. Moodie MSc and B.C.R. Ewan PhD
Contributing Author:	W. Rattigan BSc
Customer:	Energy Technology Institute
Technical Reviewer:	Phil Hooker
Editorial Reviewer:	Linda Heritage
Project number:	PE03468

Disclaimer:

This report and the work it describes were undertaken by the Health and Safety Laboratory under contract to the Energy Technology Institute. Its contents, including any opinions and/or conclusion expressed or recommendations made, do not necessarily reflect policy or views of the Health and Safety Executive.

© Energy Technologies Institute

EXECUTIVE SUMMARY

The report describes a further series of tests (Phase Two) undertaken with the existing reduced-scale model of a combined cycle gas turbine (CCGT) complete with a model heat recovery steam generator (HRSG). This test series was designed to provide additional data to fill gaps identified in the original test series (WP 2.3). The report presents the results from these additional tests together with an analysis of them. The facility provided a means of measuring the consequences of the ignition of binary mixtures consisting of hydrogen/methane or hydrogen/carbon monoxide, and ternary mixtures consisting of hydrogen/carbon monoxide/methane, when they were injected and spark ignited in the hot exhaust stream from a gas turbine.

The overall objective was to investigate at reduced scale, the consequences of a flame-out in a full-size CCGT when running on high hydrogen fuel mixtures. In so doing the intention was to provide data sets that could be used to aid understanding of the physical processes involved as well as providing data that could be used for CFD modelling of the whole process. The test parameters varied were the fuel mixture composition, the equivalence ratio and the exhaust gas temperature. The engine mass flow rate was kept the same throughout the test programme. The HRSG was designed with a series of solid finned tubes giving a blockage ratio of 48% per tube row. There were a total of 218 tubes arranged in 15 rows. All of the tests were undertaken with the end plate in position on the HRSG and with a vertical exit stack at the end of the HRSG directing the exit gases vertically upwards.

The accuracy of the various types of sensors used was examined, including in particular the performance of the pressure transducers used during the test programme. Detection of the flame was by flame ionisation and optical emission techniques, which provided complementary measurements, the optical sensors providing a "line of sight" across the HRSG, whilst the ionisation sensors were point measurement devices located just in from the side wall and detected flame that was present locally. The optical sensors were modified versions of those used previously, having been designed specifically for the weaker flame-fronts experienced during these tests. Overall the optical and pressure sensors yielded a 94% usage rate. High-speed videos of the tests were also made using two high-speed cameras, one upstream of the tube bank the other downstream. The results showed more clearly than previously (WP 2.3) the variability in flame behaviour under different conditions of fuel mixture composition and equivalence ratio.

Additional pressure sensors were used in fixed positions throughout the test series. The data from these often showed complex behaviour arising from the different sensor locations and the changing flame speed behaviour within the test facility as a consequence of the combusting flows through the HRSG. In many cases the peak pressure was of short duration, followed by longer duration lower pressure components. This may have implications for the real impact of pressure pulses on the containing structures.

Mixtures of H_2/CH_4 , H_2/CH_4 and H_2/CO were investigated with equivalence ratios (EQR's) up to 0.79 for methane alone, and down to 0.285 for hydrogen alone. A total of 55 tests were successfully completed, not including the three hydrogen tests undertaken as part of the original re-commissioning procedure. There were eight auto-ignitions observed at the higher temperature when testing mainly CO/H_2 mixtures. The highest pressure observed at the highest temperature was 2.236 barg with hydrogen alone at an EQR of 0.52. The nearest equivalent result with hydrogen at

the lower temperature was a peak pressure of 2.818 barg with an EQR of 0.45. Generally speaking, but not in every case, the lower temperature tests gave higher pressures than the equivalent high temperature tests.

There was one low temperature test with a CO/H₂ mixture which resulted in the mixture detonating and producing a maximum over-pressure of 18.228 barg. Not only did this test have a higher EQR but the lower initial temperature produced a more energetic explosion because of the higher fuel density. Although the laminar flame velocity was slightly higher (and the cell size smaller) at the higher temperature, the density ratio across the flame was higher than at the lower initial temperature. Consequently flame acceleration was promoted in the heat exchanger which governs the conditions in the highly turbulent unconfined downstream flow region where initiation took place.

The pressure and video records indicated that the peak pressures were generated around the highly turbulent heat exchanger region immediately downstream of the exit from the tube bank, where combustion intensity was greatest and with a pressure pulse width of around 5 msec. The propagation of the pressure pulse was observed within the geometry and gave rise to an approximate and temporary doubling in the region of the end plate due to reflections. Amplitude changes due to geometry changes within the HRSG system were also observed and had an effect on the maximum peak pressures. This was in line with observations from the previous test series.

The reactivities of the various mixtures, based on peak pressures and flame speeds, indicated that dilution of pure hydrogen with methane had a greater reactivity reduction effect than dilution with carbon monoxide, which again was consistent with previous findings.

Consistency in behaviour over an EQR range for the same mixture enabled a curve fit of peak pressure vs EQR to be generated for most of the cases studied and this enabled interpolation of results and a limited extension to a wider range of EQR values than those tested. It also allowed EQR values to be predicted for both high and low temperature tests that should ensure that the maximum pressures within the HRSG did not exceed some chosen value, in this case a value of 0.3 barg.

Acknowledgements

The authors wish to thank Paul Winstanley of the Energy Technologies Institute (ETI), together with their sponsors. We would also like to express our gratitude to Priyank Saxena of Solar Turbines and Gaby Ciccarelli for their continued support and technical advice throughout the project.

Acronyms

BoD	Basis of Design
CCGE	Combined Cycle Gas Engine
CCGT	Combined Cycle Gas Turbine
CFD	Computational Fluid Dynamics
CHP	Combined Heat and Power
CSV	Comma Separated Values
DDT	Deflagration to Detonation Transition
EQR	Equivalence Ratio
eStop	Emergency Stop
ETI	Energy Technologies Institute
FSO	Full-Scale Output
GDS	Gas Delivery System
HAZOP	Hazard and Operability Study
HE	Heat Exchanger
HRSG	Heat Recovery Steam Generator
HSE	Health and Safety Executive
IP	Ionisation Probe
LFL	Lower Flammable Limit
OP	Optical Probe
P&ID	Process and Instrumentation Diagram
PLC	Programmable Logic Controller
PT	Pressure Transducer
rpm	Revolutions per Minute
TDMS	LabVIEW Test Data Exchange Stream
WP	Work Package

Table of Contents

1	INTRODUCTION	7
1.1	Contractual requirements.....	7
1.2	Basis of previous WP 2.3 test programme.....	7
1.3	Objectives for Phase 2	8
1.3.1	Project value objectives	8
1.3.2	Phase 2 specific objectives.....	8
1.4	Rationale for Phase 2 programme extension	9
2	RIG SPECIFICATION.	10
2.1	Major components of the rig.....	10
2.2	Design specification for the test rig15.2	10
3	PHASE 2 TEST PROGRAMME	14
3.1	Description of the test rig	14
3.2	Description of the data logging and control system	14
3.3	Description of the instrumentation used.....	15
3.4	Phase 2 test programme.....	16
3.4.1	Additional testing at a lower temperature	18
4	RIG MODIFICATIONS FOR PHASE 2	21
4.1	Changes made to the butane supply system	21
4.2	Engine modifications.....	21
4.3	Modifications to the duct	21
4.4	Fuel and oxygen supply systems.....	21
4.5	Modifications to the HRSG and tube bank	22
4.6	Software changes.....	22
4.7	Instrument modifications	22
5	OPERATING PROCEDURES.....	24
6	RESULTS OBTAINED DURING RE-COMMISSIONING.....	26
6.1	Introduction	26
6.2	Re-commissioning tests	26
6.3	HYDROGEN-ONLY tests, with ignition.....	26
6.4	Implications of the results and auto-ignition issues	27
7	PRESENTATION OF RESULTS FROM PHASE 2.....	30
7.1	Introduction	30

7.2	Definition of Equivalence Ratio (EQR)	30
7.3	Results listings.....	31
7.4	Phase 2 Additional Information	35
7.5	Repeatability of test results	35
8	DISCUSSION OF RESULTS – COMMON FEATURES.....	37
8.1	General behaviour of flame and pressure pulses following ignition	37
9	ANALYSIS OF HIGH TEMPERATURE TESTS.....	44
9.1.1	Peak pressures obtained.....	44
10	ANALYSIS OF LOW TEMPERATURE TESTS	50
10.1	Peak pressures obtained.....	50
11	DISCUSSION OF PHASE 2 AND WP 2.3 RESULTS.....	55
11.1	Auto-ignition issues.....	55
11.2	Examination of the pressure generation zone for WP 2.3 and Phase 2 tests	58
11.2.1	The special case of Test 64.....	66
11.2.2	Graphical representation of pressure generation zone data at high temperature	69
11.2.3	Graphical comparisons of pressure generation zone data at high and low temperature for Phase 2	70
12	RIG DE-COMMISSIONING PROCEDURE.....	78
12.1	De-commissioning of the butane storage system	78
12.2	De-commissioning of the Viper gas turbine.....	78
12.3	De-commissioning of the test rig and HRSG	79
12.4	De-commissioning of the gas and oxygen delivery systems.....	79
12.5	De-commissioning of the instrumentation and data acquisition system	79
13	CONCLUSIONS.....	81
13.1	Evaluation of results overall.....	81
13.2	Safe operating modes for the fuel mixtures tested.....	81
13.3	Test rig performance.....	83
14	REFERENCES.....	84
15	APPENDICES.....	85
15.1	Position of Sensors on Experimental Rig	85
15.2	5S implementation details.....	87
15.3	Analysis of HRSG following Test 64.....	91

1 INTRODUCTION

1.1 CONTRACTUAL REQUIREMENTS

This report presents the results and final analysis of a test programme undertaken by the Science Division (SD) of the Health and Safety Executive (HSE) on behalf of the Energy Technologies Institute (ETI). The work utilised the existing heat recovery steam generator (HRSG) test rig with some minor modifications incorporated and was an extension to the original test programme. The work formed Phase 2 of the ETI funded High Hydrogen project, and was conducted under the terms and conditions of the ETI Contract Number PE03468, Schedule1, Part 1 – Project Outline, 2017.

1.2 BASIS OF PREVIOUS WP 2.3 TEST PROGRAMME

The test facility was designed to investigate, at reduced scale, the consequences of flame-outs within actual combined cycle gas turbines (CCGTs) when running on high hydrogen fuels and when such fuels passed through the turbine and into the exhaust system. In such circumstances the maximum hydrogen concentration in the downstream mixture could be as high as 10-12% v/v (when fuelled with pure hydrogen), and at temperatures as low as 157-177 °C (430 – 450 K) according to Solar. These conditions are dependent upon the exhaust composition and the degree of compression achieved in the gas turbine compressor. If ignition in the exhaust system was then assumed to occur, the project sought to assess the potential consequences, particularly the flame speeds and over-pressures that may be developed within the system by the combusting fuel/exhaust mixture.

The rig comprised a Rolls-Royce (R-R) Viper type 301 jet engine, which provided a hot vitiated airflow that exhausted through a nominal 600 mm diameter, 12 metres long duct. It should be noted that, for the purpose of any modelling undertaken, this vitiated air contains approximately 2.5% CO₂ and 3.7% H₂O by volume. Initially a series of experiments were carried out using only this duct, the results of which were reported in [1]. A further series of tests were undertaken with a scaled model heat exchanger attached to the end of the duct, representing a typical HRSG, in this case a GE 350 MW unit. The latter was attached to the exit of the duct and contained a simulated heat exchanger consisting of 15 rows of vertical finned heat exchanger (HE) tubes, giving an area blockage ratio of 48%. Fuel mixtures plus make-up oxygen were injected into the system near to the duct entrance and ignited by a high energy spark.

The test programme consisted of a series of experiments designed to measure the consequences of ignition of various fuel mixtures, at different concentrations, within the exhaust duct of the test rig. Two gas exhaust temperatures were utilised, the lowest temperature achievable with the test set-up being approximately 320 °C (593 K).

The WP 2.3 test programme had been undertaken with and without an end plate fitted to the HRSG and with an exhaust stack also fitted to the HRSG. The majority of the tests were videoed using a high-speed camera, viewing the flow after the tube bank through the end plate.

The dynamic pressures were measured using fast response Kulite pressure transducers, flame speeds were calculated from flame positioning measurements obtained using both optical and

ionising probes manufactured in-house. Gas temperatures were measured using 'K'- type 1.5 mm diameter thermocouples. The results from the WP 2.3 test programme were reported in [2].

The design and layout of the original test facility are also given in [1, 2], consequently only the implemented design changes made to meet the revised Phase 2 requirements are described in detail in this report.

1.3 OBJECTIVES FOR PHASE 2

This section covers all of the programme objectives.

1.3.1 Project value objectives

The overall project value objectives were to provide a more detailed evidence base for, and advance the state-of-the-art in, the safe and efficient operation of high hydrogen gas mixtures for energy production in order to enable the following outcomes:-

- Identify the bounds of safe design and operation of proposed high hydrogen systems to avoid unpredicted hazardous outcomes (limits of flammability, ignition and significant over-pressure potential (including DDT) in exhaust systems for a range of CHP/CCGT applications);
- Operate existing systems with more confidence within their bounds of safety in order to increase energy production and avoid unnecessary trips (for example, enabling gas engines to run at higher fuel/air ratios, or operating CCGT systems with higher trip set-points); and
- Identify specific limitations on validity, plus any further work required to increase confidence in the extrapolation process.

1.3.2 Phase 2 specific objectives.

The Phase 2 test programme objectives were based upon observations and analysis of the results from the previous WP 2.3 test programme.

The fundamental objective of the project was to further understand the impact of underlying physical processes on the behaviour of ignited flammable gas mixtures within the HRSG, by filling identified gaps in the knowledge base. This was to be achieved through extending the range of fuel mixtures and equivalence ratio (EQR) values tested. Consequently limited programmes of sensor and software upgrades were considered necessary in order to identify flame behaviour at lower EQR values than those used previously. The test programme was optimised to fill those key knowledge gaps identified in the WP 2.3 report. The whole of the test programme was undertaken with an end plate fitted to the HRSG and all of the tests were videoed using the high-speed camera system used in the previous phase of the project, together with a second camera viewing the approach flow to the HRSG tube bank from above.

A further objective was to consider the impact of rapidly decreasing exhaust temperatures, which recent information from Solar indicated could in practice fall very quickly to as low as 430 – 450 K following a flame-out. Ignitions at lower temperatures could increase the potential risk of DDT occurring with certain fuel mixtures, as was observed in [1] where the over-pressures developed were higher at lower temperatures as a consequence.

1.4 RATIONALE FOR PHASE 2 PROGRAMME EXTENSION

The rationale for an extended test programme followed from an examination of the results obtained from the tests completed previously by HSL [1, 2] and from the comments of the ETI reviewers. Collectively they identified several additional tests that would add value to understanding the underlying physical principles governing the flame-front behaviour following ignition, and its subsequent acceleration through the tube bank part of the heat recovery steam generator. These included tests at lower temperatures as previous tests had shown that such tests could generate higher pressures.

These additional tests extended the range of fuel mixtures tested and the range of equivalence ratio (EQR) values used, thus increasing the range of applicability of the data as well as filling in identifiable gaps in the existing data sets. There was, however, a fundamental difference between the WP 2.2 and WP 2.3 experiments; in the former the circular duct was filled with flame across its entire cross-section, whereas in the latter HRSG tests the flame entered the bottom of the HE section and spread upwards as it accelerated axially forward. Because of the vertical orientation of the HE tubes the flame propagation upwards was far slower than horizontally, where flame folding was considered to cause flame acceleration in this direction.

The rationale for undertaking further tests at lower temperatures also followed from the experimental flame-out tests undertaken by Solar, which had shown that there was an immediate fall in the turbine exhaust temperatures following flame-out. The temperatures can fall to as low as 157 °C (430 K) within a few milliseconds, consequently, and as shown from the limited number of lower temperature tests conducted as part of WP 2.2, there was an increase in the magnitude of the over-pressures generated following ignition. Further testing at reduced temperatures was therefore considered a necessity. The minimum temperature that was readily achieved with the current test arrangement was 320 °C (593 K).

As the test system was a one seventh scale representation of an actual CCGT the data sets could be used to aid the development and validation of the CFD explosion models currently being used to predict the consequences of flame-outs in operational CCGT systems, noting however, that the actual velocities through the test rig were the same as at full scale, and that the tube bundles were the actual size used in full scale systems. This velocity, tube spacing and dimension equivalence is important since these are the parameters which determine the turbulence generation within and immediately beyond the tube bundle rather than the overall chamber width and height. By developing the capability to model the consequences of flame-outs, operators seek to demonstrate confidence in their predictions as well as demonstrating to regulators the safety of their installations.

In summary the rationale for the proposed test programme was one of seeking to provide data sets that were a limited number of repeats of those undertaken in the WP 2.3 test programme together with an extension of the test envelope generally. In addition some of the mixtures used previously in the WP 2.2 low temperature tests were used again in a further series of low temperature tests. This approach provided as comprehensive coverage as possible of the fuel triangle ($H_2/CO/CH_4$) used to define the test envelope of interest.

2 RIG SPECIFICATION.

This section details the basic specification of the test rig.

2.1 MAJOR COMPONENTS OF THE RIG

The test rig comprises five major components/systems as follows:

1. Liquid butane storage tank and pumps for supply of liquid butane to run the engine.
2. R-R Viper Type 301 gas turbine, converted to run on liquid butane.
3. A 12 metre long by 0.6 metre diameter test duct. Comprising four 3 metre long sections bolted together, beginning with transition and diverter sections, and a removable turbulence generator. Attached to the end of the duct is an expansion section, a tube bank, end plate and an exit stack, all combining to form a scaled model of an actual HRSG. Note that this duct section does not exist in an actual gas turbine exhaust system and it is likely that its presence will add to the exhaust turbulence around the tube bundle region.
4. Fuel and oxygen supply systems, each comprising a reservoir, pressure regulator, Coriolis mass flow sensor, bursting disc, flow control valve and stop valves.
5. A central data acquisition and control system.

Changes/additions were made to all of the above items in order to meet the revised rig specification for the Phase 2 test programme. These are detailed in the following sections.

The complete rig as installed and attached to the existing WP 2.2 test rig is shown in the isometric drawing in Figure 1. An engineering drawing of the duct section is shown in Figure 2, the HRSG section is shown in Figure 3 and the heat exchanger tube bank in Figure 4. The end plate shown in Figure 3 was permanently attached for the Phase 2 test programme. A workplace business improvement process, known as 5S, was also conducted in order to improve the appearance, efficiency and functioning of the test rig and surrounding areas. This has resulted in a tidying up of the sensor cabling, together with a more logical numbering scheme for the sensors. Further details regarding implementation of the 5S process are given in Appendix 15.2.

2.2 DESIGN SPECIFICATION FOR THE TEST RIG

The design specification for the rig is given below. As well as specifying the parameters to be measured it also gives the accuracy/tolerances to which the intended measurements were made. These were the acceptance criteria used to certify that the rig was fit-for-purpose.

Design specification for WP 2.3 and Phase 2:

- Engine mass flow rates 15 kg/s to 5 kg/s as a function of engine rpm. Accuracy to be within $\pm 2\%$ of the required full scale output (FSO) value.
- Control of mass flow rates through diverter section to give velocities along the test duct of between 50 – 90 m/s (maximum mass flow rate ≈ 11 kg/s). Accuracy to within $\pm 2\%$ of the required FSO value.
- Operating temperatures in the duct (before addition of fuel and oxygen) within the range 320 to 550 °C. Accuracy to within $\pm 2\%$ of the required values.

- Capability of injecting oxygen sufficient to restore levels to 21% in the exhaust stream when operating at 15 kg/s. This is equivalent to a maximum oxygen mass flow rate of 1.12 kg/s. Accuracy to be within $\pm 2\%$ of the required FSO value.
- The fuel mixtures to comprise mixtures of hydrogen, methane, and carbon monoxide, or each gas individually, up to maximum mass flow rates of 0.2 kg/s, 1.57 kg/s and 2.74 kg/s for the three gases respectively.
- Capability of injecting fuel mixtures up to 15% by volume at the maximum mass flow rates. Accuracy to be within $\pm 2\%$ of the FSO values for the three gases.
- Measurements of exhaust gas oxygen levels. Measurements to the specified accuracy of the instrument after calibration. (A Servomex gas analyser Type: Mini MP 5200 was used.)
- Pitot-static probe measurements of the velocity and temperature profiles across the circular duct. Accuracy to be within the stated tolerances for the instruments used.
- Measurements of both the static pressures and temperatures along the duct during testing. These to be measured to within the stated tolerances of the instruments used namely, Kulite pressure sensors (0.5% of FSO) and K type thermocouples.
- Data logging and processing system. Resolution to 16 bit or better, maximum sampling rates 1 MHz, but typically 100 KHz.

NB: Complete specifications, including calibration procedures, for all of the types of instrumentation used during commissioning and on the test rig are given in the WP 2.2 and 2.3 commissioning reports [3, 4].

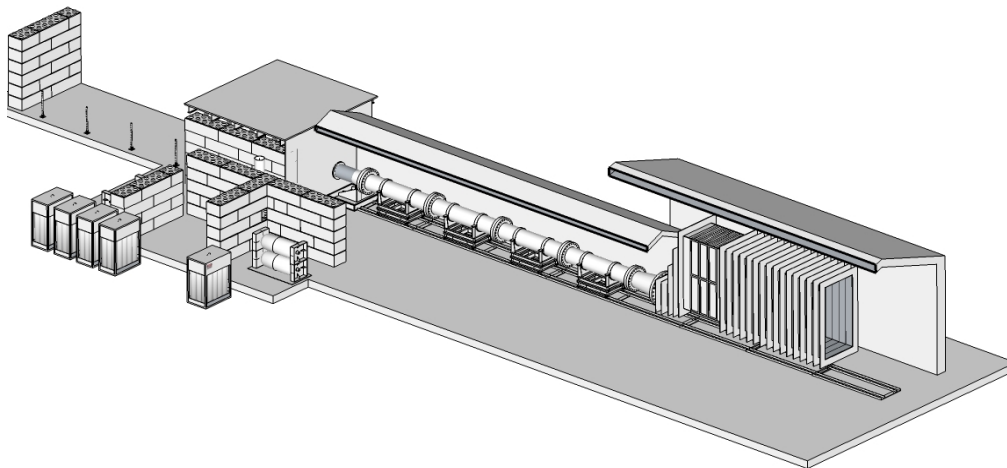


Figure 1 Isometric sketch showing physical layout of the ETI rig with HRSG extension.

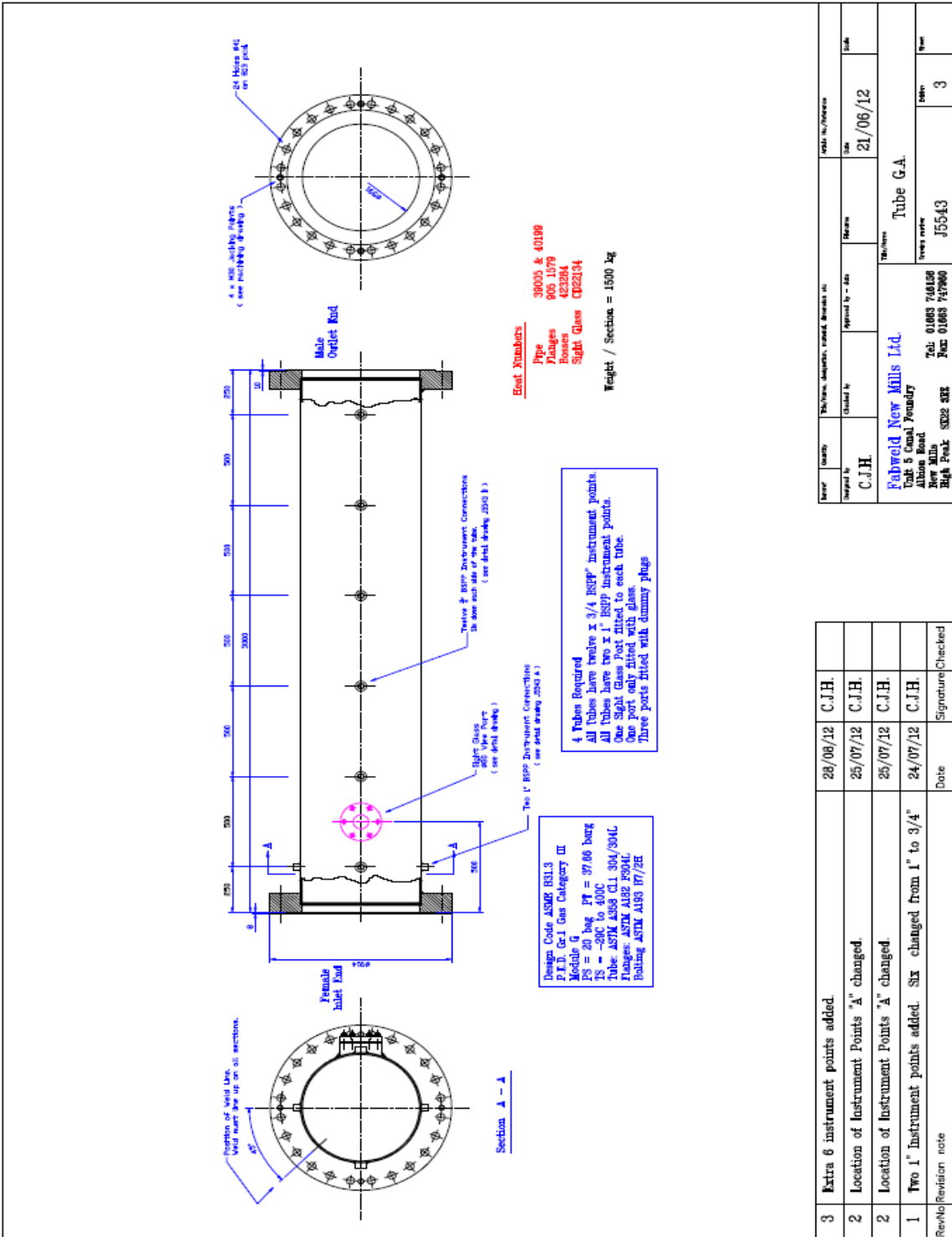


Figure 2 Circular duct engineering drawing.

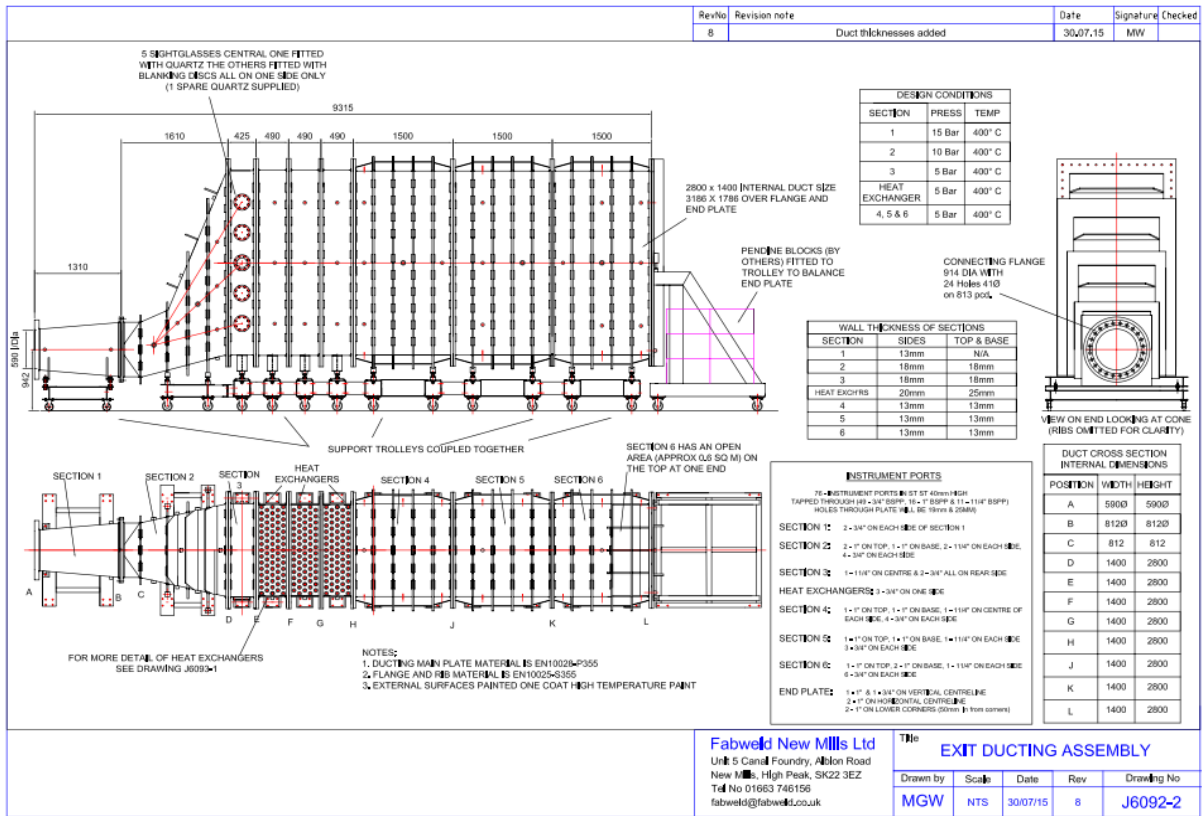


Figure 3 HRSG layout: schematic.

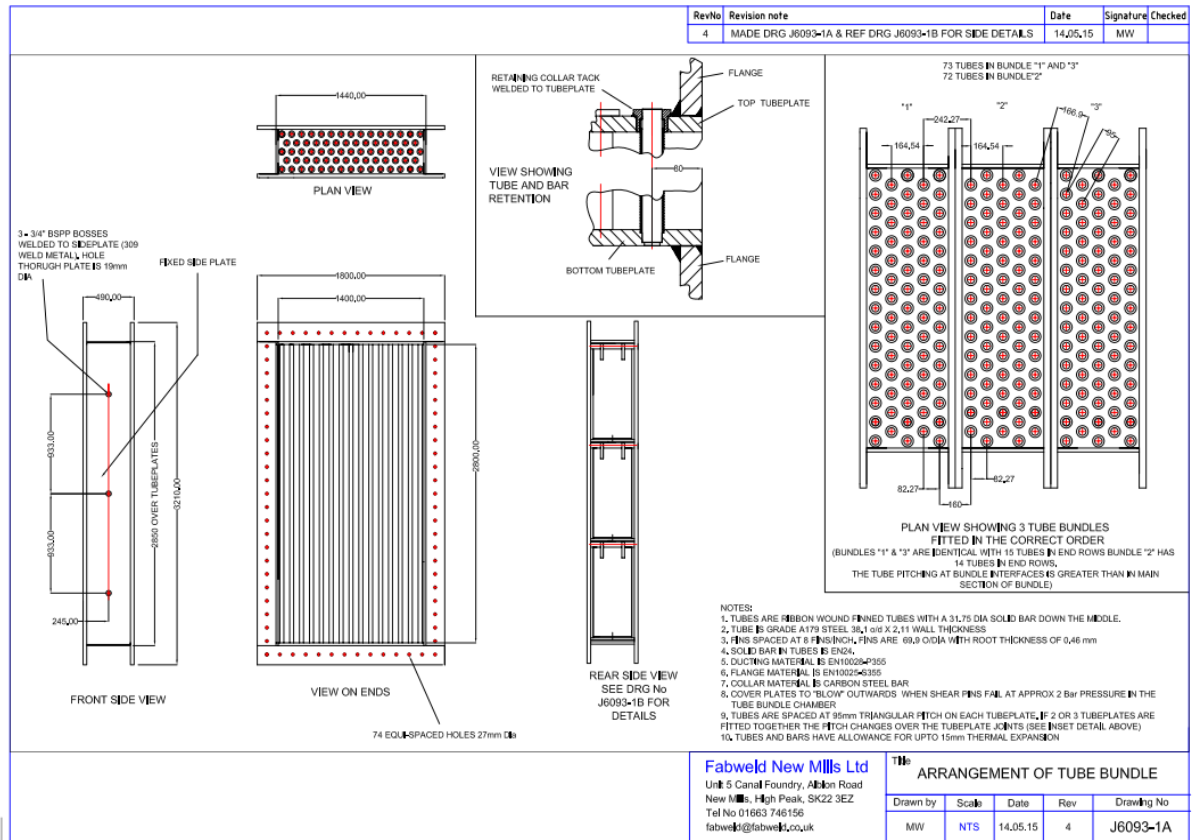


Figure 4 HRSG Tube Bank.

3 PHASE 2 TEST PROGRAMME

This section provides details of the test rig and test programme that forms the basis of this report. It also gives the rationale for the changes made to the sensors and their locations.

3.1 DESCRIPTION OF THE TEST RIG

The completed rig represented an approximately 1/7th scale model of an actual GE design of CCGT, as discussed in the Basis of design (BoD) report [5]. However, the velocities through the unit were not scaled and were the actual velocities that occurred in the full-size unit. In summary it comprised the WP 2.2 rig with the HRSG forming the WP 2.3 rig attached to the end of it. The key components were the R-R Viper 301 gas turbine, a convergent/divergent nozzle, a diverter section, an orifice plate, a transition section that contained the oxygen and fuel injection tubes, a turbulence generator, and a duct comprising four 3 metre long sections with a diameter of 600 mm. Attached to the end of the last section of duct was an expansion section that converted the circular profile of the duct to a rectangular profile as it entered the tube bank of the HRSG. The tube bank itself was made up of three separate sets of tubes, each containing 73 or 72 finned tubes, a total of 218 tubes as shown in Figure 4. The area blockage ratio of a fifteen tube row was about 48% when the finning was included, and 40% without it. After the tube bundle there was a 4.5 metre long constant area section of duct that for the Phase 2 work package was fitted with an end plate. There was a rectangular opening in the top at the end of the sixth section of the HRSG, the cross-sectional area of which increased the velocity of the exhaust gases to about 40 m/s. A stack was attached to this opening to take the outflow through the roof of the building.

A pitot-static probe was situated 500 mm along from the beginning of the fourth duct section, which could be traversed across the full width of the duct to obtain velocity and temperature profiles. There was a vertically oriented spark ignition system 250 mm along from the beginning of the second duct section.

3.2 DESCRIPTION OF THE DATA LOGGING AND CONTROL SYSTEM

The data logging and control system comprised two programmable logic controllers (PLC) systems and one programmable extended interface (PXI) system, and remained the same basic set-up-used for WP 2.2. The first PLC system was responsible for controlling the engine and for recording all engine-related parameters. It was also responsible for the safe operation of the engine and therefore had built-in logic and controls that determined in what sequence valves were activated. It also shut the engine down if any of the monitored parameters exceeded set limits. The PLC communicated with a PC located in the control room that ran the user interface and recorded, on disc, all monitored parameters at a rate of 10 Hz. Emergency stops were provided on the engine frame and in the control room which were used to shut down the engine in case of an emergency. The PLC also monitored all Estops so that it did not allow the engine to be restarted until any triggered Estops had been reset.

The second PLC unit was responsible for controlling the gas delivery system and for recording all process parameters also at a rate of 10 Hz. This system recorded the engine speed signal (the same signal that the engine control PLC was recording). This could be used to synchronise (to within 0.1 seconds) the recorded parameters of the gas delivery system with the data recorded by the

engine control system. The gas delivery system PLC communicated with a PC located in the control room that featured the user interface and also recorded all process parameters onto disc. The gas delivery system also provided digital trigger signals to the high speed data acquisition system to initiate high speed (up to 1 MHz) recording of the rig data.

The engine control PLC system started monitoring the engine speed, fuel flow and fuel supply pressure to the engine when it was on condition for an ignition test. The PLC then recorded the current parameters, taking a 5 second average. If any one of these three parameters dropped by a predefined percentage the PLC initiated software activated the Estop(s). The predefined percentage values were read from an initialisation file so that they could be altered without needing to carry out changes to the software. The software, when initiated by the Estop(s) also sent a signal to the gas delivery system PLC, which shut down the fuel and oxygen flow to the rig. When the engine user interface signalled to the engine PLC that the test was completed it stopped monitoring the three parameters and the system then operated as before. The engine user interface included a button that was activated by the operator when the test condition was reached; this notified the PLC system to start monitoring the parameters mentioned above. When this button was deactivated a signal was transmitted to the engine PLC to stop monitoring these parameters so that it would not activate the software Estop(s).

The PXI system was PC based and recorded, at high speed, the data from the experimental work being carried out. This system recorded all the experimental parameters; it also contained the software used for data processing.

3.3 DESCRIPTION OF THE INSTRUMENTATION USED

The instrumentation attached to the rig comprised thermocouples, pressure transducers and optical sensors, the latter being both flame ionisation and photodiode based sensors. The revised locations and numbering for all of the sensors are shown in Figure A1 to Figure A6 in Appendix 15.1, at the end of this report. In summary there were up to twenty-four flame ionisation sensors (IP's) positioned on the rig, together with twelve optical sensors (OP's). There were also four rakes (RA's) each containing three ionisation probes, these were fitted horizontally across the rig at the positions indicated in Figure . There were eleven Kulite pressure transducers (KU's) on the rig, four to measure pressure and wave speeds upstream of the tube bank, with the rest either in the tube bank or downstream of it, to make similar measurements. Two Kulite sensors were near to the end wall of the HRSG to measure the rise in pressure from a pressure wave impacting it and being reflected back upstream. There was a sampling probe upstream of the tube bank that was used for gas sampling but during testing it was connected to a Servomex oxygen gas analyser.

An examination of the data obtained from the optical probes placed downstream of the tube bank in the HRSG WP 2.3 test programme revealed that the responses of those furthest downstream after the tube bank were often poorly defined. This was considered the result of two potential issues; firstly, weaker flame strength, and secondly the low signal to noise ratios of some of the sensors. The latter was dealt with through modifications to the sensor design. The former was dealt with through a re-positioning of many of these sensors to locations nearer the exit of the tube bank, especially to positions lower down in the HRSG where the flame initially emerges from the tube bank. As a consequence the IPs, OPs and PTs were renumbered in a more logical sequence. The thermocouples measuring gas temperatures were also replaced with more responsive 0.8 mm

diameter units. In total there were nineteen thermocouples, four of which were the existing surface temperature measuring ones (TC1, TC3, TC5 and TC7); these are not shown in Figure A2 in Appendix 15.1. The thermocouples were also renumbered in a more logical sequence.

3.4 PHASE 2 TEST PROGRAMME

The test conditions carried over to Phase 2 from the previous WP 2.3 test programme were that the mass flow rate remained at around 9.2 kg/s, the centre-line exhaust temperature, as measured by the pitot-static probe in section four of the duct, remained at around 500-550 °C (773 - 823 K), and the corresponding centre-line velocity (as measured by the pitot-static probe) near the end of the duct and before entering the HRSG was 85 m/s. Note that the average velocity across the whole of the duct, when calculated from the mass flow rate and temperature was typically 75 m/s.

The HRSG data collected as part of WP 2.3 was obtained for relatively high EQRs, producing peak pressures of the order of 0.5 barg or higher. These values were significantly higher than the overpressures that actual gas turbine exhaust systems can tolerate. With this in mind further testing included tests at lower EQRs producing peak pressures below 0.5 barg. The additional data, along with the existing data would allow for better determination of the peak pressure vs EQR data trend, and perhaps could also be used to define maximum EQR values for the different fuels.

During the re-commissioning programme it was intended to undertake six tests, four of which were to be repeats of tests undertaken previously as part of WP 2.3. By re-running these four tests repeatability could be assessed as well as comparing the improved sensor capability with the previous set-up. The commissioning tests were in addition to the proposed revised test matrix and are shown in Table 1 below, which also shows the proposed additional tests to be undertaken as part of the Phase 2 test programme. The test programme [6], as originally proposed had the three H₂ tests, now labelled as test 3, as the intended commissioning tests and originally labelled as test 0. However following the re-commissioning programme [7] the order of testing was changed to that now shown in in Table 1. This was done in order to minimise the risk of further auto-ignitions by undertaking what were now considered the most benign of the tests first.

An important feature that can be assessed from the WP 2.2 and WP 2.3 test programmes was the transition from 1-D axisymmetric to 3-D flow, as well as any relevant scaling effects. With this in mind there was a gap in the WP 2.3 test programme as (60/40: CH₄/H₂) mixtures were not tested and logically they should be, together with the ternary mixtures (25/35/40: CH₄/CO/H₂) that was also tested in the WP 2.2 test programme, but not in the WP 2.3 programme. Also, industry uses natural gas as its primary fuel as well as for testing their systems; therefore a series of 100% CH₄ tests were included in the revised test programme for comparison with the WP 2.2 test programme. In addition it was agreed that further tests would be undertaken with both (40/60: CH₄/H₂) and (60/40: CO/H₂) mixtures in order to extend the range of EQRs tested for these two mixtures.

It is also our understanding that industry interest in using various types of syngas for fuelling and operating CCGT systems in the future remains high. This is also borne out by a general review of the power generation literature where syngas mixtures are frequently mentioned in connection with fuelling combined cycle systems running on either gas turbines or gas reciprocating engines. Syngas is a mixture of mainly carbon monoxide and hydrogen which is the product of steam or

oxygen gasification of organic material such as biomass, and is the term generally used for such mixtures of combustible gases.

Table 1 Proposed test matrix for high temperature tests.

Test Mixture	Fuel composition	Closed ¹ EQR	Closed EQR	Closed EQR	Comments
0	40/60% CH ₄ /H ₂	0.40	0.50	0.65*	Extends range & Includes repeat of WP 2.3 Test HRSG8.
1	60/40% CH ₄ /H ₂	0.50	0.60	0.70	Previously tested in WP 2.2 only.
2	100%CH ₄	0.50	0.65	0.80	Previously tested in WP 2.2 only.
3	100% H ₂	0.47	0.51	0.55*	Includes repeat of WP 2.3 Test HRSG 12.
4	100% H ₂	0.35	0.43	0.55*	Includes a second repeat of WP 2.3 Test HRSG12.
5	25/35/40 CH ₄ /CO/H ₂	0.45	0.50	0.60	Previously tested in WP 2.2 only.
6	40/60% CO/H ₂	0.40	0.50	0.60	Extends range as not tested in WP 2.3.
7	60/40% CO/H ₂	0.45	0.51*	0.60	Extends range & Includes repeat of WP 2.3 Test HRSG13.

NB: Temperature at the pitot-static probe, before injection of oxygen and fuel, to be in the range 550-510 °C (823 K) for all of the tests shown in a green background.

* Indicates repeated test from the WP 2.3 test programme.

¹ Indicates that tests marked 'closed' will be done with the end plate in position.

Typically, syngas generated at low <800°C temperatures and will contain hydrogen, carbon monoxide, carbon dioxide with potentially small quantities of methane and other hydrocarbons. However, gas generated by gasification at <800°C will have the same basic constituent but the methane content may be up to 20%. All syngas contains a level of nitrogen as this is the blanket gas used for safety and in air blown gasification there is a significant amount of nitrogen. If the gasification product contains significant amounts of non-combustible gases such as nitrogen and carbon dioxide, the term used for such mixtures is 'Producer Gas'.

As Syngas may also contain a small amount of methane, the ternary mixture already proposed together with some of the CO/H₂ mixtures can be considered as representative of Syngas. It was therefore proposed to include one further CO/H₂ mixture in the test programme, namely (40/60: CO/H₂) in order to better represent the range of syngas compositions of future interest, as well as extending the empirical modelling capability. Further justification for including this mixture comes from the highly reactive nature of hydrogen/carbon monoxide mixtures already tested, and the need to better understand their behaviour.

Another important reason for extending the test programme was the clearly identified need to provide data sets that could be used to validate CFD models, which would also enable academic studies to better understand the fundamental fluid mechanics governing the observed behaviour. Industry also needs this data to validate the CFD-based explosion modelling codes, and to predict the consequences for a range of operational scenarios.

3.4.1 Additional testing at a lower temperature

The exhaust temperature of an unburned fuel/air mixture is known to influence the extent of the pressure rise following an ignition event. A lower temperature corresponds to higher density, and thus more available energy per unit volume. Also important is that the density ratio across the flame is higher at lower initial temperature and thus more prone to flame acceleration. This can be partially offset by a lower laminar burning velocity at lower temperatures. Most of the testing (WP 2.2) in the circular duct rig was carried out at a nominal temperature of around 550 °C (823 K), with a small number of tests being done at the lower temperature of 350 °C (623 K). The latter tests did show that for the same test conditions the lower temperature tests produced a significantly higher peak pressure than did the corresponding higher temperature ones. Evidence from some limited engine testing at Solar Turbines also indicated that the initial temperature in a flame-out situation would be lower than the lowest temperature used previously in WP 2.2 and were therefore likely to result in even higher pressure rises than those obtained from the WP 2.2 test programme when comparing gas mixtures and EQR's.

It is therefore important to explore temperature effects further. To this end, the specific tests conducted by Solar Turbines with special rakes and fast acting thermocouples have better characterised the temperature history during a flame-out from different engine loads. This data has been provided to the ETI to support further work in this area. It showed that the exhaust temperatures may fall to as low as 157 °C (430 K) within a matter of milliseconds following a flame-out.

However, in an actual flame-out the mass flow will slowly decay as the engine spools down, but in the context of the timescale for ignition of fuel carried over into the exhaust it effectively remains constant. A lower gas temperature due to non-combustion then suggests that a higher gas density

and a lower velocity will result from the need to maintain continuity. Thus under constant mass flow conditions of 9.2 kg/s the velocity will fall to about 55 m/s when the exhaust temperature is 320 °C (593 K), and the average velocity across the HRSG exit plane will be 4 m/s. This temperature is the lowest that can be obtained with the current set-up.

Table 2 Proposed test matrix for low temperature tests.

Test Mixture	Fuel composition	Closed ¹ EQR	Closed EQR	Closed EQR	Comments
1	40/60% CH ₄ /H ₂	0.40**	0.50**	0.58**	Extends range tested.
2	60/40% CH ₄ /H ₂	0.50	0.60	0.70	Previously tested in WP 2.2 only.
3	100%CH ₄	0.50	0.65	0.80	Previously tested in WP 2.2 only.
4	100% H ₂	0.35**	0.45**	0.50**	Extends range tested.
5	25/35/40 CH ₄ /CO/H ₂	0.45	0.50	0.60	Previously tested in WP 2.2 only.
6	40/60% CO/H ₂	0.40	0.50	0.60	Extends range as not tested in WP 2.3.
7	60/40% CO/H ₂	0.45	0.51**	0.60	Previously tested in WP 2.2 only.

NB: Temperature at the pitot-static probe, before injection of oxygen and fuel, to be approximately 320 °C (593 K) for all of the tests shown in a green background.

¹ Indicates that tests marked closed will be done with the end plate in position.

++ Indicates repeat of low temperature WP 2.2 test.

The Phase 2 test programme at a lower temperature has therefore sought to provide data sets that were repeats of those undertaken in the higher temperature tests proposed in Table 2 above, which includes testing some of the mixtures used previously in the WP 2.2 low temperature tests. This provides as comprehensive coverage as possible of the fuel triangle when extended to the lower temperature. In view of the interest in using ternary mixtures to represent syngas fuels a low temperature test is included using the same ternary mixture proposed in Table 1. The proposed test matrix for the low temperature tests is shown in Table 2, noting that the same constant mass flow rate will be used as that for the higher temperature.

The temperatures quoted are the average centre-line values measured in the fourth section of the duct, by a thermocouple attached to the pitot-static probe. It is important to note that the temperatures measured are the exhaust temperatures prior to any oxygen or fuel injection. Injection of these gases reduces the resulting temperature of the vitiated air. Whilst the flowrate of oxygen is constant for any particular engine running condition (i.e. rpm) the amount the temperature is reduced will depend on the rate of fuel addition. These temperature reductions are not reliably measured within the experiments since the data recording begins with the fuel injection and duct thermocouples may not have fully equilibrated with the exhaust flow before ignition takes place. The most secure method of estimating the reduction for each case is to carry out an energy balance using the known mass flows and measured centreline temperature, which is performed after testing with exhaust flow alone. An example for the case of Test 32 is given below.

The Test 32 parameters are as follows:

O₂ flow rate = 0.539 kg/s

Exhaust flow rate = 9.14 kg/s

CH₄ flow rate = 0.261 kg/s

Centreline exhaust temp = 540 °C

O₂ and fuel cold temps ~ 10 °C

O₂ and exhaust Cp values, i.e. Cp(air) = 1000 J/kg/K

CH₄ Cp value = 2231 J/kg/K

An energy balance takes the following form:

$$\begin{aligned} & \text{O}_2\text{mass} \times (T_{\text{final}} - T_{\text{ref}}) \times \text{Cp}(\text{air}) + \text{CH}_4\text{mass} \times (T_{\text{final}} - T_{\text{ref}}) \times \text{Cp}(\text{CH}_4) + \text{exhaust} \times (T_{\text{final}} - T_{\text{ref}}) \times \text{Cp}(\text{air}) \\ = & \text{O}_2\text{mass} \times (T_{\text{cold}} - T_{\text{ref}}) \times \text{Cp}(\text{air}) + \text{CH}_4\text{mass} \times (T_{\text{cold}} - T_{\text{ref}}) \times \text{Cp}(\text{CH}_4) + \text{exhaust} \times (T_{\text{hot}} - T_{\text{ref}}) \times \text{Cp}(\text{air}) \end{aligned}$$

Applying the test values gives a final temperature (T_{final}) of 482 °C. This represents a change of **-58 °C**, based on the centreline value. Of this reduction around 30 °C is due to the oxygen injection alone.

4 RIG MODIFICATIONS FOR PHASE 2

This section of the report details the necessary changes made to the rig to ensure that a satisfactory mode of operation was achieved together with an acceptable set of operating parameters for the Phase 2 test programme. The changes were in addition to those made previously when the rig plus the HRSG were first commissioned for the WP 2.3 work package. Changes have been made to all five major items of the rig listed in Section 2, as discussed in the following sub-sections.

4.1 CHANGES MADE TO THE BUTANE SUPPLY SYSTEM

In order to comply with the UKLPG code of practice 22, the existing pipework was replaced with thicker walled tubing (schedule 80), and several right-angled bends were removed. The butane tank was also raised and anchored to the ground at one end. This work was undertaken by companies certified to undertake LPG installations, including pipework. The contents of the butane storage tank were decanted into another suitable vessel during the pipework replacement process. The latter was necessary as the outlet valve on the existing tank was replaced with one rated for a higher flow. A certified company was also used to pressure test and certify the final installation, which was completed in January 2018.

4.2 ENGINE MODIFICATIONS

There were no changes made to the engine other than checking the oil level and ensuring that there were no leaks on the butane supply line from the high pressure control pump. The high-pressure pump itself was re-installed after having been serviced and repaired. The inverter that runs the engine pump was replaced with a new one, which was re-housed in the control room end of the spray booth building to shelter it from the elements. The engine was re-commissioned during January/February 2018. During April 2018 the starter motor relay began sticking and had to be repaired and eventually replaced with a new one in June 2018.

4.3 MODIFICATIONS TO THE DUCT

No changes were made to the duct other than the re-positioning of several sensors. The cabling to the sensors was streamlined to meet the 5S requirements. The replacement Servomex oxygen gas analyser was also installed in the fourth duct section, downstream of the pitot-static probe used for measuring velocities and temperatures across the duct. The duct ignition system was also checked for correct operation.

Both the optical and ionisation probes were re-designed in an attempt to improve their signal to noise ratios, as also were the four rakes. High frequency noise was filtered out from these types of sensors after it was discovered that the HRSG itself appeared to be acting as an aerial.

4.4 FUEL AND OXYGEN SUPPLY SYSTEMS

This system was commissioned previously as part of WP 2.3, which included some changes at the time to the pipework and flow control system to enable it to cope with the higher flow rates required for that work. Practical experience of operating the system led to the installation, immediately downstream of the Hale-Hamilton (H-H) pressure regulator, of a bursting disc with a higher rating (70 bar) than used previously. Consequently the pipework downstream of the pressure regulator was replaced with new larger diameter pipework, which had a higher pressure rating, in

order to comply with the Pressure System Safety Regulations (2000). No further changes were made other than to install upgraded control software and to check the integrity of the revised installation, including leak and operational testing.

4.5 MODIFICATIONS TO THE HRSG AND TUBE BANK

The main changes made to the HRSG were the addition of several more sensor ports, as it was agreed that most of the sensors would be re-positioned around the entry and exit areas of the tube bank. The revised sensor positions are shown in Figure A1 to Figure A6 in Appendix 15.1 of the report as described in the previous section. An additional viewing port for a second high speed camera was also added to the sloping entry section of the HRSG. It was also agreed that the same sensor positions would be used throughout the Phase 2 test programme. This allowed the wiring to be streamlined and incorporated into the 5S improvement package.

When the tube bank was examined after completion of the WP 2.3 work package, it was noted that the fins on the first four to five rows of tubes had melted due to the high temperatures they had been exposed to for a period of several seconds following ignition of the test fuels. These were replaced with new finned tubing of the same dimensions as used previously.

4.6 SOFTWARE CHANGES

Improvements to the engine control software involved changes to those items greyed out on the control panel during different modes of operation. This was to provide more precise control of several key operating parameters by enabling them to be set individually. For example, the speed of the butane control pump cannot now be adjusted until the engine start button has been pressed, and if an Estop(s) happens before the fuel supply set-point is reached, the pump cannot now be reduced to the level required for an engine restart.

The logic controlling pressurisation of the Hale-Hamilton dome loader was modified so that over-pressurising of the bursting disk protecting the system downstream of it cannot now happen as a result of not following the correct operating sequence.

A control sequence was added to start data logging on the gas delivery system (GDS) PC once oxygen flow was initiated, as in some cases the operator could forget to initiate data logging. This improvement removed that possibility. Control logic changes were also added so that when the mixed gas flow was initiated the fast data acquisition was triggered at the same time. The filename is now displayed on the screen whereas previously it was hidden.

Changes were also made to how PID parameters are communicated from the control room PC to the GDS PC. The default experiment time was also changed from 1200 seconds to a more realistic value (30 seconds) and the default PID parameters were changed to those most commonly used.

4.7 INSTRUMENT MODIFICATIONS

A number of changes were made to the existing instrumentation to address some of the difficulties which were identified within the WP 2.3 work. There were 24 individual flame ionisation sensors (IP's) and 12 flame ionisation sensors arranged in groups of three within four tubular 'rake' geometries (RA's). The IP's were located originally on the surface of the rig at various positions and had protruded around 25 mm into the chamber, whilst the RA sensors were located within the HRSG

and across its width. The RA sensors have kept their original geometry, but the bead insulation has been replaced with ceramic tubing to provide better electrical insulation, high frequency filters have also been fitted. The IP's were lengthened to provide an insertion depth of around 80 mm at each location. The reasoning behind this change was that it was considered that some of the previous flame propagation indication was being lost due to boundary layer effects as a result of the proximity of the sensor tips to the wall.

A further issue with the behaviour of the IPs, RAs, and also the optical sensors (OPs) was the interference between sensors due to the common battery power supply powering the devices. A significant modification has therefore been the provision of each sensor with its own battery power supply making it fully independent. This has resulted in the provision of a wall-mounted 'battery box' providing an individual 6 V supply to each sensor, as well as modifications to the circuitry within each sensor body to enable it to operate with this lower supply voltage. For the IPs and RAs, flame arrival is identified with the instantaneous positive rise of the quiescent signal above its baseline. For these, the quiescent 'no flame' level is around 1.2 V. The OP sensor outputs were previously AC coupled to their op amps and the choice of circuit elements resulted in a derivative signal when a flame passed the collection lens, meaning that the flame-front could be associated with the maximum of the derivative signal. For the present circuit arrangement, the AC coupling capacitor has been increased in size meaning that it effectively acts as a short circuit to changes in input voltage. For the Phase 2 work therefore, flame arrival is associated with a positive rise of the signal from the zero voltage baseline.

There are a number of thermocouples (TC's) around the test rig; previously these were of 1.5 mm diameter. The response of these was too slow to be considered useful for the transient combustion following ignition and it was decided to replace these with 0.8 mm diameter ones. These have a shorter time response and can give some additional useful information on flame passage.

The WP 2.3 work employed a downstream high-speed colour video camera which viewed the exit plane of the HRSG tube bank through a window located on the end plate of the HRSG. In this way flame emergence and progress could be monitored and this camera provided some very useful data and enabled good insights into the dynamics of the flame around the turbulent region downstream of the tube bank. For the Phase 2 work, an additional black and white (BW) video camera has been added to the top surface of the expansion section upstream of the tube bank and looking toward the tube bank. This was planned to provide additional flame propagation information as the flame emerged from the circular duct toward the HRSG. As the results will show, this camera has also provided special insights and understanding not previously observed (i.e., Auto-ignitions). The framing rate for both the downstream colour camera and the upstream BW camera was nominally 2500/sec.

5 OPERATING PROCEDURES

The operating procedures followed those used previously and are summarised below:-

- On the designated test day, checks were made to ensure correct functioning of all the required instrumentation.
- The test gas mixture required was then made up by filling the gas reservoir with the lightest gas first then adding the next heavier component(s). The correct gas mixture ratio was obtained using partial pressures. When a toxic gas was being used any person approaching and opening the toxic gas bottle filling valve was required to wear BA. The gas mixtures were thoroughly mixed by recirculating through the Haskel gas pump for a minimum of one hour.
- The liquid butane, which fuelled the Viper gas turbine, was also recirculated through the butane supply system at approximately the same time.
- The engine control software and the data logging system were readied for operation.
- The appointed Trials Officer then placed lookouts at chosen points on the exclusion zone boundary. They were in radio contact.
- Given the all clear, the gas turbine was started and run up to the required operating speed.
- After a period of no more than two minutes, during which time the exhaust gas temperature stabilised and a series of safety checks were completed, the siren was sounded and then the actual test proceeded. For each test a target EQR was set and the required fuel mass flow rate calculated and entered into the control system parameters.
- Sufficient oxygen was then injected to restore the level in the exhaust stream to 21%. This was followed by injection of the required fuel such that the rate of injection built up to the test EQR. The points of injection into the exhaust stream were downstream of the engine turbine. This procedure reduced the exhaust stream temperature by approximately 40 -50 °C, as the oxygen and fuel were at ambient temperature prior to injection. Sufficient time after reaching the desired EQR value was allowed before ignition to ensure that the whole of the test rig was filled with the flammable mixture.
- The flammable gas/oxygen mixture injection process lasted for no more than 10 - 20 seconds, during which time ignition of the mixture was undertaken using the electrical spark situated axially downstream of the fuel injection point. This also started the data recording process. Immediately after ignition the fuel and oxygen supplies were automatically stopped by the controlling software.
- If an ignition occurred the engine was slowed down and a check made of the data obtained. It was stored and backed up for analysis later.

During the test the duct walls were heated up but at no point in the test did they reach thermal equilibrium. However, the exhaust gas heat losses to the duct walls were minimal. As an example for the duct exhaust temperatures in Test 23, at the position for TC0 (1253mm) the exhaust temperature is 452 °C and for TC6 (10258mm) is 428 °C. Note also that the wall and near wall gas temperatures were recorded throughout the test period.

After completion of testing for a day, (usually after completing two or three tests with the same fuel mixture) the dynamic pressure and static temperature profiles were measured across the diameter of the duct, using the pitot-static probe and attached thermocouple. The engine was run at the

appropriate rpm. This information was used retrospectively to calculate the exhaust mass flow rates, to check the injected mass flow rates of oxygen and fuel mixture and to update the EQR values for the particular tests to which the measurements were applicable. The re-calculated EQR value was the value quoted for each test.

The exhaust oxygen concentration was monitored using a Servomex gas analyser and this provided repeatable values at the agreed running conditions. This resulted in an oxygen make-up injection rate of between 0.48 – 0.52 kg/s depending on test requirements. Note that a deviation from this injection rate of $\pm 4\%$ results in a deviation in the exhaust oxygen level from 20.85 to 21.15%.

The composition of the engine exhaust gas has been reported in the commissioning report (4) and these values were used to calculate the molecular weight of exhaust gas, both for fuel injection calculations and sound speed estimations when required. The molar percent values used for the engine exhaust were as follows: N₂ 76.46, O₂ 16.50, H₂O 3.72, CO₂ 2.47, and Ar 0.88. The input values to this calculation were based on the user's choice for the particular test being run. For example, the fuel mixture composition was input as the mole fractions of each gas in the mixture already prepared and the oxygen mole fraction in the exhaust was measured separately with the engine running at the normal operating condition. The exhaust mass flow rate was calculated separately as previously discussed.

As had been the case for the WP 2.3 tests the recording system was triggered to start recording by the ignition spark and it was terminated by the closing of the mixture supply valve. During the WP 2.3 set of tests using carbon monoxide it was observed that auto-ignitions had occurred shortly after commencing the fuel mixture injection process and before the ignition system had been triggered. As a consequence the data recording system had not recorded the event. A modification was therefore made to the software controlling the data recording system which allowed the recording system to be started manually. This was used for the carbon monoxide based tests reported herein. It resulted initially in larger data files but these were clipped to contain only the relevant data prior to being issued.

6 RESULTS OBTAINED DURING RE-COMMISSIONING

6.1 INTRODUCTION

This section describes the tests carried out during re-commissioning together with the results obtained from the hydrogen fuelled re-commissioning tests, the details are reported in [7].

Towards completion of the WP2.3 test programme an auto-ignition occurred during test 14. The fuel was a CO/H₂ mixture and this was the second test utilising CO/H₂. A longer than normal heat-up time had occurred as a pitot-static traverse had been undertaken prior to testing. The auto-ignition resulted in burning of the fuel/air mixture and propagation of flame throughout the test rig. The problem was overcome at the time by ensuring that the oxygen was injected before the fuel and also by undertaking the pitot-static traverse after the ignition test had been completed. The subsequent tests (15, 16 and 17) were completed according to plan and nothing more was considered regarding the auto-ignition and any possible consequences.

After the test programme had been completed the HRSG was separated for inspection purposes at the junction with the expansion section. It was then observed that there had been extensive burn damage to the first few rows of the heat exchanger tube bundle, where the tube fins had melted and burnt away. The damaged tubes were replaced with new ones prior to commencing the Phase 2 test programme. At the time it was assumed that the fins on the tube bundle had been burnt away progressively during the test programme, and that as they contributed no more than 10% to the overall blockage area of the tube bundle they would have only made a marginal contribution to the level of turbulence generated by the overall heat exchanger tube bundle.

6.2 RE-COMMISSIONING TESTS

The procedure required undertaking three re-commissioning tests specified in the originally agreed programme of work. These required the injection of hydrogen only plus make-up oxygen and they were repeats of tests 9, 10 and 12 from the previous WP 2.3 test programme. They were selected to give a basis for comparing the modified instrumentation and its layout with that used previously in the WP 2.3 programme.

6.3 HYDROGEN-ONLY TESTS, WITH IGNITION

The three ignition tests used EQR values of 0.47, 0.51 and 0.55 for the tests numbered 18, 19 and 20 respectively. The exhaust stream oxygen content was adjusted to approximately 21% by means of oxygen injection.

The instrumentation used for these tests and the locations of the instruments are given in Figure A1 to Figure A6 in Appendix 15.1. Of particular interest are the pressures and flame-front speed data as recorded from the 24 flame ionisation sensors (IP's), together with the 12 optical probes (OP's) and the eleven pressure transducers. Up to 19 thermocouples were also used along with four IP rakes, a gas analyser and two high speed digital cameras. The data from these three tests was issued using the format established in the WP 2.3 test programme. A summary analysis and observations are given in the following paragraphs.

On the 20th June 2018 tests 18 and 19 were attempted, in both cases no explosion or release of smoke from the exhaust was observed. Data sets from the two tests plus video from the second test were obtained, examination of which indicated that the hydrogen fuel had ignited on a hot surface once the EQR had reached a sufficiently high value to form a flammable mixture. There was heat damage to the two rakes in the expansion section and to the fins on the heat exchanger tubes at the start of the tube bundle. The damage was consistent with the damage seen in an earlier phase of work when hot surface ignition had occurred. All of the damaged finned tubes were replaced with new finned tubes after test 20.

The thermocouples in this region had reached temperatures of around 1100 °C. The pressure transducers showed little or no increase in pressure. It was concluded that a flame had probably stabilised on the two rakes in the expansion section just before the tube bundle, or the tube fins. The flame burnt the fuel as it reached it, preventing a build-up of pressure in the HRSG. It was noted that the engine had run for almost fifteen minutes prior to the test, as a velocity traverse had been done during this time. This procedure, it was assumed, had allowed the hot surfaces in question to reach the local auto-ignition temperature prior to the test.

Test 18 was repeated on 27th June but in this case the test was run for no more than two minutes before the fuel and oxygen were injected. The test was successful and a full data set was obtained for subsequent analysis. The test had been delayed until the afternoon, but after allowing an hour for the rig to cool down, test 19 was attempted. Another auto-ignition occurred, however a data set plus video was collected. It was assumed that the same sequence of auto-ignition events had occurred again, as the data indicated. It was therefore decided to move the monochrome camera to the viewing port on the expansion section in an attempt to obtain a clearer picture of what was happening in this region.

Test 19 was successfully repeated on the morning of the 29th June 2018, and test 20 in the afternoon after allowing sufficient time for the rig to cool down. Complete data sets were obtained for both of these tests including video records. The data sets from the three successful re-commissioning tests were released to the ETI, whilst a more detailed analysis was undertaken by ourselves. One aspect of immediate concern was that the peak pressures observed were all much less than those observed in the equivalent tests previously undertaken as part of WP 2.3.

6.4 IMPLICATIONS OF THE RESULTS AND AUTO-IGNITION ISSUES

During June 2018 the rig was re-commissioned and the three commissioning tests, described in the previous section, completed. The results from these tests were not as expected as the peak pressures in all three cases were approximately half of what were the corresponding WP 2.3 test results. It was observed that the first of the commissioning tests did not go to plan initially as an auto-ignition occurred following injection of the hydrogen fuel. This was attributed to an excessive warm-up time as a pitot-static traverse had been done prior to the test. Examination of the rig and the test results suggested that the auto-ignition had occurred at the first rake (burn damage) in the expansion section just upstream of the heat exchanger tube bundle, and that it had lasted for several seconds. The problem was overcome as previously by minimising the warm-up time and by allowing time for the rig to cool down before proceeding with repeating this test and the following two commissioning tests. However upon analysing the test results from the three commissioning tests and observing the lower- than- expected pressures it was decided to re-check the calibrations

of the pressure transducers, which were shown to be correct. A visual examination of the tube bundle was then made, where upon it was observed that there had been severe burn damage to those tubes and fins that were visible from the viewing ports to the side and just upstream of the tube bundle. The damage pattern was not quite the same as previously in so much that the central area of the tube bundle was the main area damaged, whilst previously it had been the sides and upwards. It was agreed that the fire damaged tubes needed to be replaced and new ones were therefore ordered and installed.

In the meantime a more detailed analysis of the tests results was undertaken in particular examinations of the pressure losses across the tube bundle, in both the WP 2.3 and the corresponding Phase 2 tests, noting that the peak pressures arise principally from the combustion activity around the exit of the heat exchanger and its section four region. For a particular EQR, there is only so much energy per unit volume in the fuelled-up exhaust which means that, if the flame passes through the turbulent region quickly, the pressure pulse will be strong and of short duration. The converse is also true, i.e. a slower flame will release the energy more slowly and the pressure pulse will be weaker and of a longer duration. Comparisons of the pulse widths between corresponding pressure transducers for the two sets of test results show that for the WP 2.3 results the trend is towards shorter widths with increasing EQR, which makes sense since flame speed is also a function of H₂ concentration. Thus for the three WP 2.3 tests (9, 10 & 12) the pulse width corresponding to combustion in the turbulent section four region of the heat exchanger is shorter than the pulse width at the end panel and this width shortens to 3 msec for the 0.55 EQR case. The Phase 2 test widths show a marked difference, with a generally wider set of pulses (slower flames) and significantly longer in the equivalent EQR case, i.e. 13.9 msec. This behaviour is consistent with the lower peak pressures which are tied up with the slower combustion rates in the turbulent region.

A further potential indicator of the influence of the burn damage to the heat exchanger tubes was the back pressure generated immediately upstream of the heat exchanger as a result of frictional losses through it. This back pressure arose as exhaust gas was driven downstream ahead of the flame through the HRSG following ignition as the flame progresses down the circular duct. The peak pressures occur whilst the flame is around the entrance section to the HRSG and before it has reached the heat exchanger tube bundle. The pressures for the Phase 2 tests are significantly lower, approximately 50% less, than those for the corresponding WP 2.3 tests. However, it is difficult to measure accurately the actual pressures because of the poor resolution of the Kulite sensors at the low pressure levels of concern (10-100 mbar). Other things being equal these measurements indicate that the downstream obstruction, i.e. the heat exchanger is presenting less of an obstruction than was the case for the WP 2.3 tests. This suggests that the reduced pressure across the obstruction, as represented by the heat exchanger, is responsible for reduced turbulence in the section four region of the HRSG and hence lower flame speeds and reduced peak pressures.

The foregoing brings into question the validity of the WP 2.3 test results particularly the final three tests following the auto-ignition in test 14. The issue is being able to see if it is possible to identify when the fin damage took place during the WP 2.3 tests, i.e. whether it was progressive or sudden. If there was a progressive change this also has a potential impact on the robustness of those test results prior to Test 14. An examination of the heat exchanger pressure drops for the WP 2.3 tests, particularly those involving CO/H₂ mixtures (Tests 13, 15, 16 & 17) shows that the average

differential pressure drop across the heat exchanger for Tests 6 – 15 is 35 mbar, whilst that for Tests 16 & 17 is 5 mbar. However there is some uncertainty attached to the accuracy of the measurements due to the poor resolution of the Kulite sensors at these very low values. There is some additional evidence that brings into question the validity of the final three CO/H₂ tests and that is the variation in peak pressures with increasing EQR values. The results show that the peak pressures decrease with increasing EQR values and it is only for Test 17 that the peak pressure is greater than the value for Test 13. Logically a consistent pressure increase with EQR is expected as was the case for all of the other test gas mixtures together with hydrogen alone. We therefore conclude that the last 2 - 3 test results from the WP 2.3 tests are questionable due to the burn damage to the first few rows of the heat exchanger tubes that occurred as a result of an auto-ignition during the failed Test 14. It was also noted that the burn damage to the finned tubing was not progressive but the result of a single auto-ignition event taking the temperature of the fins to above the melting point for a sufficient duration to cause the damage observed.

In an effort to avoid any further auto-ignitions, improvements were made to the controlling software to limit the amount of fuel that was injected after an ignition and to ensure that only one spark was generated per test. The means for automatically closing the system down was also added should a temperature rise be detected prior to ignition. Visual inspections were also made after each test of the first few rows of the heat exchanger tube bundle in order to check for any heat damage.

7 PRESENTATION OF RESULTS FROM PHASE 2

7.1 INTRODUCTION

The arrangement of sensors around the test rig has been made in order to reveal the most important consequence of the combustion event, i.e. peak pressures, as well as providing data to inform the flame dynamics during the short term event following ignition. Raw data from each test is provided in the 'tdms' and video files but since these are large files, this report will focus on the main outputs from these files, which includes peak pressures and flame speeds throughout the system as well as an account of their relationship with the video record.

All of the results are sensitive to the nature of the mixture and of the fuel concentration as identified by the equivalence ratio (EQR). The reported results will therefore always relate to the specific mixture composition and EQR used.

7.2 DEFINITION OF EQUIVALENCE RATIO (EQR)

The definition of equivalence ratio (EQR) used throughout the work should be noted, since this is based on the mole fraction ratio of the fuel in the fuel/air mixture rather than the more commonly used mole ratio of fuel and air.

Defining the following terms:-

M_F = moles of fuel, M_A = moles of air, then the molar ratio of fuel and air is: M_F / M_A .

Under stoichiometric conditions, the stoichiometric molar fuel/air ratio is S_{mfr} , where $S_{mfr} = M_F / M_{A_s}$ and where M_{A_s} is the stoichiometric moles of air corresponding to M_F moles of fuel.

For an arbitrary number of fuel moles M_F' and air moles M_A' , the equivalence ratio EQR_{mfr} , based on fuel and air mole ratios is then:

$$EQR_{mfr} = M_F' / M_A' \times M_{A_s} / M_F \text{ i.e. } M_F' / M_A' \times 1 / S_{mfr}$$

This formula would correspond to the commonly used definition of EQR. In the present work mole fractions are used to represent the EQR parameter.

The stoichiometric mole fraction fuel air ratio, S_{mfr} , then becomes :-

$$S_{mfr} = \frac{M_F}{M_F + M_{A_s}}$$

where M_{A_s} corresponds to the stoichiometric moles of air corresponding to M_F moles of fuel.

The equivalence ratio used in the present work is then defined as EQR_{mfr} , where

$$EQR_{mfr} = \frac{M_F'}{M_F' + M_A'} \cdot \frac{1}{S_{mfr}}$$

and where M_F' and M_A' are the actual mole quantities used in a test.

It can readily be shown that a conversion between the above two definitions of EQR can be derived, and this relation is the following:

$$EQR_{mr} = EQR_{mfr} \cdot \frac{(1 - S_{mfr})}{(1 - EQR_{mfr} \cdot S_{mfr})}$$

The EQR_{mfr} values are always provided for each test and the stoichiometric mole fraction ratios (S_{mfr}) are shown in the Table 3 below for the mixtures used in the test series.

Table 3 Stoichiometric mole fractions for the mixtures used in the test series.

Fuel mixture	S_{mfr}
100% CH ₄	0.095
60% H ₂ /40% CH ₄	0.1603
40% H ₂ / 60% CH ₄	0.1304
CO	0.2957
40% H ₂ / 60% CO	0.2957
60% H ₂ / 40% CO	0.2957
H ₂	0.2957
40% H ₂ / 25% CH ₄ / 35% CO	0.1935

7.3 RESULTS LISTINGS

The test plan required tests to be undertaken at both high and low engine exhaust temperatures. The circular duct centreline velocities used for the high temperature tests were in the range 82-85 m/s, with centreline gas temperatures in the range of 480 - 520 °C. These corresponded to an average mass flow rate of 9.15 kg/s in the circular duct, based on an integrated velocity profile across the duct and with the engine running at 11,500 - 11,800 rpm. For the low temperature tests, it was considered necessary to maintain the same mass flow rate due to the nature of the compressor flow immediately following a flame-out and this condition was achieved by reducing the engine speed to 8100 rpm and modifying the inlet constriction to the circular duct, by fitting a larger orifice plate. In this way lower temperatures in the range of 310 - 330 °C were achieved for these tests.

Note that the centreline temperatures quoted are measured without the injection of oxygen and fuel, the addition of which will lower the temperature by some 40 - 60 °C immediately before ignition as the example in section 3.4.1 has shown. Note also that during the high temperature tests from 35 onwards the engine rpm was lowered to 11500 rpm to reduce the exhaust temperature and hence the likelihood of auto-ignitions occurring with H₂ and CO/H₂ mixtures. Consequently there was a small (about 2%) reduction in the average mass flow rates for these tests.

The following tables (Table 4 and Table 5) list the main test parameters for both the high temperature and low temperature tests respectively. Note that tests in which an auto-ignition occurred are not included in the tables, as these are discussed in a later section of the report. There

were no auto-ignitions observed during the low temperature tests. Note that the test numbering starts at 21 as 1 – 20 were the numbers allocated to WP 2.3 tests and the re-commissioning tests.

Table 4 List of the main test parameters for the high temperature (480 - 520 °C) tests (excluding auto-ignitions).

Mixture	Test No.	EQR	CH ₄ (vol%)	CO (vol%)	H ₂ (vol%)	Fuel mass flow kg/s	O ₂ mass flow kg/s	Comments
CH ₄ /H ₂	21	0.420	40	0	60	0.181	0.509	Engine at 11,800 rpm
CH ₄ /H ₂	22	0.325	40	0	60	0.140	0.477	"
CH ₄ /H ₂	23	0.560	40	0	60	0.250	0.458	"
CH ₄ /H ₂	24	0.580	40	0	60	0.259	0.485	"
CH ₄ /H ₂	25	0.640	40	0	60	0.290	0.491	"
CH ₄ /H ₂	26	0.650	40	0	60	0.293	0.498	"
CH ₄ /H ₂	27	0.590	60	0	40	0.288	0.511	"
CH ₄ /H ₂	28	0.710	60	0	40	0.352	0.522	"
CH ₄ /H ₂	29	0.510	60	0	40	0.244	0.511	"
CH ₄	30	0.640	100	0	0	0.344	0.539	"
CH ₄	31	0.790	100	0	0	0.435	0.538	"
CH ₄	32	0.490	100	0	0	0.263	0.539	"
H ₂	35	0.520	0	0	100	0.120	0.464	rpm to 11,500
H ₂	36	0.480	0	0	100	0.108	0.448	"
H ₂	37	0.540	0	0	100	0.126	0.443	"
H ₂	38	0.420	0	0	100	0.094	0.456	"
H ₂	39	0.350	0	0	100	0.076	0.462	"
H ₂	40	0.540	0	0	100	0.125	0.463	"
CO/H ₂	42	0.400	0	40	60	0.548	0.451	"
CO/H ₂	47	0.434	0	60	40	0.847	0.450	"
CO/H ₂	48	0.340	0	60	40	0.645	0.473	"

CO/H ₂	49	0.440	0	40	60	0.615	0.451	"
CO/H ₂	50	0.350	0	40	60	0.470	0.454	"
CH ₄ /CO/H ₂	74	0.462	25	35	40	0.470	0.449	"
CH ₄ /CO/H ₂	75	0.492	25	35	40	0.504	0.443	"
CH ₄ /CO/H ₂	76	0.440	25	35	40	0.440	0.450	"

Table 5 List of the main test parameters for the low temperature tests (310 - 330 °C).

Mixture	Test No.	EQR	CH ₄ (vol%)	CO (vol%)	H ₂ (vol%)	Fuel mass flow (kg/s)	O ₂ mass flow (kg/s)	Comments
CH ₄	52	0.650	100	0	0	0.344	0.312	Engine at 8100 rpm
CH ₄	53	0.810	100	0	0	0.430	0.311	"
CH ₄	54	0.506	100	0	0	0.261	0.311	"
CH ₄ /H ₂	55	0.600	60	0	40	0.288	0.311	"
CH ₄ /H ₂	56	0.500	60	0	40	0.238	0.313	"
CH ₄ /H ₂	57	0.705	60	0	40	0.344	0.313	"
CH ₄ /H ₂	58	0.510	40	0	60	0.218	0.310	
CH ₄ /H ₂	59	0.410	40	0	60	0.171	0.305	"
CH ₄ /H ₂	60	0.590	40	0	60	0.253	0.310	"
H ₂	61	0.450	0	0	100	0.102	0.312	"
H ₂	62	0.350	0	0	100	0.077	0.314	"
H ₂	63	0.285	0	0	100	0.062	0.318	"
CO/H ₂	64	0.513	0	40	60	0.724	0.306	"
CO/H ₂	65	0.303	0	40	60	0.398	0.312	"
CO/H ₂	66	0.352	0	40	60	0.470	0.308	"
CO/H ₂	67	0.393	0	40	60	0.533	0.310	"
CO/H ₂	68	0.397	0	60	40	0.764	0.307	"
CO/H ₂	69	0.438	0	60	40	0.856	0.308	"
CO/H ₂	70	0.323	0	60	40	0.606	0.316	"
CH ₄ /CO/H ₂	71	0.465	25	35	40	0.471	0.312	"
CH ₄ /CO/H ₂	72	0.496	25	35	40	0.506	0.307	"
CH ₄ /CO/H ₂	73	0.428	25	35	40	0.431	0.310	"

7.4 PHASE 2 ADDITIONAL INFORMATION

In addition to the information presented in this report there have been separate data sheets issued following each test together with the relevant high- speed video records of the tests. The Excel data sheets provide peak pressures, indicative flame speeds, gas temperatures, weather conditions, and sensor positions.

The high- speed video records were taken at framing rates of 2500 to 3000 fps, and are all time stamped. There is an upstream video of the flame front entering the tube bank in black and white, followed by a colour video showing the flame-front exiting from the tube bank and travelling through the last four sections of the exhaust duct. This was the same camera position used previously for the WP 2.3 test series. A study of the two high-speed videos for each test shows the passage of the flame front into the tube bank and its emergence from it. The time difference and the width of the tube bank giving a measure of the speed of the flame front through it, noting that as a general rule the shorter the time the higher the peak pressure generated. MP4 versions of the video sequences have also been made available. There are also several photographs of the rig both before and during operation. This data together with the information presented in the report needs to be considered collectively in order to obtain as comprehensive a picture of the overall performance of individual fuel mixtures.

7.5 REPEATABILITY OF TEST RESULTS

The experimental test programme was not set up to explore in detail the repeatability of each data set. Consequently sufficient repeat data sets were not available to establish statistically the level of accuracy to which each test could be repeated. During re-commissioning three hydrogen tests were repeated from the previous WP 2.3 test programme as discussed in section 6.3. The results from these showed that the peak pressures were considerably lower than previously observed, with no obvious explanation being apparent. However the results from these three tests were consistent in that for a given fuel the peak pressures observed increased with increasing EQR. This consistency was observed for the completed set of Phase 2 results and furthermore, where relevant, they fitted into the WP 2.3 results without showing any obvious inconsistencies. Whilst the foregoing in itself does not establish the accuracy of each data set it does at least indicate that within the accuracy of the sensors and the data processing that the results are consistent and that trends within the data could be established. For each data set a best fit curve was established and the degree of scatter around each best fit curve is a rough indication of the level of repeatability. For much of the data, but not all this, scatter is relatively small and at present this is the best measure we have of the repeatability of tests.

Regarding the measurement of peak pressures and the accuracy to which these were made. The Kulite pressure transducers at worst measured to an accuracy of 0.5% of FSO, thus giving a tolerance of 35 mbar for a 7 bar pressure gauge output. A separate calibration check on each individual transducer channel using a "Druck" calibrator, which has a resolution of 0.1 mbar showed that for the eleven sensors used the average error was 14.7 mbar.

The frequency response of the Kulite sensor's was of the order of 50 to 100 kHz, thus when seeking to measure the peak pressure a degree of subjective judgement was used, taking into account the fact that several data points would be present over the whole of the wave form of interest. This

allowed peaks due to noise to be eliminated such that if a peak data point was much larger than its neighbouring points then it would be ignored. No filtering programmes were used nor did they simply pick off the peak value irrespective of its context.

8 DISCUSSION OF RESULTS – COMMON FEATURES

In this section the common features across both the high and low temperature tests are discussed, in particular the pressure behaviour and flame speeds.

8.1 GENERAL BEHAVIOUR OF FLAME AND PRESSURE PULSES FOLLOWING IGNITION

There is an extensive body of results and their main features can be depicted in a number of ways to aid understanding. In all cases where a successful ignition occurred (i.e., did not auto-ignite) a flame-front travelled down the duct at a velocity dependent upon the test conditions. Its progress being tracked by the optical sensors located in the duct (see Figure A1 and Figure A3 in Appendix 15.1). Because of the asymmetry of the expansion section geometry, the unburned gas flow induced by the flame produces a wall jet on the bottom of the channel. The flame-front travels faster in this high speed flow near the bottom of the expansion section and thus reaches the tube bank first. The key feature is the influence of the tube bank in generating flame acceleration through turbulence, and the associated pressure wave. The pressure wave travels through the tube bank at a low level before spreading upwards and sideways in the first section of the HRSG after the tube bank, see Figure 3 HRSG layout: schematic. Before the flame arrives at the tube bundle there is a pressure gradient developed in the tube bundle that is associated with the flow restriction. Consequently the flame enters the tube bundle in which there is an already existing pressure gradient. The flame velocity in the expansion section is not sufficiently high to have a significant pressure wave associated with it. The combustion and pressure generation in the tube bundle is rather complex where a pressure “pulse” develops ahead of the flame as a result of the acceleration process. The flow immediately after the tube bundle is highly turbulent due to the turbulence convected downstream from the tubes. Once the flame reaches this turbulent region rapid combustion of the gas can lead to further pressure pulse generation, which amplifies the pressure pulse (associated with the flame acceleration) that leaves the tube bundle. The speed at which this process occurs is dependent upon the nature and strength of the fuel mixture being tested. The pressure pulse travels along the length of the last three HR sections at the relevant sound speed before being reflected backwards off the end wall. There is venting of the combusted gas out through the stack, at the end of the HRSG, which reduces the strength of the reflected pressure wave.

A useful starting point to illustrate these features of the combustion event following ignition of the mixture are the following graphs. Figure 5 shows three of the main events following ignition, which are characteristic of the whole series of test results. The upper trace shows the flame ionisation signal as flame passes the exit of the circular duct (IPO). This flame progresses through the expansion section into the heat exchanger (HE) tube bank where it is identified as shown on the middle trace, by IP9 located on the side of the middle panel.

The flame accelerates through turbulence generation within the tube bank into the region immediately downstream of the tube bank in HR4, see Figure 3. This is a turbulent flow region, where the main combustion driven pressure wave is generated. Since the turbulent region is finite and assumed to be of the order of 1m in length, (based on a typical pulse width of 5msec and flame speed in HR4 of around 100 - 200m/s), the pressure generated in this region cannot be maintained as the flame progresses further along the exhaust duct (HR4-HR6) due to a reduced rate of combustion. This results in a pressure pulse of finite width as shown in the KU5 and KU6 traces of

Figure 5. The duration of this pressure pulse will depend on the intensity of combustion in HR4, on the fuel mixture components and upon its concentration (EQR).

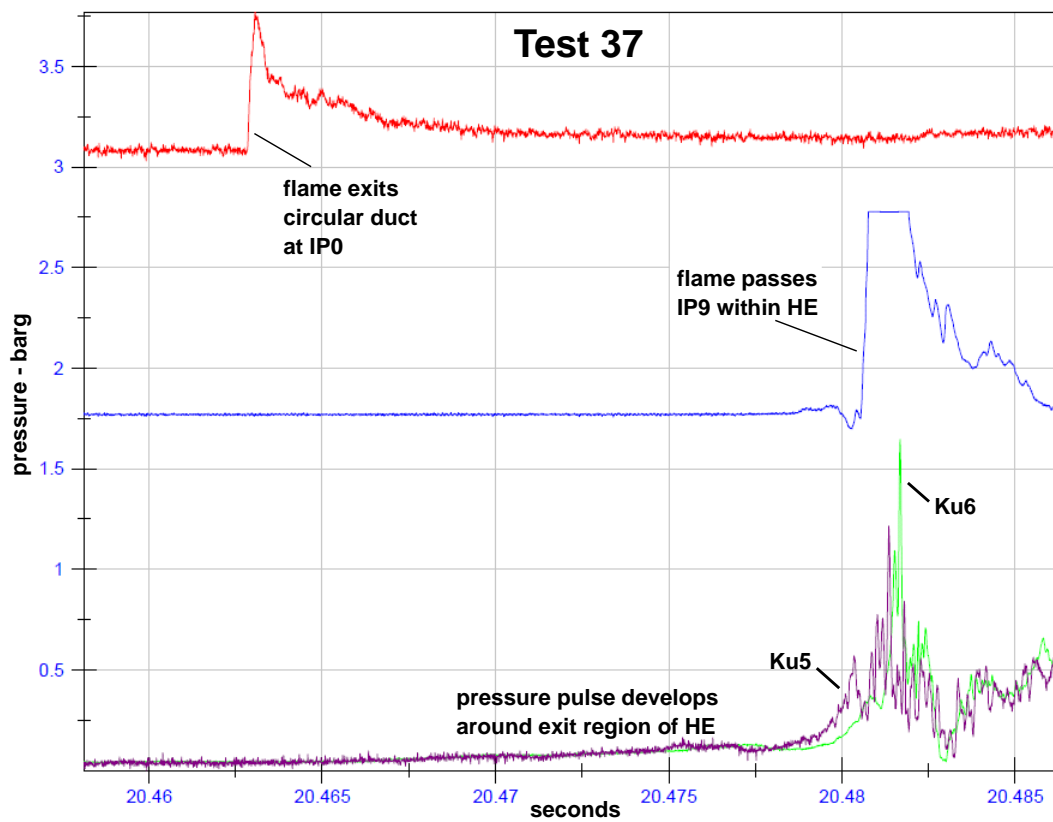


Figure 5 Pressure and flame front traces for a typical test (37: H₂, EQR: 0.54).

The pulse duration is illustrated by the two cases shown in Figure 6 and Figure 7. In Figure 6 an initial pressure pulse can be seen as recorded on Kulite 6 (KU6) of around 5 ms width and 0.64 barg in amplitude. In this same figure a second pulse can be seen around 15.6 ms later on KU6, which arises from the pressure pulse reflection off the downstream end plate. It is important to note that this initial pressure pulse (at around 21.39 s) is the origin of subsequent pressure pulse behaviour within the whole system and that the evolution of this initial wave arises through normal propagation, reflection and pulse sharpening associated with regular shock behaviour. These fluid dynamic effects often result in the propagated wave being greater in amplitude than the original wave, even within the region where it first originated. Due to the importance of this initial pressure wave around the heat exchanger, it is given special attention, and subsequent plots of pressure vs EQR use this initial wave as the basis for comparison between different test conditions.

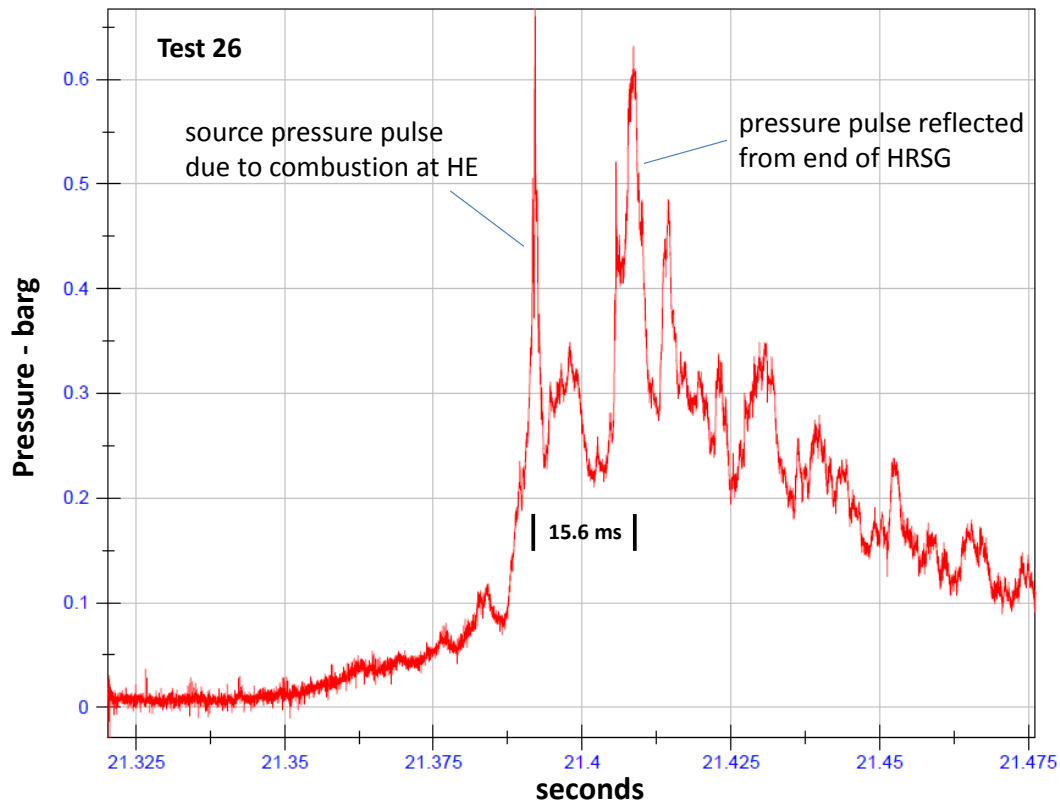


Figure 6 Typical pressure pulse profile for Ku6 for a fast combustion event (Test 26: CH₄/H₂. EQR: 0.65).

The combustion associated with the test case shown in Figure 7 is much more sluggish resulting in a wider initial pressure pulse of lower amplitude. Due to its width, the reflected pulse merges with the initial pressure growth, resulting in a much broader event recorded at KU6. Both the amplitude and time width of this initial pressure pulse are important features characterising the intensity of the combustion event and is referred to at length in the representation of the results in the following sections of the report.

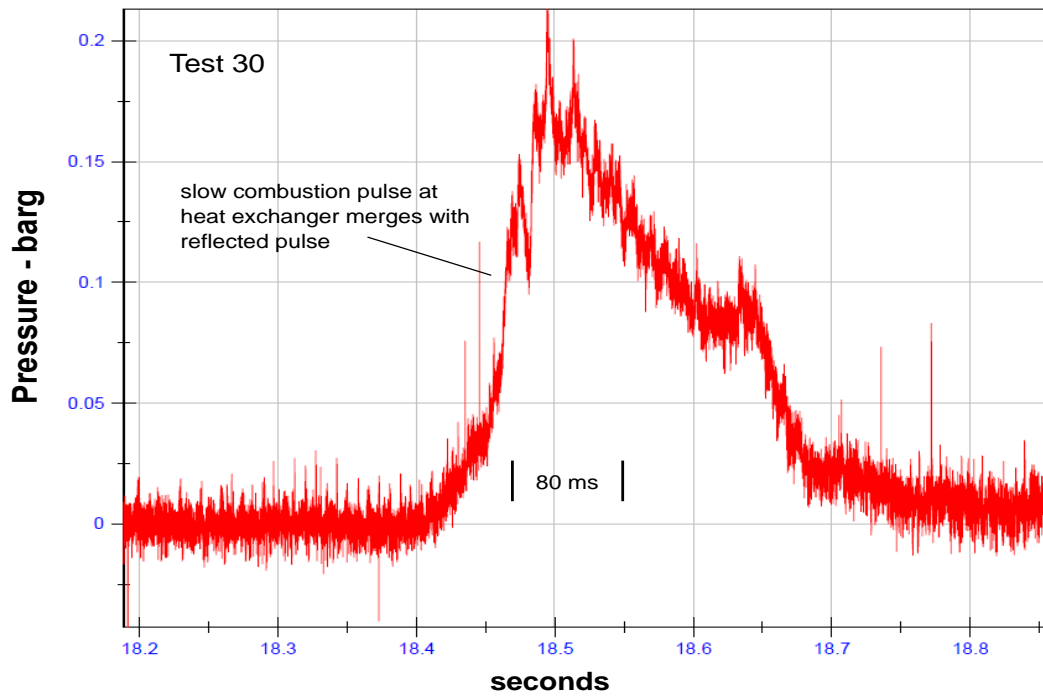


Figure 7 Pressure profile for a slow combustion event (Test 30: CH₄. EQR: 0.64).

The finite combustion energy contained in the turbulent region will be released during the period represented by the initial pulse width shown in Figure 6. If this is short due to fast combustion, then the peak pressure will be higher than that occurring with a more sluggish combustion event as typified by the initial pulse shown in Figure 7.

Another pressure pulse feature observed, and illustrated from Test 40 in Figure 8, is a series of short pressure pulses recorded just after the tube bundle by KU6. This is associated with more reactive mixture conditions, and is assumed to be a feature of the unsteady flow and highly turbulent region around the tube bank exit and immediately downstream of the tube bank. The time period of around 15 ms for the reflected wave to reach KU6 represents a velocity of around 600 m/s, the sound speed in the hot gas mixture through which it travels.

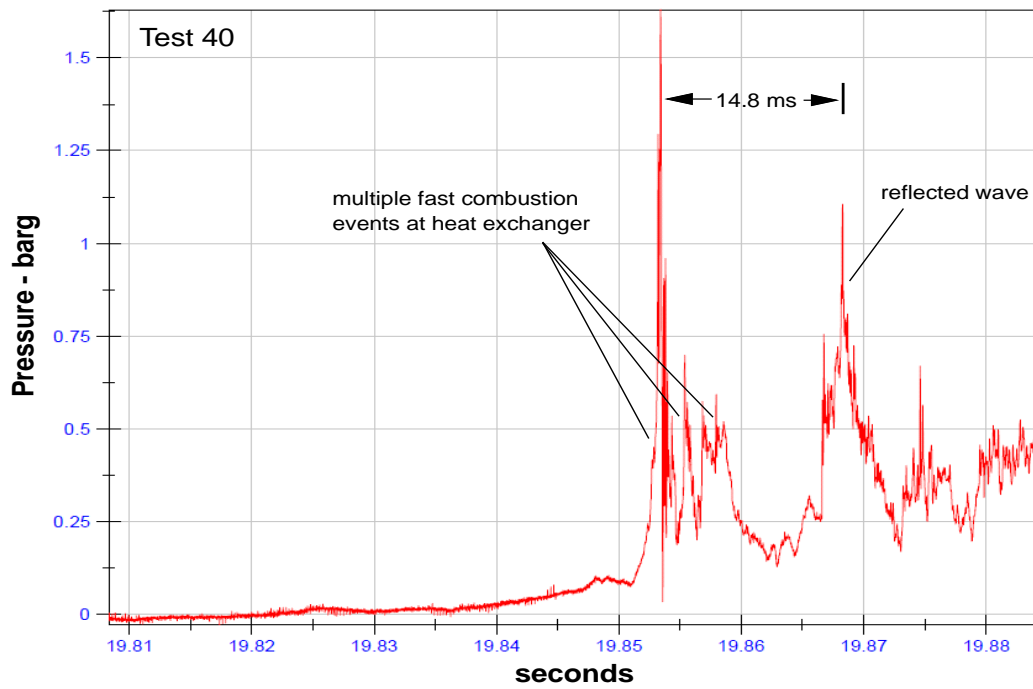


Figure 8 Multiple fast combustion events at the heat exchanger (Test 40. H2. EQR: 0.54).

Figure 9 shows the relationships between the pressure measurements in the duct and those downstream in the HRSG. In particular the back pressure created by the flame-front as it leaves the duct and later the backwards travelling pressure pulse from the reflected pulse off the end wall coming back through the heat exchanger tube bank.

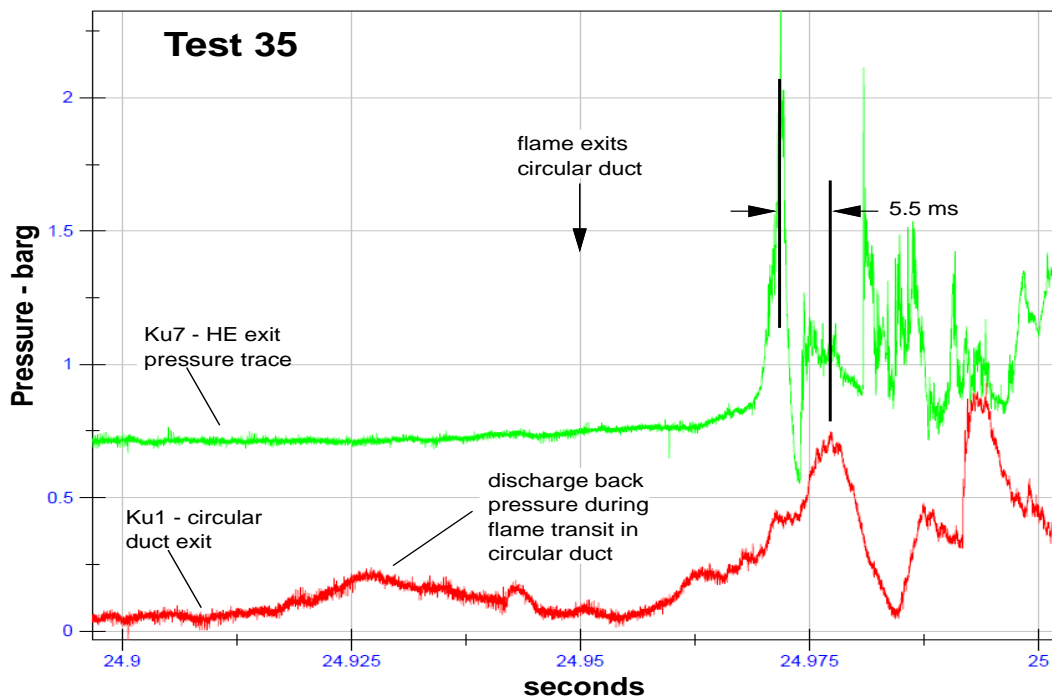


Figure 9 Pressure traces from end of section 4 of HRSG and end of circular duct (Test 35, H2, EQR: 0.52).

The trace from KU7 illustrates the amplification of the initial pressure pulse (flame-front) as it emerges from the turbulent region immediately downstream of the tube bank, and also shows the delay before this pressure pulse reaches the upstream KU1 pressure sensor in the circular duct. This pressure pulse is lower in magnitude than the following wave that has been reflected from the end wall of the HRSG. The time point at which the flame leaves the circular duct (based on IPO) is also indicated.

The features shown in Figure 5 to Figure 9 are typical of the test results from both the high and low temperature tests. The timings and magnitudes of the pressures observed depending on the fuel mixture, the test temperature and the EQR of the fuel mixture.

The pressure front and flame front ultimately emerge from the vertical chimney at the end of the HRSG, as shown in Figure 10 below, taken from Test 57. The extent of the visible flame depends on the strength of the pressure wave, which itself is dependent upon the fuel composition and the EQR of the test fuel.



Figure 10 Flame emerging from the vertical chimney at the end of the HRSG.

9 ANALYSIS OF HIGH TEMPERATURE TESTS

This section examines the pressures generated during the high temperature tests, together with the overall behaviour of the various fuel mixtures tested, including flame speeds.

9.1.1 Peak pressures obtained

Table 6 shows the fuel mixture compositions tested together with the highest pressures recorded both in the duct and in the HRSG downstream of the tube bank.

For the purposes of this table, the maximum peak pressures are divided into three groups, those near the end of the circular duct, those between the heat exchanger and the end plate (KU6-KU9) and the pressure sensor at the end plate (KU10). Within the second group, as has been discussed previously, the origin of the pressure pulse is the rapid combustion in the heat exchanger and immediate downstream HR4 region and this is indicated on the initial pressure recorded on KU6. The KU6 pressure pulse is always the first to be seen on the time axis and this then propagates to the other sensors in the system, appearing later both upstream and downstream. The KU6 pressure is not always the highest pressure to be found within the first group for reasons of fluid dynamic and acoustic behaviour of the initial wave.

KU10 measures the pressure reflected back off the end plate and as such represents the maximum pressure seen within the test rig in about 50% of the tests. When it is not the maximum it is because the reflected wave travels back through what is combusted gas and cannot therefore strengthen as a result of further combustion. The reflected pressure wave always (except for the detonation test) first travels through unburned gas (ahead of the flame) and then through combustion products. It is never reinforced by combustion because there is no combustion wave associated with it. The distance between the incident pressure wave and the trailing flame will govern how much time the reflected wave travels through unburned and burned gas. For more energetic events this distance will be smaller. The magnitude of the reflected wave reaching the tube bundle is probably governed by these relative times because of the large difference in sound speed in these two gases. In addition pressure decays due venting of gas (first unburned and then burned) through the stack, the process of which sends a series of expansion waves back towards the tube bank.

It can be seen from Table 6 that the maximum pressures recorded both downstream and upstream of the tube bank are in general increasing with increasing EQR, irrespective of the fuel mixture. The highest pressures for each test occurred with the 100% hydrogen fuel, whilst the lowest pressures were associated with 100% methane. The other fuel mixtures produce intermediate values. These results were consistent with the known reactivity of the fuel mixtures used as reported in [2, 8].

Table 7 presents a more detailed analysis of the peak pressures and flame speeds throughout the test rig. In Table 7, a flame speed is quoted for each section of the system. These flame speeds should be interpreted with care since they represent average values over some extended distance within each section. When IP's have been used to extract these values, they have always been selected using flame sensors on the same side of the test rig since it is recognised that the flame-front is not necessarily normal to the direction of propagation, as a simple propagation model might predict. The use of OP's for this purpose has fewer constraints since these are line-of-sight measurements, although these may also require careful interpretation where the flame front is not

normal to the duct axis. Also need to be aware that the OPs on the side-wall in the expansion section and HR4 section are problematic as the flame shape is far from uniform from top to bottom so signal can be very misleading. The OPs on the top wall are more useful as they provide the flame speed for the leading edge no matter the vertical flame front distribution.

Table 6 Summary of test pressures from high temperature tests. (NB. Kulite 6 pressures also presented separately in section 11).

Mixture	Test No.	Eq. Ratio	CH ₄ (vol%)	CO (vol%)	H ₂ (vol%)	KU0 - KU1 highest pressure (barg)	KU6 - KU9 highest pressure (barg)	KU10 peak pressure (barg)
CH ₄ /H ₂	21	0.420	40	0	60	0.199	0.116	0.122
CH ₄ /H ₂	22	0.325	40	0	60	0.02	< 0.02	< 0.02
CH ₄ /H ₂	23	0.560	40	0	60	0.429	0.475	0.512
CH ₄ /H ₂	24	0.580	40	0	60	0.502	0.573	0.511
CH ₄ /H ₂	25	0.640	40	0	60	0.694	0.727	0.842
CH ₄ /H ₂	26	0.650	40	0	60	0.666	0.876	0.990
CH ₄ /H ₂	27	0.590	60	0	40	0.488	0.410	0.390
CH ₄ /H ₂	28	0.710	60	0	40	0.738	0.947	1.211
CH ₄ /H ₂	29	0.510	60	0	40	0.250	0.190	0.155
CH ₄	30	0.640	100	0	0	0.385	0.277	0.239
CH ₄	31	0.790	100	0	0	0.791	0.929	0.967
CH ₄	32	0.490	100	0	0	0.117	0.061	0.058
H ₂	35	0.520	0	0	100	0.84	2.196	2.154
H ₂	36	0.480	0	0	100	0.714	0.991	1.158
H ₂	37	0.540	0	0	100	1.020	2.725	3.115
H ₂	38	0.420	0	0	100	0.476	0.595	0.601
H ₂	39	0.350	0	0	100	0.232	0.251	0.210
H ₂	40	0.540	0	0	100	1.046	3.430	3.029
CO/H ₂	42	0.400	0	40	60	0.328	0.336	0.315

CO/H ₂	47	0.434	0	60	40	0.598	0.633	0.699
CO/H ₂	48	0.340	0	60	40	0.123	0.060	0.051
CO/H ₂	49	0.440	0	40	60	0.150	0.079	0.069
CO/H ₂	50	0.350	0	40	60	0.072	<0.02	<0.01
CH ₄ /CO/H ₂	74	0.462	25	35	40	0.464	0.204	0.215
CH ₄ /CO/H ₂	75	0.492	25	35	40	0.553	0.253	0.269
CH ₄ /CO/H ₂	76	0.440	25	35	40	0.361	0.174	0.187

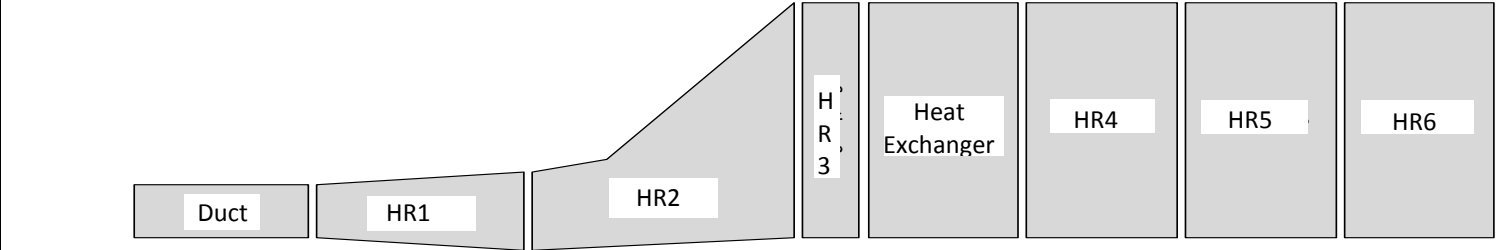
Table 7 Distribution of peak pressures and flame velocity estimates through duct and HRSG system - high temperature tests.

Duct										
HRSG Tests	Test No.									
40CH ₄ /60H ₂ EQR = 0.420	21	Vel m/s	256		109	85	40	25	7	7
		P bar	0.199		0.205	0.119	0.09	0.073	0.116	0.122
40CH ₄ /60H ₂ EQR = 0.325	22	Vel m/s	130		50	-	52	-	-	-
		P bar	0.02		< 0.02	< 0.02	< 0.02	< 0.02	< 0.02	< 0.02
40CH ₄ /60H ₂ EQR = 0.560	23	Vel m/s	303		164	65	112	144	25	23
		P bar	0.429		0.307	0.322	0.288	0.350	0.475	0.512
40CH ₄ /60H ₂ EQR = 0.580	24	Vel m/s	333		211	178	111	157	32	18
		P bar	0.502		0.277	0.339	0.403	0.381	0.573	0.511
40CH ₄ /60H ₂ EQR = 0.640	25	Vel m/s	370		200	120	144	274	28	18
		P bar	0.694		0.399	0.477	0.494	0.526	0.687	0.842
40CH ₄ /60H ₂ EQR = 0.650	26	Vel m/s	370		190	112	170	245	66	23
		P bar	0.666		0.379	0.450	0.544	0.657	0.876	0.990
60CH ₄ /40H ₂ EQR = 0.590	27	Vel m/s	322		184	231	76	146	49	23
		P bar	0.488		0.249	0.318	0.395	0.314	0.410	0.394
60CH ₄ /40H ₂ EQR = 0.710	28	Vel m/s	370		221	225	154	274	27	17
		P bar	0.738		0.509	0.509	0.589	0.621	0.817	1.211
60CH ₄ /40H ₂ EQR = 0.510	29	Vel m/s	204		117	219	126	60	19	16
		P bar	0.250		0.138	0.149	0.204	0.155	0.190	0.155

Table 7 Distribution of peak pressures and flame velocity estimates through duct and HRSG system - high temperature tests (cont).

HRSG Tests	Test No.									
100CH ₄ EQR = 0.640	30	Vel m/s	238		135	109	89	144	47	34
		P bar	0.385		0.196	0.213	0.249	0.212	0.277	0.239
100CH ₄ EQR = 0.790	31	Vel m/s	370		247	199	204	347	29	19
		P bar	0.791		0.543	0.569	0.612	0.613	0.929	0.967
100CH ₄ EQR = 0.490	32	Vel m/s	158		77	93	34	42	12	19
		P bar	0.117		0.066	0.070	0.076	0.046	0.054	0.058
100H ₂ EQR = 0.520	35	Vel m/s	333		237	213	232	218	32	19
		P bar	0.840		1.685	0.540	0.857	0.908	2.104	2.154
100H ₂ EQR = 0.480	36	Vel m/s	286		216	178	175	106	22	27
		P bar	0.714		0.400	0.432	0.519	0.583	0.991	1.158
100H ₂ EQR = 0.540	37	Vel m/s	370		269	199	282	190	38	40
		P bar	1.020		1.397	0.682	1.181	1.598	2.452	3.115
100H ₂ EQR = 0.420	38	Vel m/s	278		184	114	191	176	25	-
		P bar	0.476		0.371	0.317	0.386	-	0.491	0.601
100H ₂ EQR = 0.350	39	Vel m/s	250		170	98	109	56	17	-
		P bar	0.232		0.157	0.189	0.220	0.162	0.251	0.210
100H ₂ EQR = 0.540	40	Vel m/s	357		203	208	255	187	24	-
		P bar	1.046		1.175	0.929	1.249	3.430	2.748	3.029

Table 7 Distribution of peak pressures and flame velocity estimates through duct and HRSG system - high temperature tests (cont).



HRSG Tests	Test No.	Vel m/s	278		137	190	138	137	27	-
60H ₂ /40CO EQR = 0.400	42	P bar	0.328		0.188	0.226	0.239	0.227	0.336	0.315
60CO/40H ₂ EQR = 0.434	47	Vel m/s	333		209	204	102	196	-	8
		P bar	0.598		0.357	0.389	0.431	0.433	0.580	0.699
60CO/40H ₂ EQR = 0.340	48	Vel m/s	169		73	43	26	23	-	-
		P bar	0.123		0.063	0.048	0.058	0.036	0.060	0.051
40CO/60H ₂ EQR = 0.440	49	Vel m/s	182		81	21	21	23	7	-
		P bar	0.150		0.074	0.077	0.080	0.048	0.079	0.069
40CO/60H ₂ EQR = 0.350	50	Vel m/s	137		48	-	-	-	-	-
		P bar	0.072		<0.01	<0.01	<0.01	<0.01	<0.01	<0.01
25CH ₄ /35CO /40H ₂ EQR = 0.462	74	Vel m/s	278		126	85	134	66	11	14
		P bar	0.464		0.202	0.200	0.141	0.167	0.164	0.215
25CH ₄ /35CO /40H ₂ EQR = 0.492	75	Vel m/s	276		157	138	161	66	25	-
		P bar	0.553		0.263	0.259	0.186	0.252	0.224	0.269
25CH ₄ /35CO /40H ₂ EQR = 0.440	76	Vel m/s	248		129	121	153	60	11	19
		P bar	0.361		0.183	0.176	0.156	0.141	0.137	0.187

10 ANALYSIS OF LOW TEMPERATURE TESTS

This section examines the pressures obtained from the low temperature results.

10.1 PEAK PRESSURES OBTAINED

The results are presented in Table 8 below in a similar way to those for high temperature. A similar interpretation is also applicable. Note that a blank indicates the pressure was too low to measure.

Table 8 Summary of test result pressures - low temperature tests (NB. Kulite 6 pressures also presented separately in section 11).

Mixture	Test No.	Eq. Ratio	CH ₄ (vol%)	CO (vol%)	H ₂ (vol%)	KU0 - KU1 highest pressure (barg)	KU6 - KU9 highest pressure (barg)	KU10 peak pressure (barg)
CH ₄	52	0.650	100	0	0	0.394	0.214	0.177
CH ₄	53	0.810	100	0	0	0.831	0.672	0.514
CH ₄	54	0.506	100	0	0	0.102	0.062	-
CH ₄ /H ₂	55	0.600	60	0	40	0.514	0.302	0.350
CH ₄ /H ₂	56	0.500	60	0	40	0.123	0.082	0.093
CH ₄ /H ₂	57	0.705	60	0	40	1.415	3.105	1.668
CH ₄ /H ₂	58	0.510	40	0	60	0.182	0.157	0.176
CH ₄ /H ₂	59	0.410	40	0	60	0.064	0.030	0.037
CH ₄ /H ₂	60	0.590	40	0	60	0.542	0.604	0.640
H ₂	61	0.450	0	0	100	1.826	2.818	2.739
H ₂	62	0.350	0	0	100	0.502	0.319	0.349
H ₂	63	0.285	0	0	100	0.278	0.159	0.157
CO/H ₂	64	0.513	0	40	60	3.402	15.118	18.228
CO/H ₂	65	0.402	0	40	60	0.292	0.181	0.192
CO/H ₂	66	0.352	0	40	60	0.464	0.440	0.496
CO/H ₂	67	0.393	0	40	60	0.898	0.658	0.783
CO/H ₂	68	0.397	0	60	40	1.386	0.666	0.680
CO/H ₂	69	0.438	0	60	40	1.904	2.712	2.281

CO/H ₂	70	0.323	0	60	40	0.317	0.156	0.166
CH ₄ /CO/H ₂	71	0.465	25	35	40	0.584	0.425	0.414
CH ₄ /CO/H ₂	72	0.496	25	35	40	1.322	0.782	0.815
CH ₄ /CO/H ₂	73	0.428	25	35	40	0.326	217	244

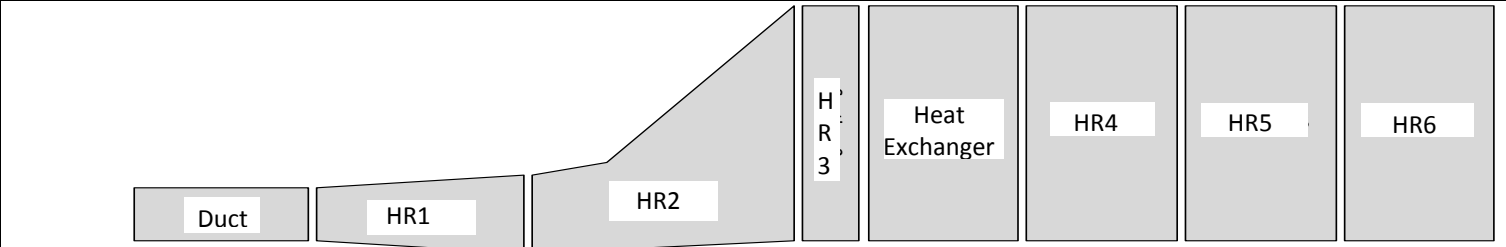
Table 9 Distribution of peak pressures and flame velocity estimates through duct and HRSG system - low temperature tests.

HRSG Tests	Test No.									
100CH ₄ EQR = 0.650	52	Vel m/s	227		156	-	90	52	8	-
		P bar	0.394		0.238	-	0.211	0.142	0.156	0.177
100CH ₄ EQR = 0.810	53	Vel m/s	286		279	63	47	30	9	-
		P bar	0.831		0.596	-	0.479	0.476	0.451	0.514
100CH ₄ EQR = 0.506	54	Vel m/s	110		52	10	8	-	-	-
		P bar	0.102		-	-	0.069	0.062	0.050	-
60CH ₄ /40H ₂ EQR = 0.600	55	Vel m/s	232		157	38	51	155	10	-
		P bar	0.514		0.298	-	0.215	0.239	0.259	0.350
60CH ₄ /40H ₂ EQR = 0.50	56	Vel m/s	161		74	14	20	58	39	3
		P bar	0.123		0.097	-	0.085	0.070	0.061	0.093
60CH ₄ /40H ₂ EQR = 0.705	57	Vel m/s	345		221	106	142	251	45	42
		P bar	1.415		-	-	0.816	3.105	1.174	1.668
40CH ₄ /60H ₂ EQR = 0.510	58	Vel m/s	185		109	24	31	108	12	12
		P bar	0.182		0.151	-	0.167	0.124	0.123	0.176
40CH ₄ /60H ₂ EQR = 0.410	59	Vel m/s	112		35	7	11	17	-	-
		P bar	0.064		0.034	-	-	0.021	0.019	0.037
40CH ₄ /60H ₂ EQR = 0.590	60	Vel m/s	238		148	161	139	153	13	-
		P bar	0.542		0.410	-	0.334	0.377	0.412	0.640

Table 9 Distribution of peak pressures and flame velocity estimates through duct and HRSG system - low temperature tests (cont).

HRSG Tests	Test No.										
100H ₂ EQR = 0.450	61	Vel m/s	256		145	152	296	214	28	18	
		P bar	1.826		2.164	-	1.063	1.487	1.542	2.739	
100H ₂ EQR = 0.350	62	Vel m/s	196		89	83	97	45	13	-	
		P bar	0.502		0.304	-	0.222	0.267	0.245	0.349	
100H ₂ EQR = 0.285	63	Vel m/s	133		81	70	54	40	12	-	
		P bar	0.278		0.136	-	0.134	0.140	0.129	0.157	
40CO/60H ₂ EQR = 0.513	64	Vel m/s	384		414	135	277	1475	1862	1876	
		P bar	3.402		7.247	-	5.871	6.496	7.312	18.172	
40CO/60H ₂ EQR = 0.303	65	Vel m/s	196		89	43	20	44	20	-	
		P bar	0.402		0.161	0.166	0.179	0.148	0.156	0.192	
40CO/60H ₂ EQR = 0.352	66	Vel m/s	212		105	59	78	86	51	48	
		P bar	0.464		0.339	0.286	0.297	0.320	0.327	0.497	
40CO/60H ₂ EQR = 0.393	67	Vel m/s	268		153	152	113	126	24	-	
		P bar	0.898		0.514	0.412	0.445	0.481	0.503	0.783	
60CO/40H ₂ EQR = 0.397	68	Vel m/s	245		131	112	122	165	27	23	
		P bar	1.386		0.476	0.406	0.402	0.433	0.586	0.680	
60CO/40H ₂ EQR = 0.438	69	Vel m/s	322		201	139	154	195	192	74	
		P bar	1.904		1.734	0.652	0.988	2.712	1.317	2.281	
60CO/40H ₂ EQR = 0.323	70	Vel m/s	214		83	70	67	60	28	14	
		P bar	0.317		0.149	0.152	0.174	0.135	0.135	0.166	

Table 9 Distribution of peak pressures and flame velocity estimates through duct and HRSG system - low temperature tests (cont).



HRSG Tests	Test No.		Duct	HR1	HR2	HR3	Heat Exchanger	HR4	HR5	HR6
25CH ₄ /35CO /40 H ₂ EQR = 0.465	71	Vel m/s	279		155	103	131	100	107	-
		P bar	0.584		0.355	0.305	0.358	0.272	0.310	0.414
25CH ₄ /35CO /40 H ₂ EQR = 0.496	72	Vel m/s	318		177	161	152	214	30	-
		P bar	1.322		0.498	0.572	0.298	0.446	0.556	0.815
25CH ₄ /35CO /40 H ₂ EQR = 0.428	73	Vel m/s	236		127	102	80	55	13	22
		P bar	0.326		0.210	0.201	0.169	0.195	0.174	0.244

11 DISCUSSION OF PHASE 2 AND WP 2.3 RESULTS

11.1 AUTO-IGNITION ISSUES

Before discussing the main body of results, it is important to note that some of the mixture cases were more difficult to undertake due to auto-ignition, i.e. ignition occurring before the application of the spark. This was referred to as a pre-ignition event and was assumed to arise from hot surface ignition for certain mixtures, particularly those involving hydrogen and carbon monoxide. This was only observed for the high temperature tests.

It is recognised that pure hydrogen represents a more reactive fuel than methane and also hydrogen/methane mixtures but it has also been shown during the earlier phase of the project [8] that carbon monoxide in combination with hydrogen is as reactive as pure hydrogen. This latter behaviour was also seen during the phase 1 WP2.3 HRSG study and the behaviour manifests itself in the pre-ignition of the hot fuel/air mixture within the ironwork of the duct/HRSG system without the aid of an active ignition spark.

This behaviour has been observed in the present Phase 2 tests, both with pure hydrogen and hydrogen/carbon monoxide mixtures. These events can be damaging to the test rig since the flame may attach itself to some of the components which protrude into the flow resulting in a hot flame jet impinging on the more delicate fin structures of the tube bank. Such stable flames would be much hotter than the calculated normal exhaust temperature, e.g. 1700 °C, and, due to their non-transient nature, can melt the fin structures in a few seconds. Modifications to the ignition control system were introduced to detect such pre-ignition events by monitoring certain thermocouples for significant temperature deviations from the average baseline prior to active ignition, in order to immediately shut down the fuel injection.

Due to these pre-ignition events, certain of the planned EQR values at the higher end for pure H₂ and H₂/CO mixtures could not be achieved and the EQR values already quoted were the result of this limitation. It should be noted that this limitation was also a function of the temperature condition of the test rig prior to a test. For example, if a lower EQR test had already been completed, the internal surfaces could be 100 - 200 °C hotter than a test starting from cold, with the result that an ignition test may suffer pre-ignition through starting from a hotter condition. The exact conditions prevailing at the moment of pre-ignition could not be determined with certainty since the target EQR value had not been fully reached and held for a number of seconds. However, an approximate value can be determined from the mass flows prevailing at the moment of ignition as evidenced by the first appearing flame signals within the test rig.

Table 10 below gives the data from all of the auto-ignition tests for future reference.

Table 10 Details of tests where an auto-ignition occurred.

Mixture	Test No.	Approximate EQR at ignition	Ignition location	Comment
100% H ₂	33	0.275	?	rpm at 11800
100% H ₂	34	0.387	?	rpm at 11800
40 CO/ 60H ₂	41	Not measurable	?	rpm at 11500
40 CO/ 60H ₂	43	Not measurable	?	rpm at 11500
60 CO/ 40H ₂	44	Not measurable	Tube bank	rpm at 11500
60 CO/ 40H ₂	45	Not measurable	Tube bank	rpm at 11500
60 CO/ 40H ₂	46	Not measurable	Tube bank	rpm at 11500
40 CO/ 60H ₂	51	Not measurable	Tube bank	rpm at 11500

The upstream video camera looks toward the entry of the heat exchanger tube bank and in a few of the pre-ignition cases this camera was triggered during the pre-ignition event. In those cases, it was clear that the pre-ignition was arising within the tube bank and, where available, this has been indicated in the table. A number of sequential frames are shown in Figure 11 below, from Test 44 showing the development of the flame kernel within the body of the finned tube array as it moves upstream toward the camera.

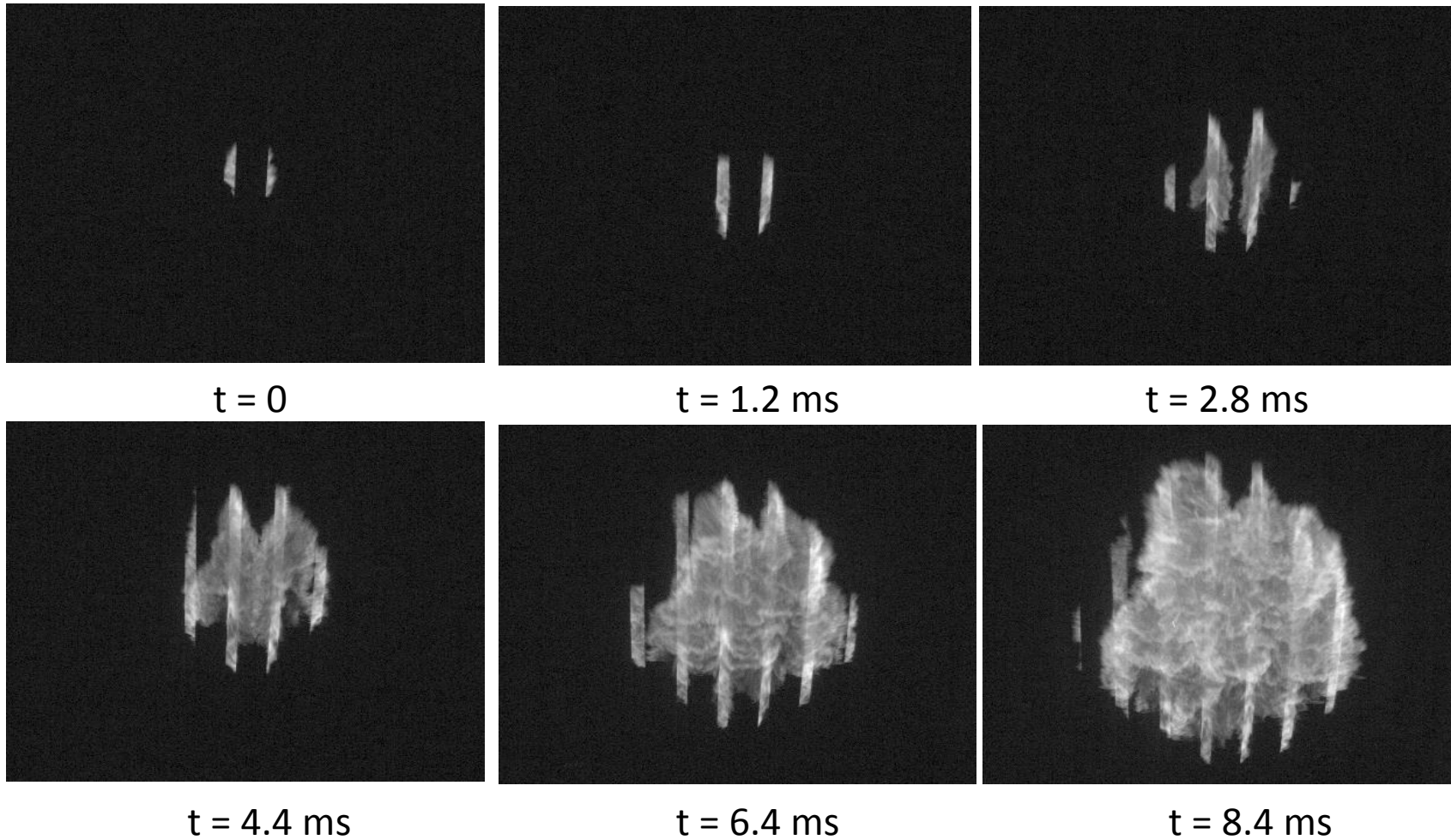


Figure 11 Frame sequence from upstream high- speed camera showing the progress of flame following an auto-ignition event from Test 44. (This record confirms that ignition originates within finned tube array, with flame progressing back upstream between t=0 and t= 8.4 msec).

The causes for the pre-ignition events with H₂ and H₂/CO mixtures are unknown at this stage of the work. The exhaust temperature on the centreline of the circular duct for an engine running at 11800 rpm is just above 500 °C and at 11500 rpm, is just below 500 °C. Hydrogen is known to have an auto-ignition temperature of 500 - 550 °C and, whilst it is likely that the fins of the heat exchanger tubes will be close to the maximum exhaust temperature, there is still a temperature deficit to be accounted for. There are other components within the system which are likely to be running at similar temperatures, e.g. the flame ionisation sensor tips on the upstream 'rake' devices, but no camera evidence was identified to implicate these as possible ignition points. It should be noted that the carbon steel fins within the HE had a significant degree of rust coverage and a mechanism involving this surface interaction remains to be investigated. Reference to the lowering of auto-ignition temperatures by ferric oxide associated with rusty surfaces is limited but a reference from 1972 [9] indicates that this was demonstrated for a number of organic species with AIT values above 290 °C.

It is also noted that the Fischer–Tropsch process is a collection of chemical reactions that converts a mixture of carbon monoxide and hydrogen into liquid hydrocarbons. These reactions occur in the presence of metal catalysts, such as iron, typically at temperatures of 150–300 °C (302–572 °F) and pressures of one to several tens of atmospheres. They are highly exothermic. These conditions would appear to exist in the tube bank, which is constructed from iron- based tubes and fins; it is therefore considered possible that such reactions may be occurring within the HRSG leading to auto-ignitions at the reduced temperatures observed, but only for H₂/CO mixtures.

11.2 EXAMINATION OF THE PRESSURE GENERATION ZONE FOR WP 2.3 AND PHASE 2 TESTS

It has been mentioned previously that the main region of pressure generation is the heat exchanger and the turbulent region immediately downstream of the heat exchanger in the HR4 section, and this is monitored by Kulite 6 (KU6) for the Phase 2 work (or occasionally KU7) and KU2 or KU4 for Phase 1 WP 2.3. The KU6 (or KU2/KU4) pressure is not necessarily the highest pressure recorded in the system, since this pressure may sharpen through normal shock behaviour and also increase in magnitude for the reflected wave. The peak value of the pressure in the HR4 section however, is an important indicator of the rapidity of combustion in this region and deserves particular highlighting for discussion. A further measure is the width of this pressure pulse, since the rate of energy release in this region is expected to be related to the peak pressure which results. Also noting that the impulse is a measure of the total energy release, which is a good measure of explosion intensity.

Table 11 and Table 12 below collect this data together for the WP 2.3 and Phase 2 results at the higher temperature and separately for the low temperature tests of Phase 2. These include the pressure pulse half width, defined as the pulse width at half the peak pressure.

Table 11 Comparison of HR4 peak pressures and pressure pulse half widths for WP 2.3 (labelled 1) and Phase 2 (labelled 2) tests - high temperature.

HRSG Test (WP 2.3 / 2)	Mixture	Eq. Ratio	CH ₄ (vol%)	CO (vol%)	H ₂ (vol%)	Pressure at Heat exchanger (barg)	Pressure pulse half width (msec)
32 (2)	CH ₄	0.490	100	0	0	0.042 (KU6)	-
30 (2)	CH ₄	0.640	100	0	0	0.150 (KU6)	23.7
31 (2)	CH ₄	0.790	100	0	0	0.683 (KU7)	6.6
22 (2)	CH ₄ /H ₂	0.325	40	0	60	-	-
21 (2)	CH ₄ /H ₂	0.420	40	0	60	0.071 (KU6)	19.1
3 (1)	CH ₄ /H ₂	0.550	40	0	60	0.35 (KU2)	7.2
6 (1)	CH ₄ /H ₂	0.550	40	0	60	0.39 (KU2)	9.5
23 (2)	CH ₄ /H ₂	0.560	40	0	60	0.282 (KU6)	8.2
24 (2)	CH ₄ /H ₂	0.580	40	0	60	0.385 (KU6)	6.5
4 (1)	CH ₄ /H ₂	0.620	40	0	60	0.63 (KU2)	3.6
7 (1)	CH ₄ /H ₂	0.620	40	0	60	0.59 (KU2)	5.6
25 (2)	CH ₄ /H ₂	0.640	40	0	60	0.392 (KU6)	8.5
5 (1)	CH ₄ /H ₂	0.650	40	0	60	1.41 (KU2)	1.4
8 (1)	CH ₄ /H ₂	0.650	40	0	60	1.30 (KU2)	1.5
26 (2)	CH ₄ /H ₂	0.650	40	0	60	0.659 (KU6)	1.7
29 (2)	CH ₄ /H ₂	0.510	60	0	40	0.117 (KU6)	28.0
27 (2)	CH ₄ /H ₂	0.590	60	0	40	0.262 (KU6)	1.9
28 (2)	CH ₄ /H ₂	0.710	60	0	40	0.534 (KU6)	6.4
39 (2)	H ₂	0.350	0	0	100	0.145 (KU6)	18.9
38 (2)	H ₂	0.420	0	0	100	0.472 (KU6)	5.8
9 (1)	H ₂	0.470	0	0	100	0.39 (KU2)	7.2
36 (2)	H ₂	0.480	0	0	100	0.475 (KU6)	3.6/4.9
10 (1)	H ₂	0.510	0	0	100	0.92 (KU2)	3.4
35 (2)	H ₂	0.520	0	0	100	0.710 (KU6)	1.4/3.1
37 (2)	H ₂	0.540	0	0	100	1.626 (KU6)	0.4/0.7
40 (2)	H ₂	0.540	0	0	100	1.639 (KU6)	0.4/0.6/2.4
12 (1)	H ₂	0.550	0	0	100	1.79 (KU2)	0.7/0.3

42 (2)	CO/H ₂	0.400	0	40	60	0.21 (KU6)	-
50 (2)	CO/H ₂	0.350	0	40	60	0.015 (KU6)	-
47 (2)	CO/H ₂	0.434	0	60	40	0.433 (KU6)	4.5
48 (2)	CO/H ₂	0.340	0	60	40	0.038 (KU6)	-
13 (1)	CO/H ₂	0.510	0	60	40	0.42 (KU4)	5.5
15 (1)	CO/H ₂	0.560	0	60	40	0.52 (KU4)	5.3
16 (1)	CO/H ₂	0.590	0	60	40	0.59 (KU4)	6.2
17 (1)	CO/H ₂	0.620	0	60	40	1.21 (KU4)	2.6/3.9

In some of the cases above the combustion event is so weak that it is difficult to assign a value and the peak pressure column is left empty. In the very weak pressure cases the pulse half width is also sometimes difficult to determine.

In general the peak pressure magnitudes and the pulse half widths show a strong correlation for the reasons described above. In some cases two values are shown in the pulse width column and this indicates that within the time scale of combustion immediately downstream of the heat exchanger, around 1 -1.5 m in dimension, more than one pressure pulse can be seen in the pressure traces. It is possible that this could be accounted for by variability in combustion intensity within and beyond the heat exchanger, with each surge contributing a pressure surge on its own timescale.

For completeness the Table 12 results show a similar correlation between KU6 pressure and the associated pressure pulse half width as did Table 10 for the high temperature tests, and the same reasoning would apply. The very unique result for Test 64 will be discussed separately.

Table 12 Comparison of HR4 peak pressures and pressure pulse half-widths. Phase 2 tests - low temperature.

HRSG Test (Phase 2)	Mixture	Eq. Ratio	CH ₄ (vol%)	CO (vol%)	H ₂ (vol%)	Pressure at Heat exchanger (KU6, barg)	Pressure pulse half width (msec)
52	CH ₄	0.650	100	0	0	0.142	-
53	CH ₄	0.810	100	0	0	0.303	9.8
54	CH ₄	0.506	100	0	0	0.380	-
55	CH ₄ /H ₂	0.600	60	0	40	0.210	8.5/5.5
56	CH ₄ /H ₂	0.500	60	0	40	0.053	15.9
57	CH ₄ /H ₂	0.705	60	0	40	0.760	3.2/4.2
58	CH ₄ /H ₂	0.510	40	0	60	0.104	24
59	CH ₄ /H ₂	0.410	40	0	60	0.023	-
60	CH ₄ /H ₂	0.590	40	0	60	0.376	6.6
61	H ₂	0.450	0	0	100	1.487	0.5/0.6

62	H ₂	0.350	0	0	100	0.266	5.8
63	H ₂	0.285	0	0	100	0.115	-
64	CO/H ₂	0.513	0	40	60	6.49	0.14/0.13
65	CO/H ₂	0.303	0	40	60	0.150	15
66	CO/H ₂	0.352	0	40	60	0.320	4.5
67	CO/H ₂	0.393	0	40	60	0.480	4.9/7.6
68	CO/H ₂	0.397	0	60	40	0.435	6.5/7.6
69	CO/H ₂	0.438	0	60	40	1.412	0.9/3.9
70	CO/H ₂	0.323	0	60	40	0.110	20
71	CH ₄ /CO/H ₂	0.465	25	35	40	0.240	13.5
72	CH ₄ /CO/H ₂	0.496	25	35	40	0.440	8.5
73	CH ₄ /CO/H ₂	0.428	25	35	40	0.156	28
74	CH ₄ /CO/H ₂	0.462	25	35	40	0.161	23
75	CH ₄ /CO/H ₂	0.492	25	35	40	0.199	14
76	CH ₄ /CO/H ₂	0.446	25	35	40	0.119	22

The confirmation of the simple correlation between the above KU6 peak pressures and the half width of the associated pulses is represented graphically in Figure 12 below. This measure of the fast combustion timescale is also apparent from a review of the video records. Note that the data below excludes the special case of Test 64.

It has been emphasised that the origin of the pulse half width lies in the rate of combustion in the immediate heat exchanger downstream region and this is a region which is monitored by the downstream high-speed video camera. Over the WP2.3 Phase 1 and Phase 2 tests, this camera has recorded the emergence of flame from the tubes of the heat exchanger at a rate of between 2500 and 3000 fps, which gives a sufficiently good resolution to evaluate the progress of the flame from its first appearance around the base of the heat exchanger tubes to around the top of the chamber. It is considered that this time period is that associated with most of the generation of pressure within the system and therefore is also intimately associated with the rate of turbulent combustion in this important region.

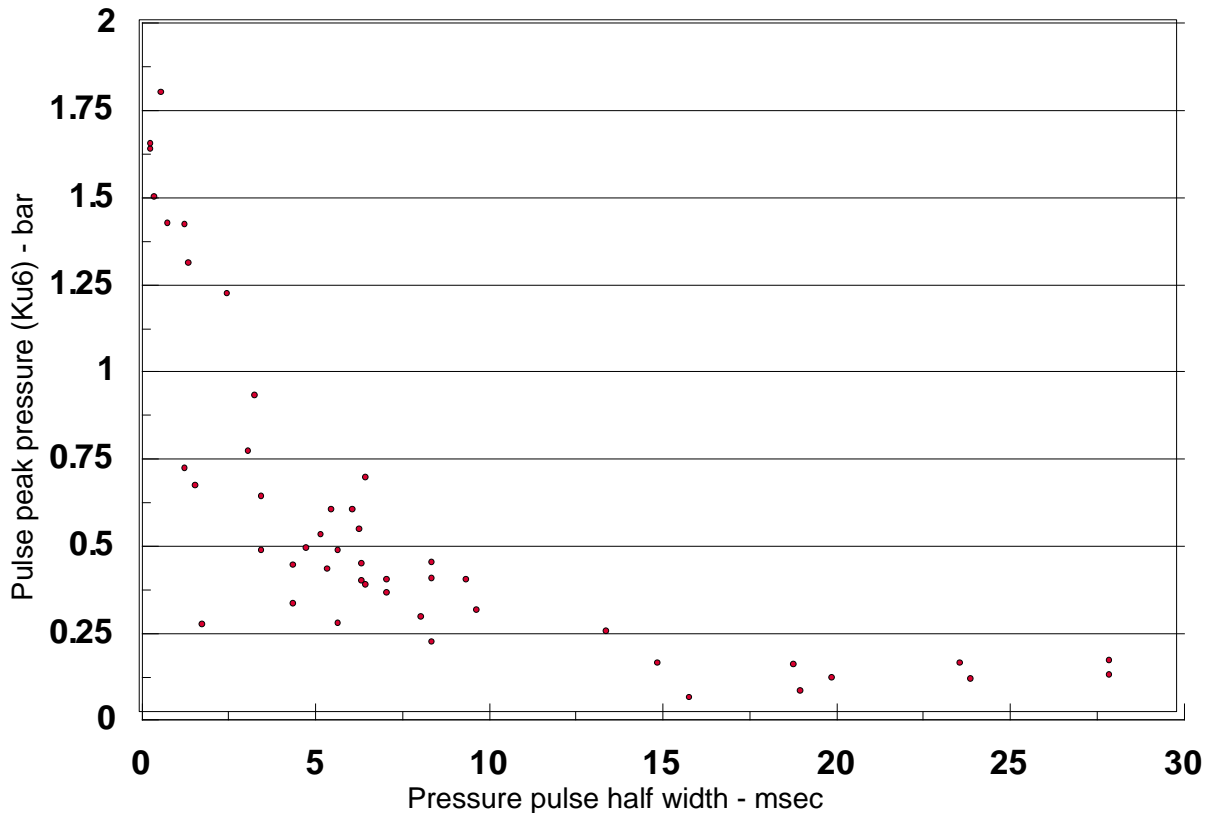


Figure 12 Graph of the data of Table 10 and Table 12 between the KU6 peak pressure and its associated pulse half width.

It is therefore of interest to determine if the correlation between the pressure pulse half width and peak pressure shows a similar behaviour to that of the variation of peak pressure and flame progress time from the bottom to top of the HRSG on first emergence. Similarity should allow us to conclude that the peak pressure and combustion rates in this region are correctly linked.

The extraction of data from the video record is illustrated in Figure 13, which is a sequence of frames from Test 40. In this case the flame progress time is around 1.6 msec. This is a short time period and the majority of such times are in the range of 3 - 10 msec, however some progress times can be as long as 30 msec, as the example for Test 29 shows in Figure 14. In this latter case the KU6 peak pressure is weak at 0.117 barg. It is clear from this video that the vertical progression of the flame in the tube bank leads the flame progression downstream of the tube bank (see the bright fingers along the top). This means that the vertical flame propagation is driven by combustion in the tube bank and not in HR4. Of course the flame propagation in HR4 still has a strong effect on the peak pressure measured in HR4.

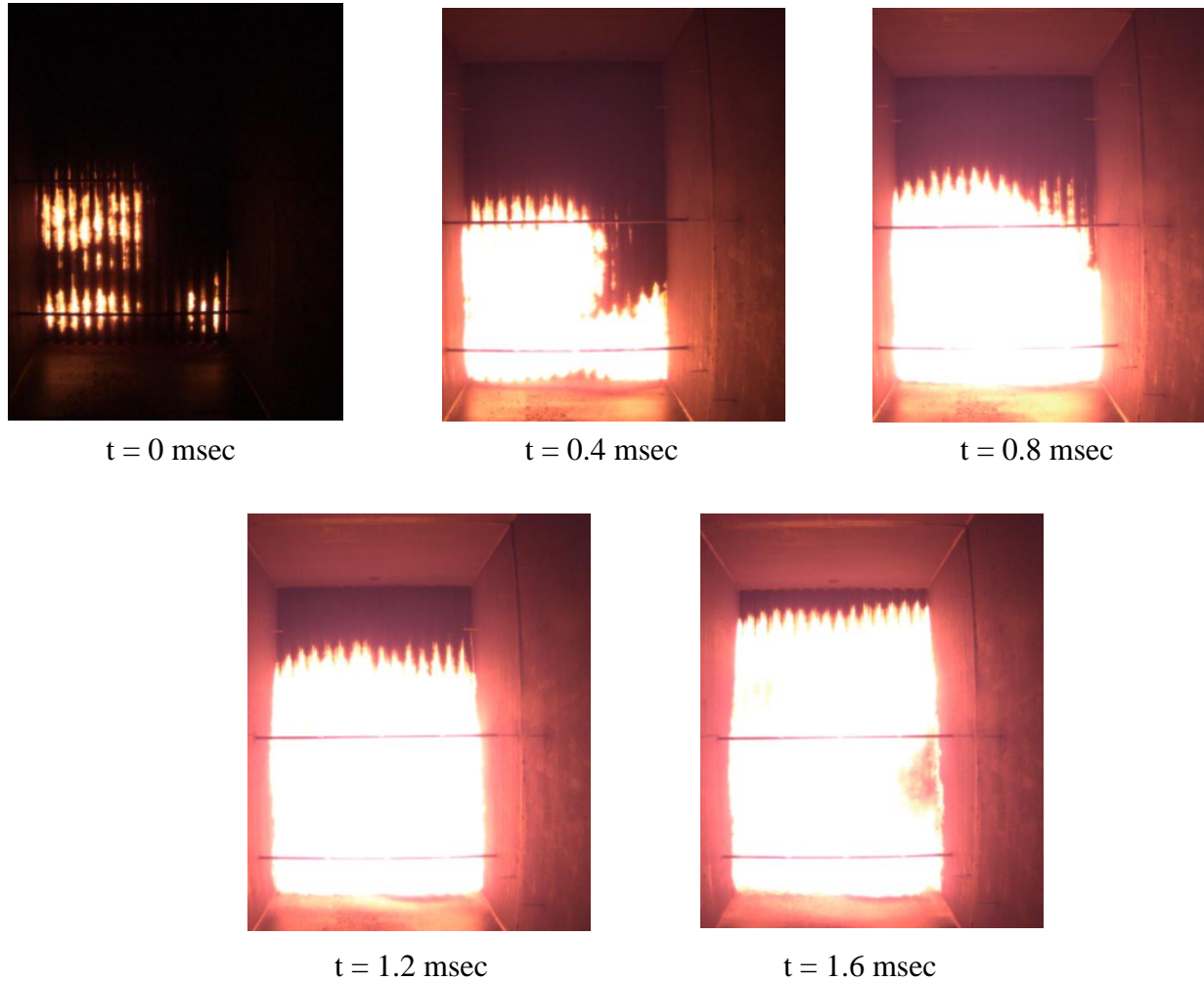


Figure 13 Video record from downstream high- speed video camera looking at flame emergence from the heat exchanger. Illustration of flame timings extracted from this record for Test 40 for flame progressing from bottom to top of HRSG - time is approximately 1.6 msec for this case.

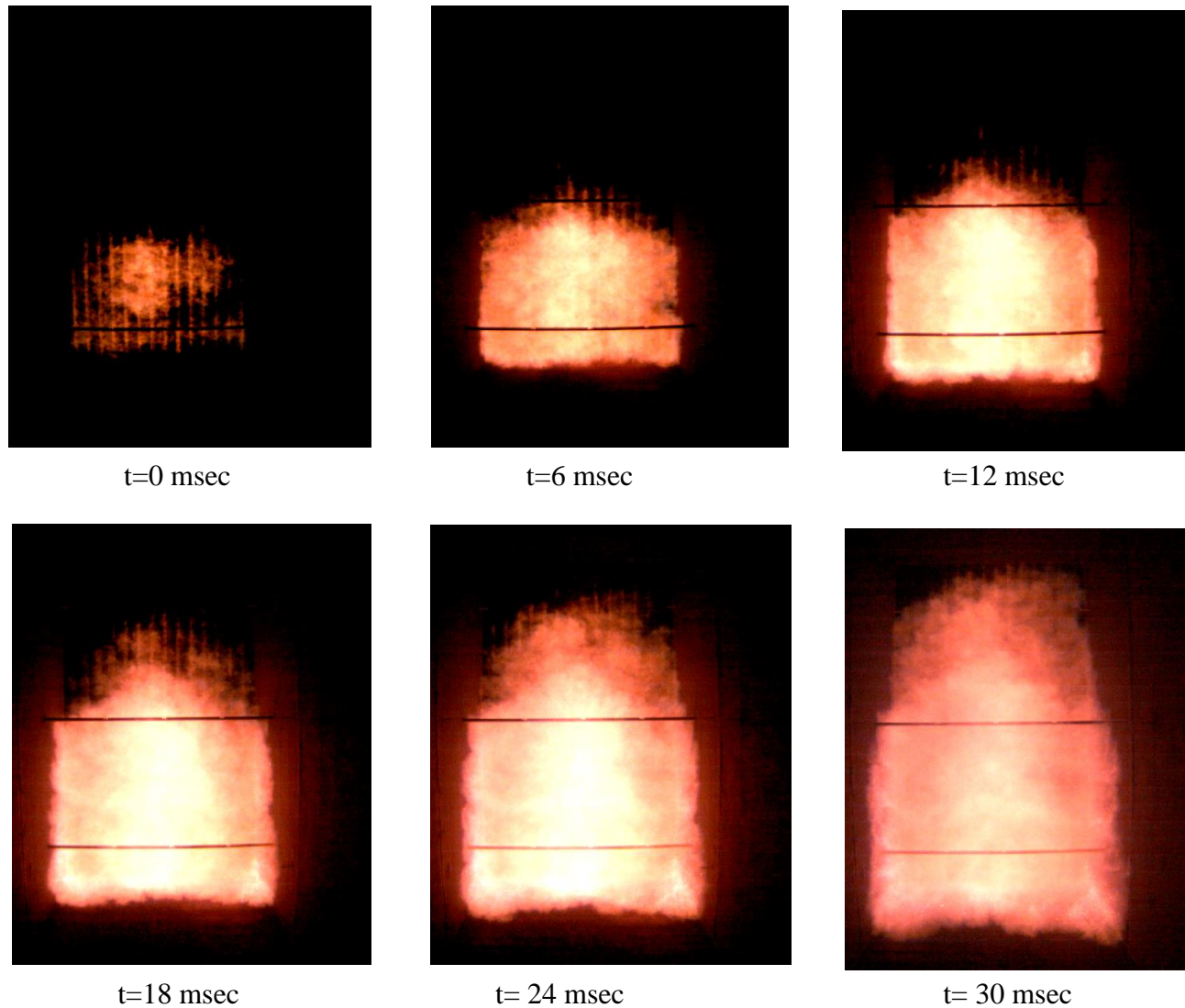


Figure 14 Video record from downstream high- speed video camera looking at flame emergence from the heat exchanger. Illustration of flame timings extracted from this record for Test 29 for flame progressing from bottom to top of HRSG - time is approximately 30 msec for this case.

The majority of video files arising from the WP2.3 and Phase 2 work have been examined in the same way as for Figure 13 and this data has been linked with the corresponding peak pressure data in the heat exchanger region e.g. KU6 data for Phase 2. Figure 15 plots this peak pressure data against the video timing data.

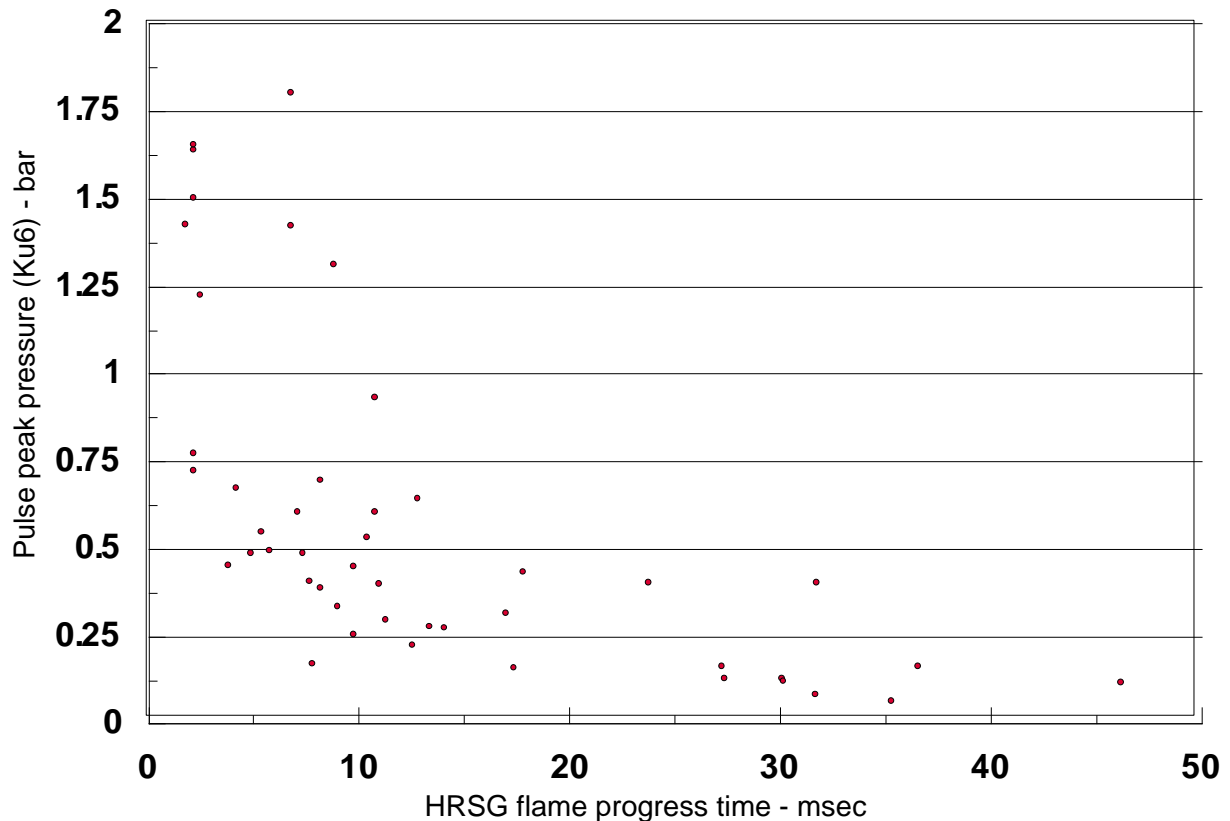


Figure 15 Variation of heat exchanger peak pressure wave amplitude (KU6 for Phase 2, KU2 or KU4 for WP 2.3) with flame progress time from video record.

As with Figure 12 shown previously, the data shows a measure of scatter but still allows the conclusion to be drawn that weak pressure pulses are associated with slow rates of turbulent combustion within the immediate downstream region. A further point to make in this connection is that all of the cases reviewed are associated with composition, EQR and temperature since the engine exhaust mass flows are the same. In addition both high and low temperature exhaust data has been combined. A final point to note is that no consideration has been given in this work to the mechanical response of the large HRSG structure to the relatively short duration pressure pulses observed. With the data now developed from this work, studies such as FE analysis are now on a stronger footing to explore the potential damage which may actually result from these events.

11.2.1 The special case of Test 64

Test 64 was the first of the proposed group of low temperature tests involving a 40%CO /60%H₂ mixture and followed from two high temperature tests (42 and 50) with the same mixtures.

Table 13 shows the first pressure peak amplitudes recorded within the HR4 region from KU6 for these three tests. Tests 42 and 50 show very modest peak pressures in this generation region and

did not provide a suggestion of the very fast combustion rate which would be seen for Test 64, with the consequent exceptionally high peak pressure of 6.49 bar recorded on KU6. Table 8 has shown that the end plate pressure recorded on KU10 was 18.2 barg.

Table 13 Summary of KU6 pressures recorded for the 40 CO/60 H2 mixtures.

Test	Mixture	EQR	CH ₄ , %	CO, %	H ₂ , %	Peak pressure bar
42	CO/H ₂	0.400	0	40	60	0.21 (KU6)
50	CO/H ₂	0.350	0	40	60	0.015 (KU6)
64	CO/H ₂	0.511	0	40	60	6.49 (KU6)

The sample video sequence of Figure 13 for Test 40 for flame progress from the bottom to top of the HRSG on its first emergence from the heat exchanger indicates one of the higher combustion rate cases, which produced a KU6 peak pressure of 1.64 barg. This can be compared with the corresponding sequence of Figure 16 for the case of Test 64, which shows a flame progress time of 0.8 msec. It is impossible to tell if detonation starts in the tube bundle or in HR4. More than likely detonation occurs in HR4 where there are no length-scale limitations to the development of a detonation wave.

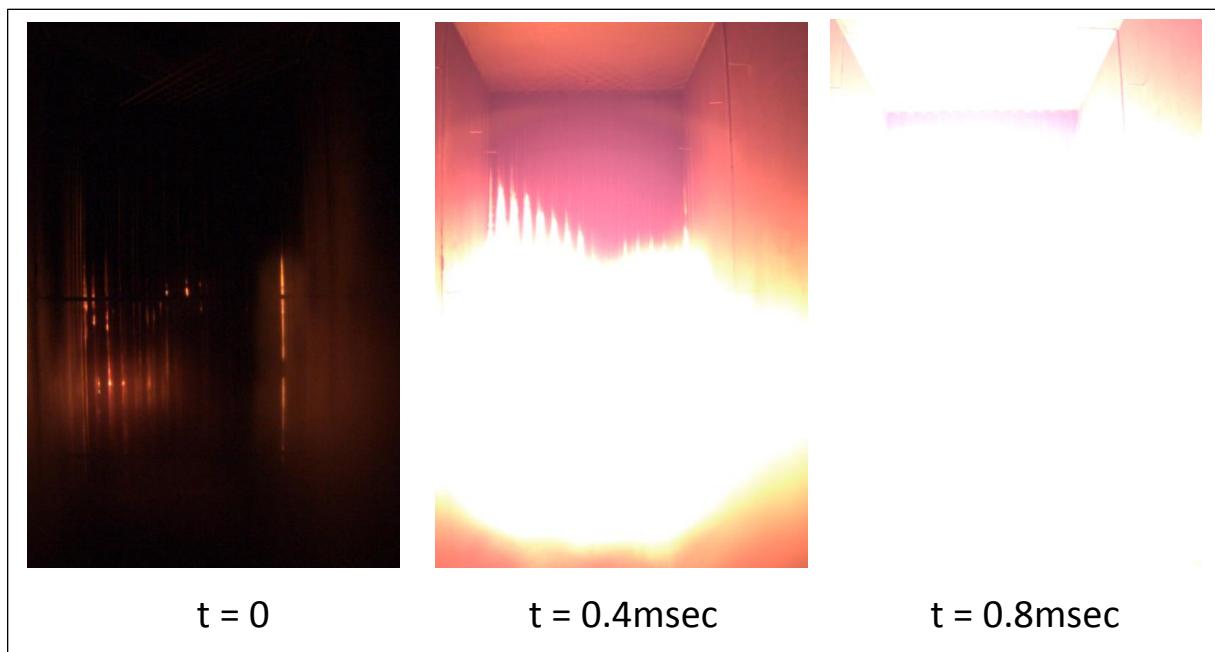


Figure 16 Flame progress sequence on first emergence from heat exchanger for Test 64.

Table 9 indicates that the estimated flame speeds within the HRSG section are close to 2000 m/s, which is consistent with development of a detonation event occurring in the region between the

heat exchanger and the end plate. Further evidence of this comes from an examination of the relationship between the flame arrival downstream and the corresponding pressure wave. Figure 17 below shows the passage of flame across IP 23 (at 19,985 mm) and the recorded pressure step at KU9 (at 20,575 mm). The pressure wave speed under the conditions within the HRSG and at the KU9 pressure of 12.5 barg (13.5 bara) is calculated using normal shock theory as 1805 m/s. This implies a time separation between the IP signal at IP23 and the pressure signal at KU9 of 0.33 msec. This is consistent with the time separation observed in Figure 17 indicating that the passage of the pressure wave and flame-front are almost coincident, i.e. consistent with the passage of a detonation wave.

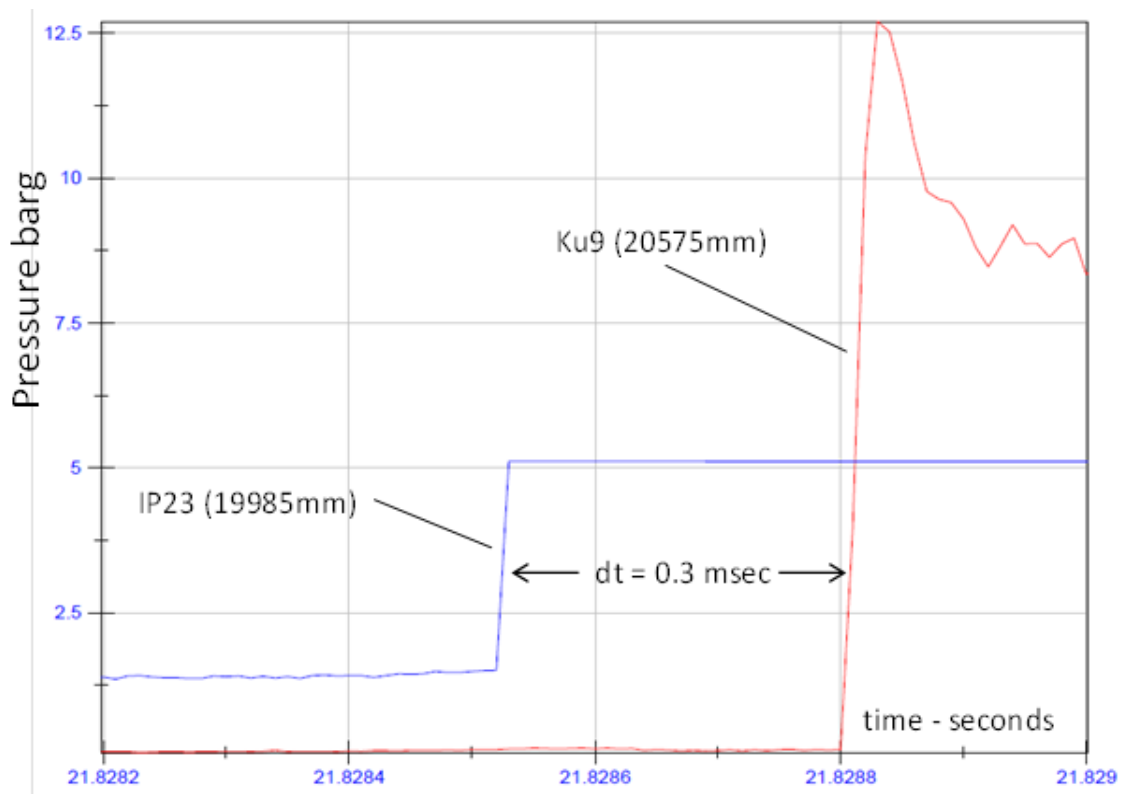


Figure 17 Indication of the arrival of the flame sensor and pressure wave signals at IP23 and KU9 respectively.

The 40CO/60H2 tests were performed at the higher temperature, where there was very little over-pressure and the maximum EQR tested was 0.443. The conditions for test 64 were 40CO/60H2 and an EQR of 0.51 at 320°C. Not only did this test have a higher EQR but the lower initial temperature would naturally produce more energetic explosions because of the higher fuel density. Although the laminar flame velocity was slightly higher (and the cell size smaller) at higher temperature, the density ratio across the flame was higher than at the lower initial temperature. Consequently flame acceleration would be promoted in the heat exchanger which governs the conditions in the highly turbulent unconfined downstream flow region where initiation took place. Detonation initiation within the heat exchanger is not possible because of the relatively small spacing between tubes compared to the expected detonation cell size. Consequently the most likely position for detonation initiation was at rakes 3 or 4 in section HR4, when the reflected lead shock arrived.

11.2.2 Graphical representation of pressure generation zone data at high temperature

Whilst the data tables above provide a numerical record of the pressures and flame arrival events, comparison of trends between different mixtures and temperatures are more easily revealed when results are compared graphically. These may involve different mixtures at the same temperature or the same mixtures at the two different temperatures used. The graphs below attempt to identify the main similarities and differences between the cases tested to allow an overview to be developed of the main influences in pressure generation and the operation limits which should be adhered to.

For some Phase 2 tests carried out, these were intended to extend the EQR range of the previous WP2.3 test regime and in these cases the full data set from WP2.3 has been included in the comparisons. All of the tests show a variation of downstream heat exchanger peak pressure (HR4 peak pressure) as a function of mixture EQR and can be related back to the data from Table 10 and Table 11.

Figure 18 shows the high temperature comparison of 60H₂/40CH₄ and 40H₂/60CH₄. Although the 60H₂/40CH₄ data set shows a degree of scatter, it is considered that there is sufficient difference between the two data sets to justify curve fitting the data sets separately. At EQR values below 0.55, the mixture behaviours cannot easily be separated but above this value, the higher H₂ content mixture appears more reactive as would be expected.

By way of an example of how the data could be used for comparing mixture scenarios; if a limiting pressure value of say 0.3 barg is chosen to identify an EQR limit for operation in industrial systems, but noting that this HR4 pressure may be doubled on reflection at the end plate. On this basis, Figure 18 suggests an EQR limit of 0.57 for both mixtures.

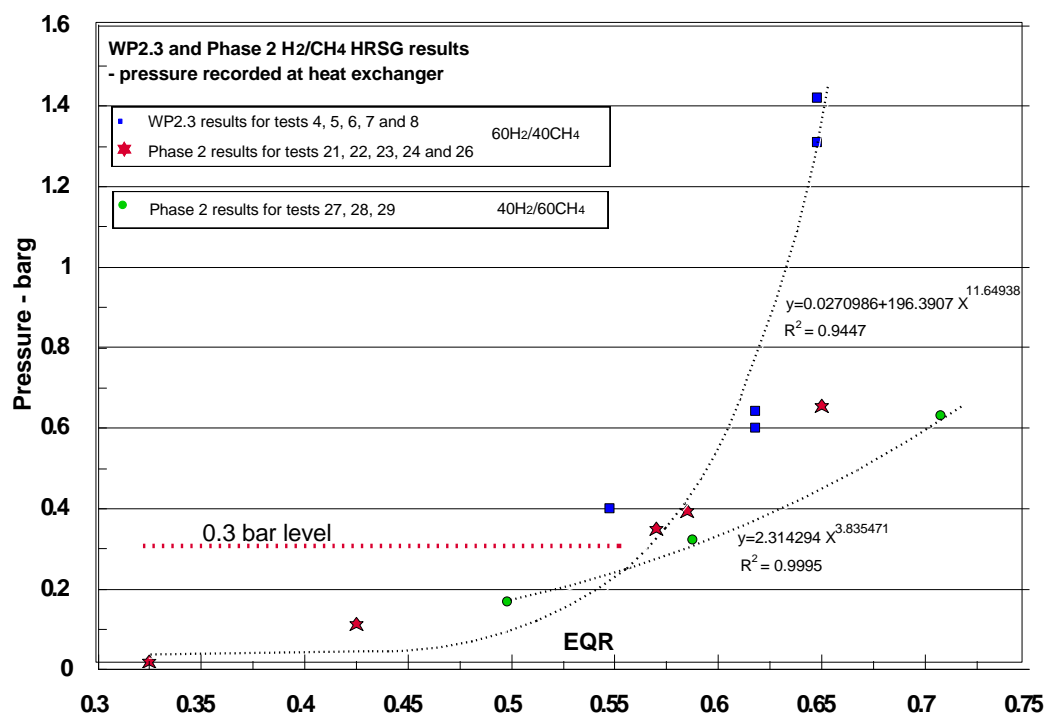


Figure 18 WP2.3 and Phase 2 data for HR4 peak pressures for 60H₂/40CH₄ compared with Phase 2 pressures for 40H₂/60CH₄ mixture at high temperature.

Figure 19 shows the corresponding high temperature comparison between 40H₂/60CO and 60H₂/40CO. In this case there is significant scatter in the data and at the EQR values tested for the 60% H₂ content, no distinction can be made from the 40H₂/60CO mixture. For this reason, only a single best fit curve has been drawn through the data. For these mixtures, an EQR limit of 0.5 is indicated.

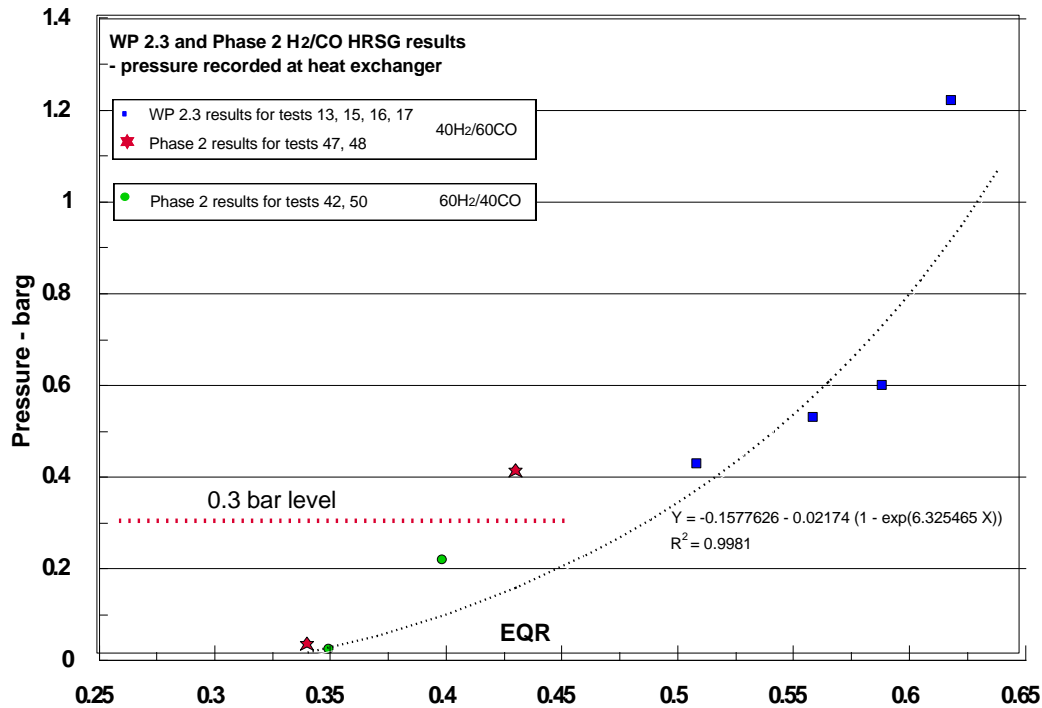


Figure 19 WP2.3 and Phase 2 data for HR4 peak pressures for 40H₂/60CO compared with Phase 2 pressures for 60H₂/40CO mixture.

11.2.3 Graphical comparisons of pressure generation zone data at high and low temperature for Phase 2

Further comparisons arise between cases at the different exhaust temperatures used and these are presented in the following.

Figure 20, using 40%CH₄/60%H₂ and 60%CH₄/40%H₂ mixtures at the lower temperature can be compared with the higher temperature data for the same mixtures from Figure 17. At this lower temperature there is a definite difference in peak pressure variation with EQR between the two mixtures, which suggests that the higher H₂ content mixture has the greater reactivity of the two. For the 60% H₂ mixture an EQR limit of 0.56 is indicated, as for the high temperature cases, whereas for the 40% H₂ mixture a higher limit of around 0.62 is suggested, which is higher than that indicated on the comparable high temperature cases, although the latter carried greater data scatter.

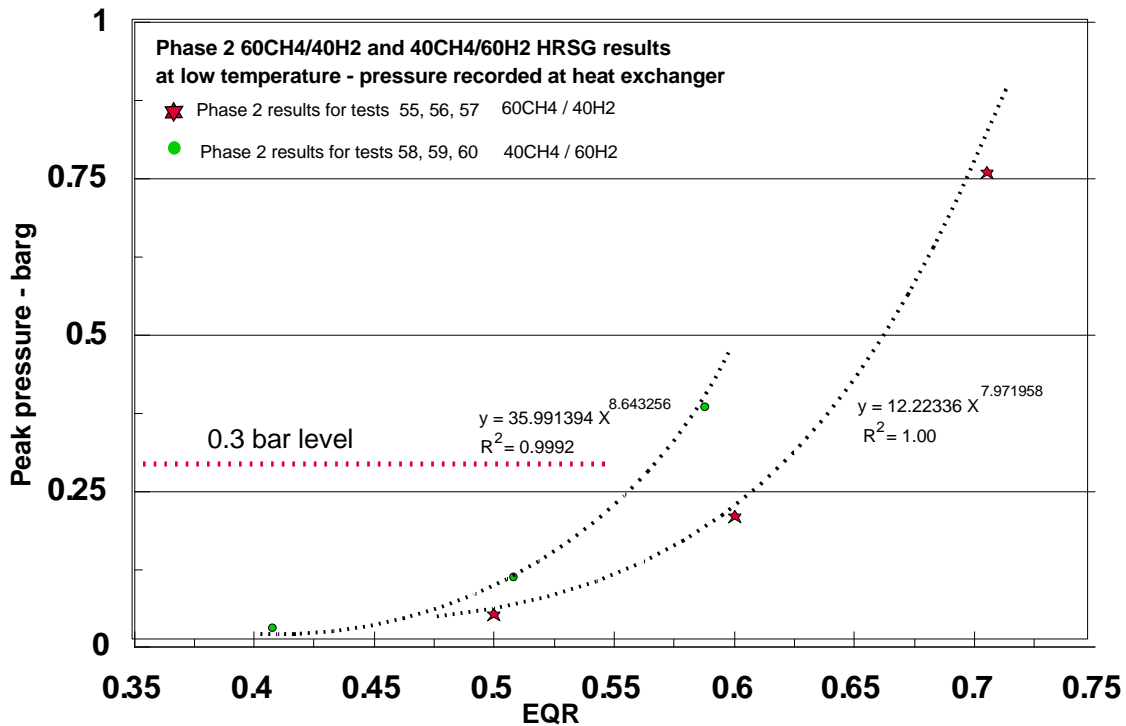


Figure 20 Comparison of Phase 2 data for HR4 peak pressures for 40%CH₄/60%H₂ and 60%CH₄/40%H₂ at low temperature.

Figure 21 shows the comparison of pressure behaviour using 40%CO/60%H₂ and 60%CO/40%H₂ at the lower temperature. For the lower EQR range, the 60% H₂ mixture shows higher peak pressures, although this approaches, and may cross over, the 40% H₂ pressure curve. It is noted that the replacement of CH₄ by CO markedly reduces the EQR limit behaviour. For the 60% H₂ mixture this EQR value is around 0.35, whereas for the 40% H₂ mixture it is around 0.38. This difference between the H₂/CH₄ and H₂/CO mixtures appears to be greater at lower temperature than at the higher temperature.

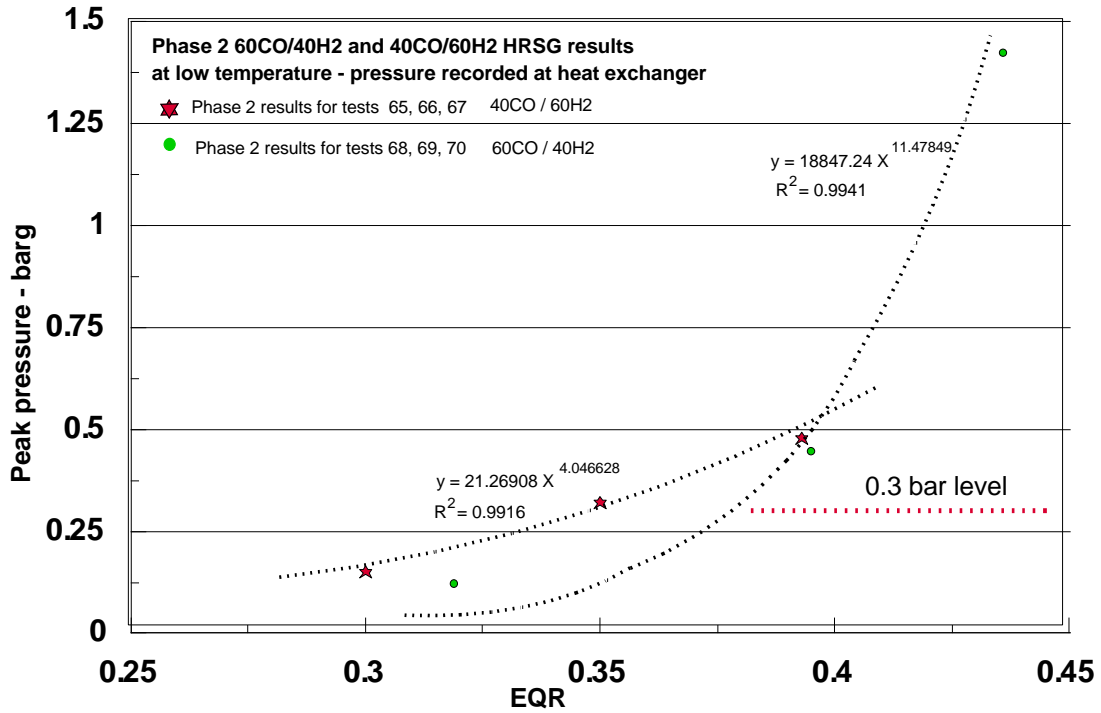


Figure 21 Comparison of Phase 2 data for HR4 peak pressures for 40%CO/60%H₂ and 60%CO/40%H₂ at low temperature.

The next set of graphs compare the pressure behaviour of the same mixtures at high and low temperatures. Figure 22 shows the result for 100% CH₄.

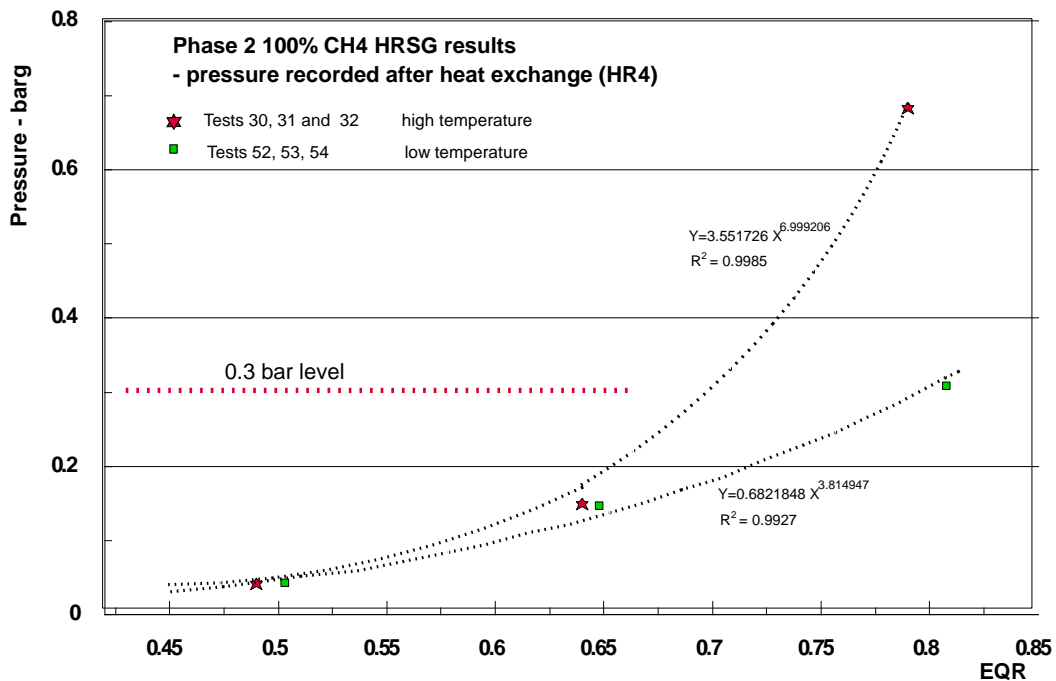


Figure 22 Comparison of Phase 2 data for HR4 peak pressures for 100% CH₄ at high and low temperature.

For EQRs below 0.65 there is no effect of initial temperature on the measured peak pressure. Contrary to expectation, the lower temperature case shows a lower pressure than the high pressure curve over a similar EQR range. The assumption has been that at constant pressure, the higher molecular density at lower temperature would result in higher chemical rates of combustion. However, reaction rates are also affected by temperature and since peak pressures are connected with these rates, the interplay between the two opposing factors may work toward a lowering of rates with temperature for this mixture. Kinetic modelling developments by others may shed more light on these aspects. The suggested EQR limits for pure methane are suggested as 0.7 for the high temperature and 0.77 for the low temperature cases.

Again the peak pressure is not affected by temperature at low EQRs (below 0.35). By contrast, the 100% H₂ comparisons in Figure 23 show the opposite behaviour and also significantly lower limit EQR values. Figure 23 also incorporates the WP 2.3 data for H₂ at high temperature. For the low temperature case, an EQR limit of 0.36 is suggested, whereas for the high temperature case this would be 0.43.

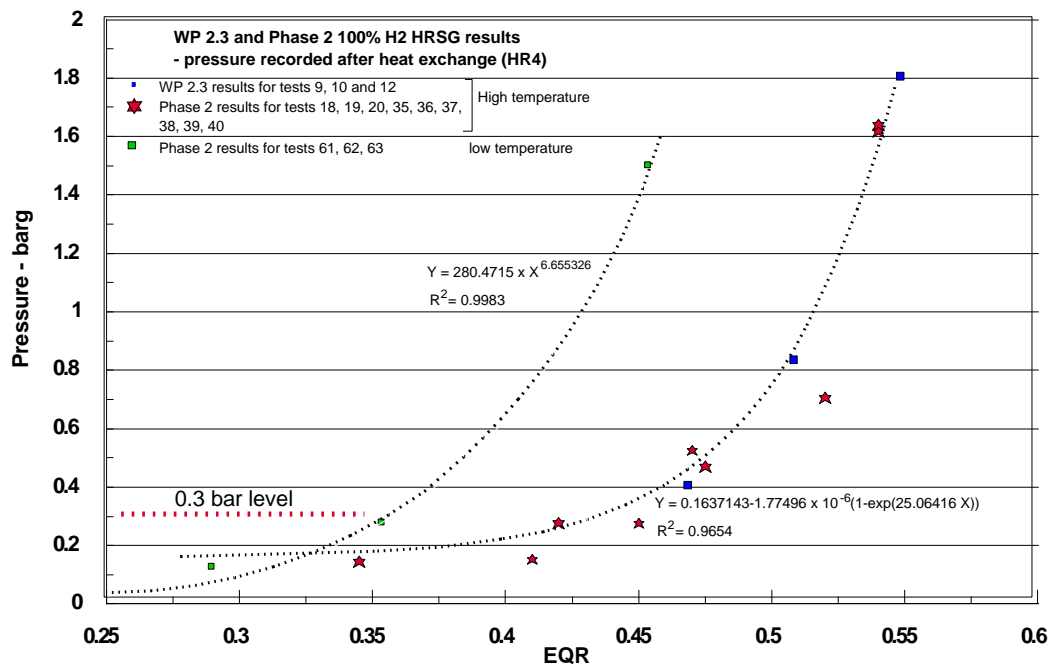


Figure 23 Comparison of WP2.3 and Phase 2 data for HR4 peak pressures for 100% H₂ at high and low temperature.

Figure 24 revisits the high temperature 60%CH₄/40%H₂ case, this time comparing it with its low temperature equivalent. The differences between the two temperatures are not so clear cut for this mixture but the R² value for the curve fits indicate a good level of confidence in the representation of the behaviour and therefore justifies treating their behaviour as distinct. The crossing point of the curves happens to occur around the 0.3 barg level therefore suggesting an EQR limit for both temperatures of 0.63. The graphs again imply that the variation of mixture reactivity via temperature and molecular density versus its variation via EQR is one which only appropriate modelling will properly reveal.

Note that it is not expected that the curves can simply be extrapolated back to zero pressure, as the expectation is that at some lower EQR value ignition will not occur (LFL), at which point the curves cease to have any meaning in respect of pressures generated.

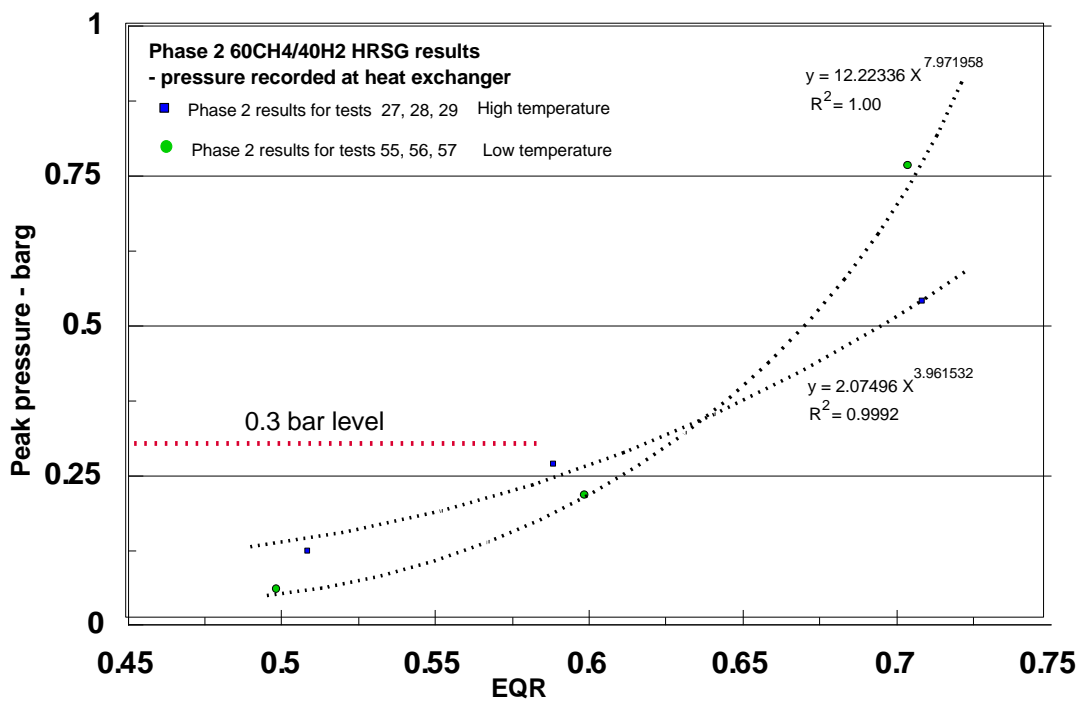


Figure 24 Comparison of Phase 2 data for HR4 peak pressures for 60%CH4/40%H2 at high and low temperatures.

The effect of increasing the amount of hydrogen to make a 60%H₂/40%CH₄ mixture is revealed in Figure 25, where the results include the WP2.3 test cases for this mixture.

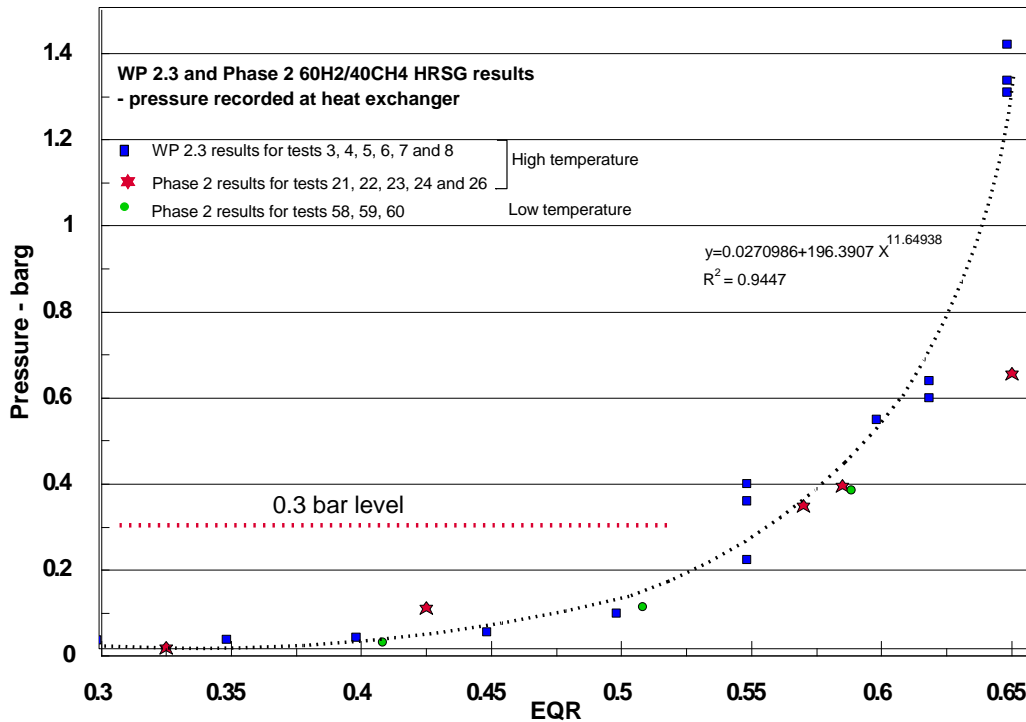


Figure 25 Comparison of WP 2.3 and Phase 2 data for HR4 peak pressures for 40%CH4/60%H2 at high and low temperatures.

For this comparison the data sets cannot be separated and only a single curve fit is provided. In this case an EQR limit value of 0.57 is indicated.

Figure 26 shows the high/low temperature comparison using 40%CO/60%H₂. The low temperature results were more easily obtained and were not prone to auto-ignition behaviour, therefore allowing a good curve fit to be presented. From the graph it appears that the high temperature data tends to be lower in peak pressure across the EQR range although the low peak pressures are being treated with caution, particularly in view of the detonation behaviour of Test 64 at low temperature at an EQR value of 0.513. The limit EQR value suggested by Figure 25 would be 0.35, based on the behaviour of the low temperature case, which would also be a conservative strategy for the high temperature mixture.

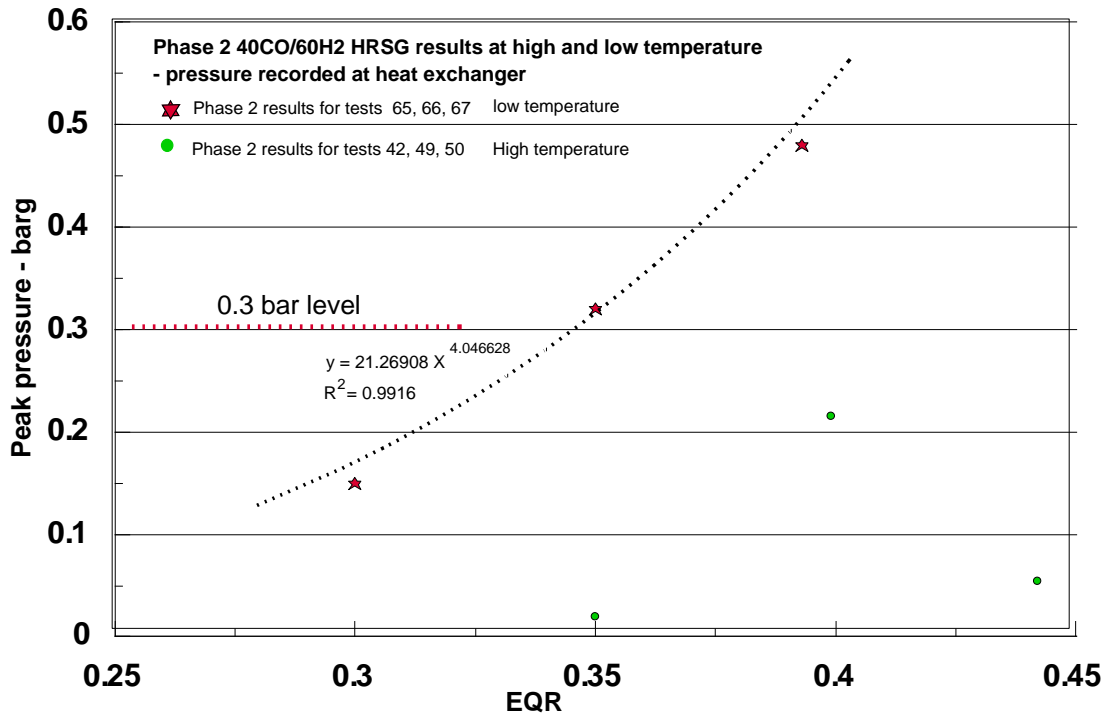


Figure 26 Comparison of Phase 2 data for HR4 peak pressures for 40%CO/60%H₂ at high and low temperatures.

Figure 27 shows the results for 60%CO/40%H₂ mixture and although Phase 2 provided only two data points at the higher temperature, there is more consistency in the behaviour of these. No curve has been drawn for these since only two points are available. The lower reactivity of the 40% H₂ case appears to result in slightly lower peak pressures for the same EQR meaning that at the low temperature a limit EQR value of around 0.38 can be taken, whilst for the high temperature it would be 0.39. The difficulties in working with H₂/CO mixtures at the higher temperature have been discussed previously and a further outcome has been that some of the results under this condition have been variable and more difficult to interpret.

The ternary mixture result for 25%CH₄/35%CO/40%H₂ is shown in Figure 28. The ratio of CO/H₂ is close to 1:1 and in the absence of CH₄, the mixture might be expected to behave somewhere between the 40CO/60H₂ and 60CO/40H₂. In fact one can see that the peak pressures in Figure 28 are significantly lower than either of those of Figure 26 and Figure 27 for the low temperature cases and this is also true with some certainty for the high temperature case of Figure 27 showing the mitigating effect of methane in the mixture. The data of Figure 28 also shows good consistency providing confidence in the curve fit via the R² value. Limit EQR values for this mixture would be deduced as 0.48 for low temperature and around 0.52 for high temperature.

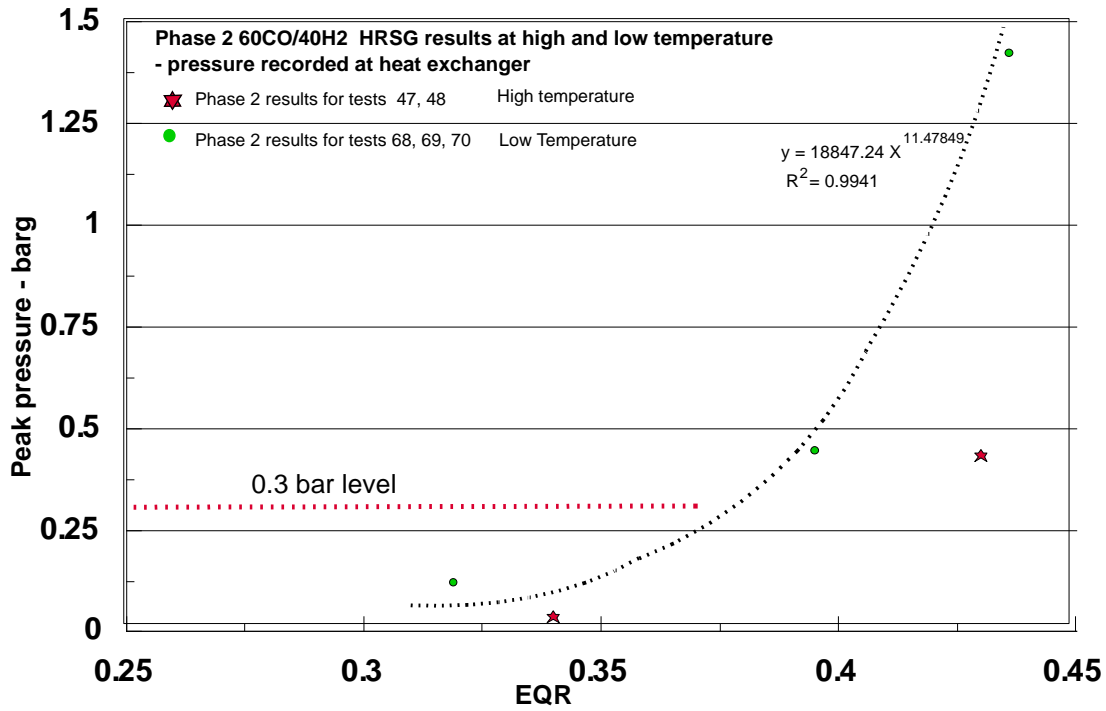


Figure 27 Comparison of Phase 2 data for HR4 peak pressures for 60%CO/40%H2 at high and low temperatures.

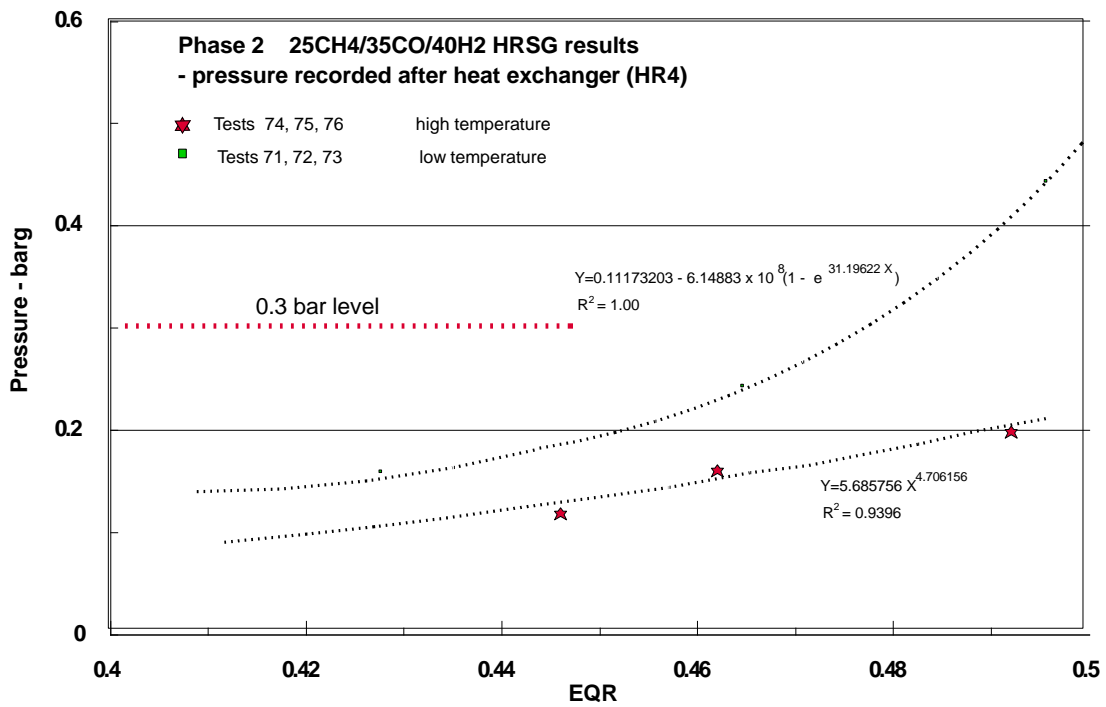


Figure 28 Comparison of Phase 2 data for HR4 peak pressures for 25%CH4/35%CO/40%H2 at high and low temperatures.

12 RIG DE-COMMISSIONING PROCEDURE

This section describes the steps that will be taken to de-commission (mothball) the ETI test rig should further commercial work not be forthcoming within a reasonable time period from completion of the Phase 2 test programme. The proposed procedures should allow the rig to be maintained in a near- operational state for up to two years, without the need for more extensive de-commissioning procedures being necessary. This will enable experiments to be undertaken with 30 days' notice. The key rig systems will remain in place and be maintained in an operational state. All measurement instrumentation installed on the duct and HRSG will be removed and placed into the spray booth building. The flammable gases (methane and hydrogen) and the toxic (carbon monoxide) inventory will be removed from the test site. Some butane inventory (~55%) will remain in the bulk tank (subject to other maintenance tasks being undertaken). This will enable the engine to be run every two to three months. The oxygen bulk tank will be left with some inventory to facilitate purging and also to prevent organic ingress. In order to do this, the statutory / good practice examinations (e.g. Pressure systems, lifting examinations and electrical) need to be kept in date. The spray booth will remain heated to maintain the stored equipment in an efficient state, as will the main control building.

12.1 DE-COMMISSIONING OF THE BUTANE STORAGE SYSTEM

The butane storage system consists of a standard nine tonne butane storage tank contained in a suitable enclosure and connected to the gas turbine through a pipework system. It supplies butane fuel to run the engine and is installed in accordance with the UKLPG code of practice 22, the existing pipework being thick walled tubing (schedule 80). The butane tank is also raised and anchored to the ground at one end. The installation work was undertaken by companies certified to undertake LPG work, including pipework. A certified company was also used to pressure test and certify the final installation, which was completed in January 2018.

The following will be undertaken: - Keep the PSSR working examinations up to date. Inspect pipework during engine running. Ensure daily security checks are made. Operate butane valves during engine runs and check tank level gauges and associated instrumentation. Vegetation management needs to be checked as part of engine run exercise. Also need to follow maintenance regime on the bulk tank pump and engine butane pump.

12.2 DE-COMMISSIONING OF THE VIPER GAS TURBINE

The gas turbine is a Rolls-Royce Viper type 301 jet engine operating without the convergent jet nozzle in place. Consequently the engine produces a hot exhaust gas stream at minimal back pressure with an oxygen concentration of approximately 17%. The engine was modified initially by Reaction Engines to run on liquid butane instead of aviation fuel. It is controlled by a high- pressure fuel pump which controls the flow of butane to the engine, and hence its speed. The engine also has an oil supply which has to be topped up manually as required. The engine is turned over to start it using a 24 volt battery supply. The engine is housed within a blast walled test area providing partial protection from the weather.

The following will be undertaken: Run engine every two to three months to maintain bearing lubrication and also to provide a hot gas stream to dry out the rig. The engine intake needs blanking

off to protect the engine from the weather when it is not being run. The oil sump can be left with oil in it, sufficient to allow the engine to be turned over periodically on the starter motor. The engine starter batteries will be kept on trickle charge.

12.3 DE-COMMISSIONING OF THE TEST RIG AND HRSG

The test rig is shown in Figure 1 of the report, whilst detailed drawings of the key components are shown in Figure 2 to Figure 4. The initial sections of the duct including the diverter and gas injection tubes are made from stainless steel and are housed within the blast protected area and the purpose built enclosure. They are reasonably well protected from the weather, apart from the two exhausts from the diverter which need protective covers fitting over them.

The expansion section, the tube bank and the HRSG are manufactured from various carbon steels, hence may rust if exposed to inclement weather. The exhaust stack on the end of the HRSG is particularly vulnerable to the ingress of water and must therefore be protected with a suitable cover. There are also numerous instrument ports throughout the rig, which need to be sealed in order to avoid water ingress. Periodic running of the engine will be undertaken to dry out the test rig should it become apparent that water ingress is proving a problem.

12.4 DE-COMMISSIONING OF THE GAS AND OXYGEN DELIVERY SYSTEMS

The gas and oxygen delivery systems each comprise two gas storage vessels with a total capacity of 440 litres, operating at pressures up to 200 barg. Each system has a Hale-Hamilton pressure regulator, a Coriolis flow meter and an Emerson flow control valve, all of which are operated remotely from the control room.

The following will be undertaken:- Empty flammable / toxic gases from bulk tank and purge with nitrogen. Leave nitrogen pressure of ~ 150 bars in bulk tank in order to permit functional testing of valves. Test valves and pressure regulator by injecting nitrogen into duct during engine testing. Also spray valve spindles with silicon grease or similar. Maintain working examination in accordance with PSSR. Remove flammables, toxics and nitrogen MCP from site. Check maintenance / cycling requirements of the Haskel boost pump.

Leave oxygen pressure of ~ 150 bars in bulk tank in order to permit functional testing of valves. Test valves and pressure regulator by injecting oxygen into duct during engine testing. Also spray valve spindles with approved oxygen lubricant. Maintain working examination in accordance with PSSR. Remove oxygen MCP from site. Check maintenance / cycling requirements of the Haskel boost pump.

Other related requirements are to isolate and drain the water supply, and to check and undertake maintenance requirements for the diesel- driven air compressor, including PSSR compliance.

12.5 DE-COMMISSIONING OF THE INSTRUMENTATION AND DATA ACQUISITION SYSTEM

The principal items of instrumentation fitted to the rig are the optical (IP and OP) sensors, the Kulite pressure transducers and the thermocouples. All of these sensors will be removed from the rig, checked for correct functioning and stored in a warm secure environment. The cabling fittings will be protected and any unused cabling removed from the system. The instrument ports on the rig will be sealed off.

The data acquisition system: some is housed in the spray booth in a relatively warm environment, and some is housed in the main control room in a thermostatically controlled temperature environment. The complete system will be powered down and left in situ. Site standard operating procedures will assure security of the buildings housing this equipment.

13 CONCLUSIONS

13.1 EVALUATION OF RESULTS OVERALL

The purpose of the Phase 2 tests has been to extend the mixtures and EQR values tested in WP2.3 to fill gaps in the data, and to extend the data to lower EQR values, which are consistent with the normal limits of industrial operations. The programme has been broadly successful in meeting this objective and the results carry a large degree of consistency with those of WP2.3, both in terms of continuity in behaviour in extending the WP2.3 results to lower EQR but also in the relationship of newly tested mixtures with similar mixtures previously tested.

Sensor performance has been generally good, particularly in view of the challenging test environment - both from the point of view of thermal stresses and also from often harsh weather conditions. Over all of the Phase 2 tests, and excluding thermocouple sensors, the flame and pressure sensors have yielded a useful measurement for 94% of the individual sensor measurements made.

The flame behaviour has reproduced that seen in the WP2.3 tests and the interpretation of the origin of the main pressure wave as being associated with the turbulent region immediately downstream of the heat exchanger has been reaffirmed. Combustion in this region has been semi-quantitatively related to the observed pressure pulse width in the same region as well as flame progress data extracted from the high speed video evidence. This has provided the necessary insight into possible mitigation methods and this may now be pursued in further work through limiting the amount of turbulent flammable gas entering the HRSG in the event of a flame-out event, or by burning such gas prior to its entry into the heat exchanger.

Consistency in behaviour over an EQR range for the same mixture has enabled a curve fit of peak pressure vs EQR to be generated for most of the cases studied and this now enables interpolation of results and extension to a wider range of EQR values than those tested.

One of the cases tested (Test 64) gave rise to a detonation event and this was against expectations based on similar mixtures previously tested. This provides a note of caution against extrapolating the existing data points much beyond their tested EQR range since for most mixtures, it is expected that there are strong non-linearities which develop at higher EQR values associated with flame acceleration. A basis for judging the range of safe operation is discussed in the following section.

13.2 SAFE OPERATING MODES FOR THE FUEL MIXTURES TESTED

Sections 11.2.2 and 11.2.3 have examined the variation of peak pressures arising in the HR4 region immediately downstream of the heat exchanger for a range of mixtures and at high and low temperature and drawn some basic conclusions on the limits of EQR values for each condition based on a HR4 peak pressure of 0.3 barg. The reasons for this choice are discussed in these sections. This level of HR4 peak pressure is also indicated on the graphs of Figures 14 - 24. For most of the data, curve fit equations were able to be provided to represent each case as a function of EQR and therefore alternative choices may readily be made based on these curves if alternative HR4 peak pressures need to be considered.

The EQR values determined in the previous sections are summarised in the Table 12 below.

Table 14 Summary of EQR limit values based on HR4 peak pressures of 0.3 barg.

Mixture, %	Exhaust Temperature	EQR limit value
100 CH ₄	HIGH	0.7
	LOW	0.77
100 H ₂	HIGH	0.43
	LOW	0.36
60 CH ₄ / 40 H ₂	HIGH	0.63
	LOW	0.63
40 CH ₄ / 60 H ₂	HIGH	0.57
	LOW	0.57
60 CO / 40 H ₂	HIGH	0.39
	LOW	0.38
40 CO / 60 H ₂	HIGH	-
	LOW	0.35
25 CH ₄ / 35 CO / 40 H ₂	HIGH	0.52
	LOW	0.48

High Temperature: ~ 520° C.

Low Temperature: ~ 320 °C.

The immediate conclusions to be drawn from this table are that the implied reactivities of the different mixtures are consistent with the previous WP2.3 observations and also with those of the report conclusions from ref. [8].

These can be summarised as follows:

1. Methane is the least reactive of the group, allowing the greatest EQR values to be used.
2. Increasing the hydrogen content in the methane mixture will increase the reactivity and reduce the value of any EQR limit value based on a chosen maximum explosion peak pressure level.
3. Carbon monoxide/hydrogen mixtures behave in a very similar way with respect to their contribution to the reactivity of the mixtures. In this regard 40%H₂/60%CO mixtures behave in a closely similar way to 60%H₂/40%CO mixtures. This is confirmed by the similar EQR limit values in Table 14, particularly for the low temperature cases, where the data is more complete.
4. Carbon monoxide/hydrogen mixtures behave in a similar way to pure hydrogen - again the low temperature EQR limit values provide an indication of this.

5. Methane provides a mitigating effect on the rate of combustion and therefore on the peak pressures developed. This is confirmed from the behaviour of the 25%CH₄ /35%CO/40%H₂ mixture and it would be reasonable to assume from Table 14, that as the methane content varies from 25% to 100%, the EQR limit value will vary from the indicated value of 0.77 at low temperature to around 0.35 for a CO/H₂ mixture.

It is also interesting to observe that there is a degree of similarity in the high and low temperature EQR limit values for a number of cases, despite the indications from the graphs of Sections 11.2.2 and 11.2.3 that there are usually distinct differences in peak pressure behaviour with change in temperature. Since the limit pressure has been set at 0.3 barg, this is usually at the lower end of the pressure vs EQR curve, whilst much of the divergence in the peak pressures occurs at the slightly higher pressures.

13.3 TEST RIG PERFORMANCE

The HRSG was designed and manufactured in accordance with [5] and commissioned as reported in [4, 6]. During the course of the Phase 2 test programme a detonation occurred (Test number 64), which resulted in higher than expected dynamic pressures being generated within the rig, together with the explosion relief panels opening and damage to the vent stack on the HRSG and the buildings around it. In the course of repair work several structural checks were carried out to provide assurance that the rig had not been permanently damaged beyond repair.

Details of the modelling work are given in Appendix 15.3, this was based upon the Finite Element modelling that had been done originally for the HRSG as described in [5]. In summary modelling of the peak pressure pulse showed that there was no plastic strain of the HRSG webbing beyond the 0.2% proof stress, and that the explosion relief panels could have open with a velocity not exceeding 75 m/s.

14 REFERENCES

- 1) ETI WP2, Task 2. Interim Project Report: Experimental results and detailed analysis. K.Moodie, B.C.R. Ewan et Al. MHU/15/138. 15th January 2016. (Restricted)
- 2). ETI Project Report: Experimental results, detailed analysis, evaluation and recommendations. K. Moodie, B.C.R. Ewan, H. Michels, M. Christodolou, W. Rattigan and J.T. Allen. MH/16/169. 27th February 2017. (Restricted)
- 3). Commissioning Report for WP2 Task 2 Test Rig. K. Moodie and B.C.R. Ewan. V.0.01. 9th May 2014. (Restricted)
- 4). HSL Commissioning Report for WP2 Task 3 Test Rig. K Moodie, BCR Ewan, W Rattigan and JT Allen. MH/16/28. 8th March 2016. (Restricted)
- 5). Basis of Design Document for HSL WP2 Task 3 HRSG Test Rig for ETI. Version V.0.11. K. Moodie. 20th July 2015. (Restricted)
- 6). Proposed ETI High Hydrogen Phase 2 Test Programme. K. Moodie, MSc and B.C.R. Ewan, PhD. EA/18/02 Rev: 2. 24/10/2018. (Restricted)
- 7). Re-commissioning report for the High Hydrogen Phase 2 project utilising the HRSG test rig. K. Moodie, MSc and B.C.R. Ewan, PhD. EA/18/29. (Restricted)
- 8). Results from IC WP2.1 Report, H. Michels. 2015. Imperial College London. (Restricted)
- 9). Auto-ignition temperatures of organic chemicals, Hidalgo, C.J., Clark, S. W., Chemical Engineering 79, 75 - 80 (1972).

15 APPENDICES

15.1 POSITION OF SENSORS ON EXPERIMENTAL RIG

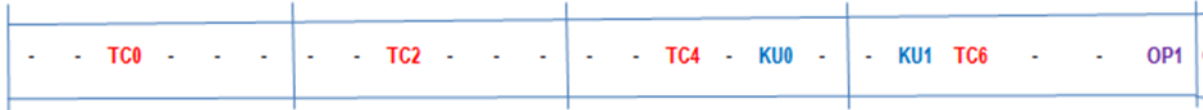


Figure A1 Circular Duct, right-hand side.

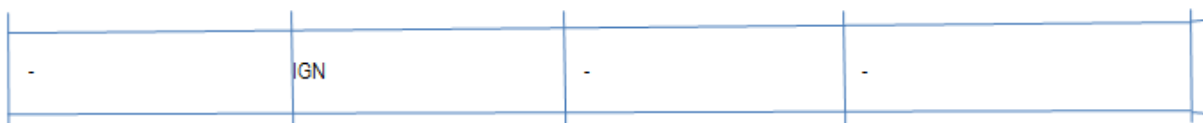


Figure A2 Circular duct, top.

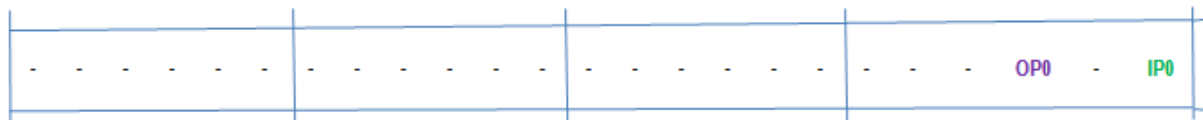


Figure A3 Circular duct, left-hand side (mirrored).

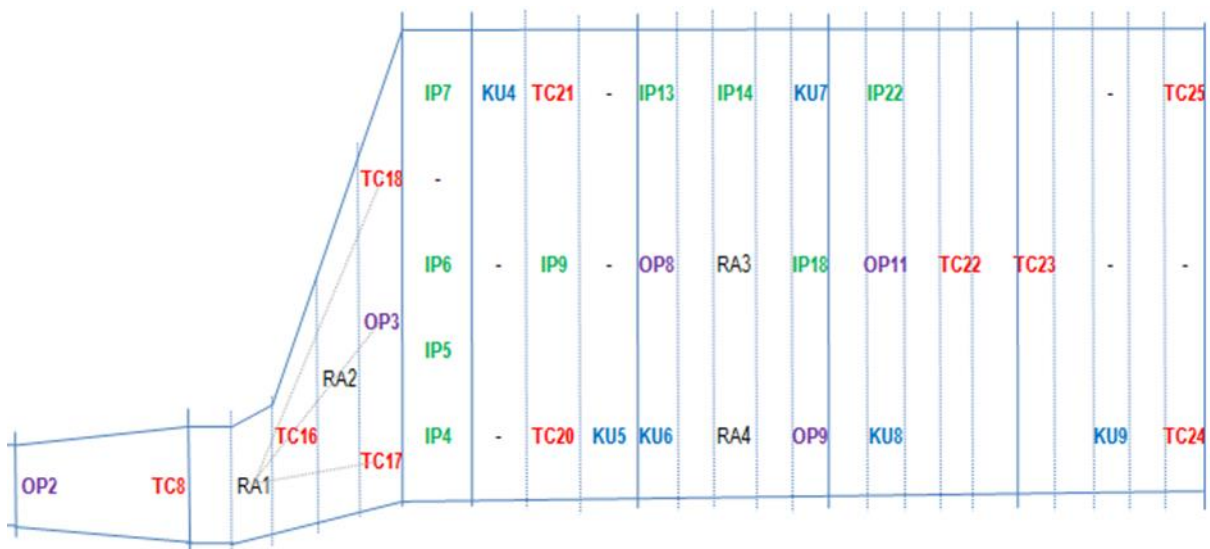


Figure A4 HRSG, right-hand side.

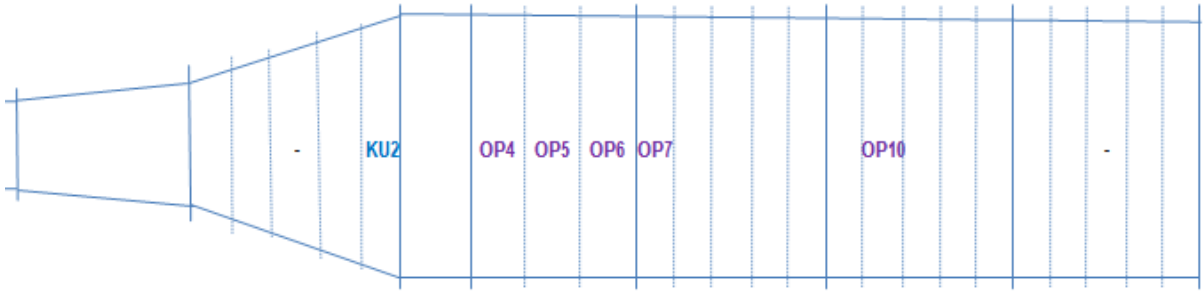


Figure A5 HRSG, top.

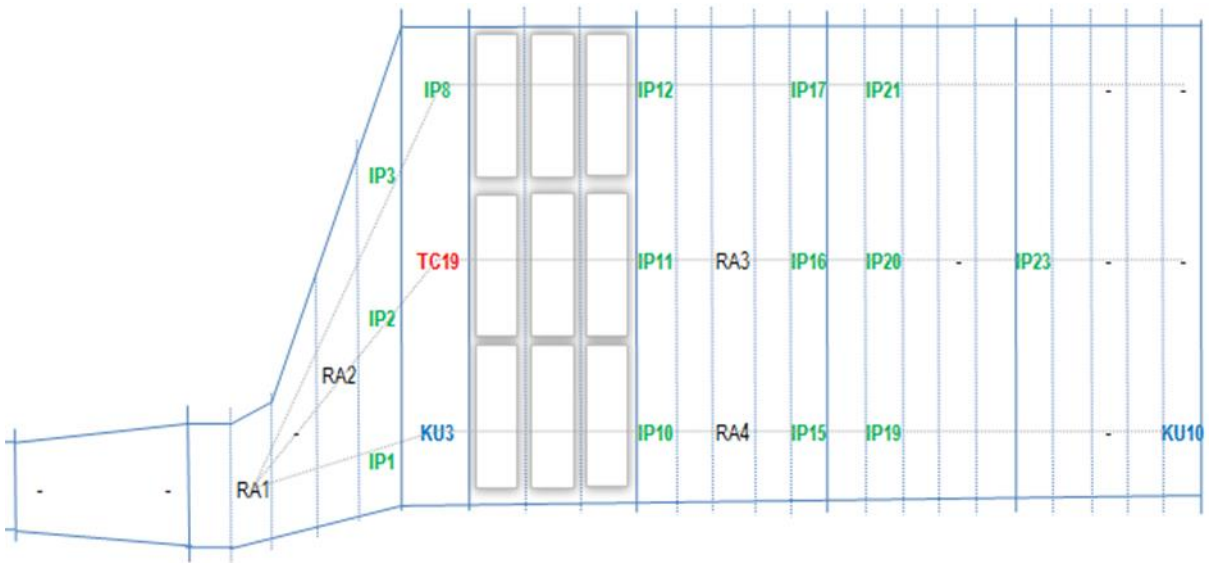


Figure A6 HRSG, left-hand side (mirrored).

15.2 5S IMPLEMENTATION DETAILS.

The ETI 5S project ran from June 2017 to May 2018. The aim of this project was to address concerns from the customer that the ETI Rig was not being managed and maintained to an acceptable standard, to identify and resolve any shortcomings, and to establish a system to sustain the resulting improvements. The 5S methodology was chosen as the tool to help facilitate the improvements. The 5S project comprised the following five stages:- SORT, STRAIGHTEN, SHINE, STANDARDISE & SUSTAIN. These were intended to address all the listed project objectives.

The physical scope of the project was:

- The ETI Rig and the surrounding external site;
- The Control Room in Building 66; and,
- The Spray Booth - Storage Building.

The objectives of the project were to:

- Remove waste and non-essentials through a 5S Red Tag Exercise;
- Address any Health & Safety (H&S) issues;
- Correct any structural and compliance inadequacies;
- Complete any ground and structural maintenance;
- Complete any cleaning requirements;
- Design new work area layouts, if needed, to support delivery;
- Purchase any supporting equipment for the new layouts;
- Reorganise the contents and label home positions;
- Introduce signage and other visual management solutions;
- Introduce Work Area Standards;
- Appoint a Work Area Owner to oversee the Standards;
- Have the Work Area Owner conduct regular 5S checks and audits and provide feedback on the findings and required actions to the user team.

Problem Statement:

The project objectives came from customer feedback. The ETI, as the customer, had raised concerns about the condition of the ETI rig and the wider experimental area. The customer felt that maintenance standards had fallen and the aesthetics of the rig looked unprofessional. The customer requested a 5S intervention to address, in particular:

- **Cable safety** – neatly securing cables and installing new cable trays.
- **Maintenance of the site** – cutting back vegetation in an identified radius of the ETI rig and keeping it at a consistently, low level.
- **Equipment left from previous projects in the ETI Rig experimental work areas** – removing and disposing of waste items and returning reusable equipment to their home positions, eliminating trips and maintenance hazards and flagging up to the project manager the need to introduce a dismantling activity to all applicable, future project plans.

- **Resource** – ensuring that the work area owner, or designee, have the maintenance/physical safety role for the ETI rig work areas in their performance management plan going forward, to ensure that focus and time are available.
- **Aesthetics** – ensuring that the physical structure and support areas are maintained to a professional standard, thereby reflecting the quality of the scientific staff and the high standard of work they produce.

Improvement & Benefits:

5S SORT: During this stage, all work area contents that did not relate to the work being done were removed and returned to their home position, or disposed of, if applicable. The improvements and benefits of this stage included, the removal of waste and non-essentials from the work areas, thereby freeing up work and storage space to be used more effectively, reducing trips hazards, identifying additional safety issues to address, providing a complete overview of assets and identifying tools and equipment needing repair or replacement.

5S STRAIGHTEN: During this stage, the layout of the work areas and the storage of contents were reviewed. The improvements and benefits of this stage in each of the scoped work areas were as follows:

ETI Rig:

- New cable supports were installed and the cabling in and around the ETI Rig was re-positioned, streamlined and secured neatly.
- Additional safety solutions were introduced, to include, steps to traverse over protruding equipment and foam on a low-lying, overhead metal bar, to prevent head injuries. Safety signage ('Mind your Head' and 'No Unauthorised Access') was purchased and positioned to provide visual management solutions and to ensure worker safety;

Control Room, Building 66:

- A future state floor plan was developed for the control room/building 66 and related purchases were processed and received.
- Two low cabinets were purchased for under-bench storage of tools and equipment.
- Large metal cabinets were purchased and positioned for work in progress to be stored.
- The tools, equipment and supplies were organised and 'home positions' labelled for visual management purposes.
- A first aid box was obtained from the Health & Safety team and mounted on the wall to address minor injuries, if they occurred.
- Four sign holders were purchased and positioned for awareness and safety signs (to include a 'First Aid' sign and 'Caution Hot Water' sign).
- Long, heavy duty matting was purchased and stretched between the two building doors, to keep the muddy boots of 'walk-through traffic' off the floor.
- Blinds for the windows, on the car park side of the building, were purchased and installed to protect the confidentiality of the work taking place inside.
- A bulletin board was purchased and positioned, to hold safety notices and other key announcements for the team.

Spray Booth-Storage Building:

- A future state floor plan was developed for the spray booth storage building and related purchases were processed and received.
- New racking and crates were purchased to appropriately house large tools and equipment.
- A tool box and trolley were purchased to create a mobile solution and 'home position' when using small tools in and around the ETI rig.

5S SHINE

During this stage, a thorough cleaning of the work areas and some equipment took place. Maintenance issues were reported to the facilities management team for prompt resolution.

The improvements and benefits of this stage included:

- Facilities management staff completed the grass cutting and weeding requirements around the experimental area. They have increased the frequency of maintaining the area from every 2 months to every 2 weeks.
- Facilities management staff conducted a thorough cleaning of building 66 (Control room, kitchenette and WC) and have increased the frequency and scope of future cleaning routines.
- The major hazards team cleaned the spray booth and ETI rig and equipment.
- Cleaning equipment, supplies and heavy duty bins were purchased for all three work areas, to ensure the spaces are kept clean and free of rubbish at all times.

5S STANDARDISE

During this stage, work area standards were agreed with the user team and communicated to all area users to ensure that the standards are maintained on an ongoing basis. Challenges in sustaining these were also discussed and solutions identified to address them.

The improvements and benefits of this stage included:

- Baseline work area standards were discussed and developed by the user team. They created the solution, which increases 'team ownership' and responsibility of work areas.
- Visual management signs were created and displayed to reinforce the new work area standards to work area users.
- The new work area standards were communicated to all users of the ETI rig, spray booth/storage building and building 66.
- A suitable person was appointed as the work area owner to monitor and manage the three scoped work areas.

5S SUSTAIN

The Work Area owner, has ensured that the work areas have been maintained to standard since the completion of the 5S project in May 2018, with 5S checks and corrective actions on a weekly basis

throughout the remainder of 2018. Since January 2019, the more formal monthly 5S audits have been introduced, using the Audit Checklist and has addressed the few arising deficiencies.

The improvements and benefits of this stage included:

- A work culture being created, on which further continuous improvement efforts can be built.
- The maintenance of 5S standards, which has increased work area effectiveness, efficiency and ownership.
- A sense of pride in the work areas from users, which has rubbed off on other staff.
- The creation of a safe, clean, well-maintained and professional-looking work environment.

15.3 ANALYSIS OF HRSG FOLLOWING TEST 64

Effect of detonation pressure on HRSG walls: The model consisted of a quarter model (two planes of symmetry) of a length of ducting (1.4 m wide and 2.8 m in height), with stiffening ribs, approximately 254 mm wide, 25 mm thick, spaced at 300 mm intervals, as shown in Figure. Additional bracing was added between the ribs at the corners. The model consisted of approximately 30 000 shell elements.

A pressure pulse was applied to all the interior surfaces of the duct. The pulse, ramping up from 0 bar to 18 bar over 1 ms, then down to 0 bar again over another 1 ms was applied to all the surfaces simultaneously (i.e. the pressure did not progress along the duct). Therefore, the results are likely to be a worst case.

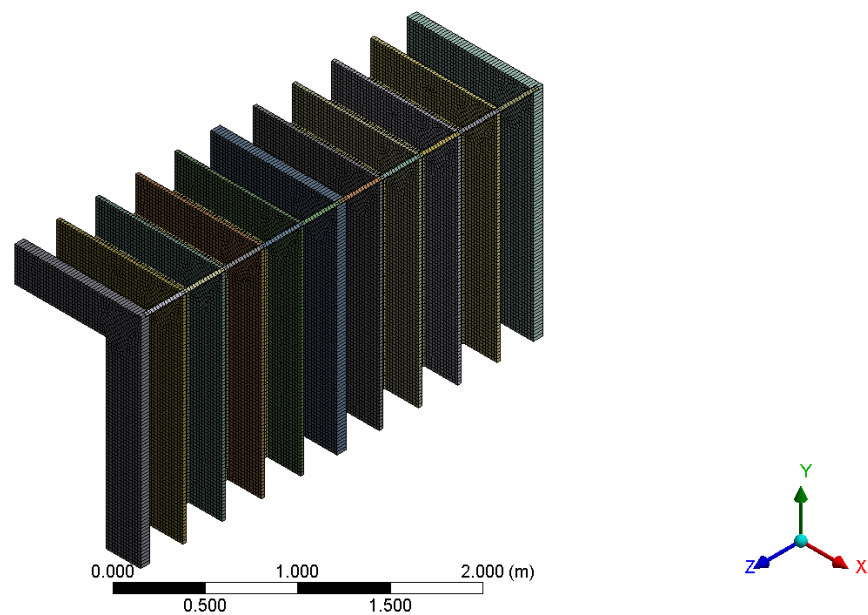


Figure A7 Geometry of duct model

The deflection results are shown in Figure A8. The maximum deflection of 11 mm occurred 3 ms after the peak pressure. The maximum plastic strains recorded were less than 0.5% and occurred in the ribs. Due to some oscillations after the pressure pulse, some reverse bending occurred which caused compressive plastic strains to counter some of the tensile plastic strains that initially occurred. By the end of the modelled time-frame (20 ms), the maximum plastic strain was under 0.2%, as shown in Figure A9.

I: Copy of New Design 25 mm ribs with corner supports
 Total Deformation
 Type: Total Deformation
 Unit: mm
 Time: 5.0004e-003
 Cycle Number: 8157
 25/03/2019 15:11

11.073 Max
 9.8437
 8.6142
 7.3848
 6.1553
 4.9259
 3.6965
 2.467
 1.2376
 0.0081366 Min

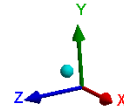
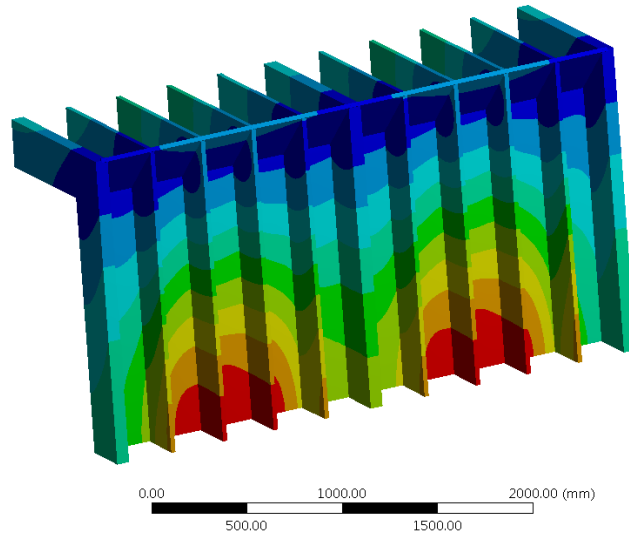


Figure A8 Maximum deflection

I: Copy of New Design 25 mm ribs with corner supports
 Equivalent Plastic Strain
 Type: Equivalent Plastic Strain - Top/Bottom
 Unit: mm/mm
 Time: 2.0001e-002
 Cycle Number: 32620
 25/03/2019 15:15

0.0015137 Max
 0.0013244
 0.0011352
 0.00094603
 0.00075683
 0.00056762
 0.00037841
 0.00018921
 0 Min

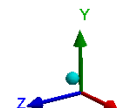
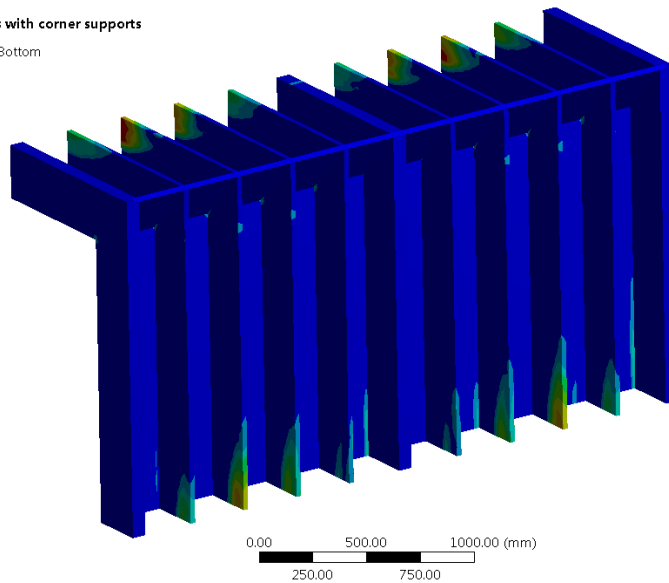


Figure A9 Plastic strain

Blast door movement: The movement of a hinged blast door in response to a defined pressure pulse has been modelled. Standard structural steel material properties were used, i.e. density of 7850 kg/m³ and Young's modulus of 200 GPa. No yield limit was set. The geometry of the door and the boundary conditions are shown in Figure A10. A plate thickness of 20 mm resulted in an overall mass of 50.9 kg, compared to a stated mass of 47.45 kg. An additional model with the plate thickness increased to 22 mm was also run as some of the doors were of this thickness. This increased the mass of the door to 56.0 kg.

The door was meshed using 3204 quadrilateral shell elements.

The top of the door was constrained in all directions for displacement, but allowed rotation, enabling the door to pivot open. Friction in this hinge was not modelled. Also, no air resistance was modelled.

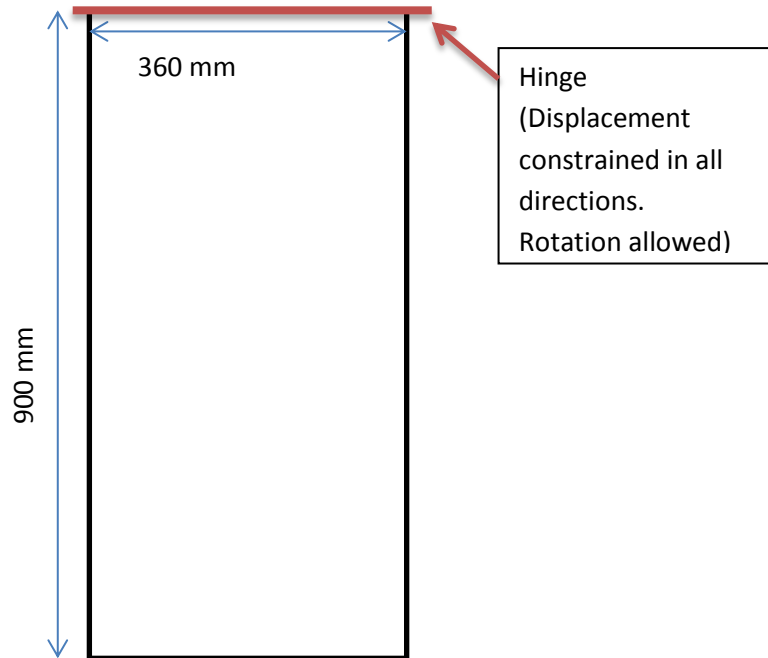


Figure A10 Geometry of hinged blast door

A pressure pulse was applied to one side of the door, across the full surface. Two different pulses were modelled, as shown in Figure A11, these represented the two most likely loading scenarios based up on the measured pressures. In each case, the pulse had a square profile. The resulting velocities of the door are listed in Table A1 for each condition modelled. As there was some flexure of the door, the velocity of the bottom (free end) of the door oscillated. This effect was more noticeable in the thinner door, and for the shorter pulse. Therefore, the velocities quoted are average values once the pressure pulse had stopped.

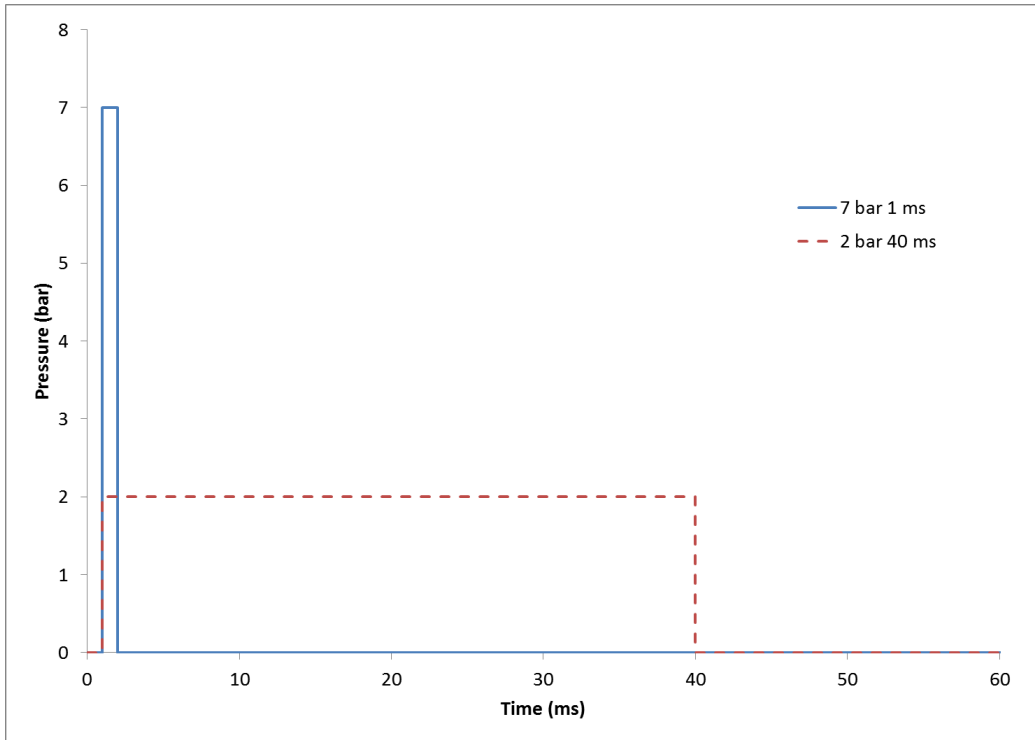


Figure A11 Pressure pulses applied to surface of blast door

The velocity results for the lower pressure, longer pulse were approximately ten times higher than for the shorter pulse. This agrees with the difference in impulse in the two pressure pulsed (7 bar·ms compared to 80 bar·ms). Increasing the thickness of the plate (and therefore the mass) by ten percent resulted in a corresponding reduction in velocity of approximately ten percent.

The results represent idealisations, where a number of effects have not been taken into consideration. Gravity and friction were not included, although the effect of these would be likely to be small. The effect of air resistance may be larger, especially for the longer pulse event, where velocities of 70 m/s were predicted. Air resistance at this velocity would be likely to be significant on a flat panel. Also, the effect of venting on the pressure pulse has not been taken into account, which again could have a significant effect especially on the longer pulse model. All the simplifications would result in higher estimates of velocity, and therefore the values shown in Table A1 below should be viewed as upper bound values.

Table A1 Results of average velocity estimates of bottom of door.

Pressure Pulse	Average Velocity (m/s)	
	20 mm plate	22 mm plate
7 bar 1 ms	7.5	6.8
2 bar 40 ms	75	70



HEALTH & SAFETY
LABORATORY

HSL: HSE's Health and Safety Laboratory is one of the world's leading providers of health and safety solutions to industry, government and professional bodies.

The main focus of our work is on understanding and reducing health and safety risks. We provide health and safety expert advice and consultancy, research, specialist training and products.

At HSL, we have been developing health and safety solutions for over 100 years. Our long history means that we're well placed to understand the changing health and safety landscape, and anticipate future issues.

We employ over 450 scientific, medical and technical specialists, including occupational health and risk management experts to help our clients manage a wide range of issues in workplace health and safety.

ISO 9001 OHSAS 18001



Health and Safety Laboratory

Harpur Hill

Buxton

Derbyshire

01753 611111